REGULATION OF NF-κB AND p53 IN THE LIVER AND SKELETAL MUSCLE OF THE FREEZE TOLERANT WOOD FROG, *RANA SYLVATICA*

By

Craig Brooks

B.Sc. Honours Queen's University, 2007

A Thesis Submitted to the Faculty of Graduate Studies and Research in partial fulfillment of the requirements for the degree of

Master of Science

Department of Biology

Carleton University

Ottawa, Ontario, Canada

Your file Votre référence
ISBN: 978-0-494-60198-3
Our file Notre référence
ISBN: 978-0-494-60198-3

Abstract

The wood frog, *Rana sylvatica*, is the primary model animal used for studying vertebrate freeze tolerance. During Canadian winters, wood frogs can endure the freezing of about 70% of their total body water and then thaw and resume life in the spring. Frogs have multiple ways to protect themselves against potential freezing injuries including adaptive changes to intermediary metabolism and gene expression. One way that wood frogs deal with freezing stress is via upregulation of several freeze-responsive genes. Previous studies provided excellent presumptive evidence for the involvement of the NF-κB and p53 transcription factors in freeze tolerance. The studies in this thesis used Western blotting to quantify levels of NF-κB subunits p50 and p65, its inhibitor, p-IκB, and downstream targets (ferritin heavy chain, manganese superoxide dismutase) as well as protein levels of p53, post-translationally modified p53, and some p53 downstream genes in the muscle and liver of control versus frozen wood frogs. Nuclear distributions of NF-κB and p53 were also assessed. RT-PCR was used to quantify transcript levels of select targets of NF-κB and p53. Significant increases in the expression levels of NF-κB and its downstream targets as well as in levels of p53, post-translationally modified p53, and its downstream targets were observed during freezing. These findings suggest the activation of NF-κB antioxidant defenses in the wood frog during freezing in anticipation of reperfusion during thawing and the activation of p53 in the wood frog which would lead to cell cycle arrest in the frozen state.

Acknowledgements

First of all, I would like to thank my thesis supervisor, Dr. Kenneth B. Storey for giving me the opportunity to be a part of and contribute to the Storey Lab and also for his motivation and guidance that have enabled me to learn a lot over the past two years. I would also like to thank Jan Storey for her help with the editing of my thesis. Her insight was much appreciated while putting this thesis together as was her support and encouragement throughout my time at the Storey lab.

I would also like to thank the Storey lab members namely Anastasia, Amal, Ben, Rabih, Neal, Chris, Kyle, Jing, Shannon, Marcus, Allan, Mike, Alyx, Judeh, and Ryan for their help and especially Jacques and Oscar who taught me a great deal.

I would like to give special thanks as well to my parents, Lydia and Brian, and my sister, Ana, for their tremendous love and support throughout the duration of my studies at Carleton.

I would also like to give special thanks to Mary, who never ceased to provide me with support and encouragement as I performed experiments and wrote my thesis.

Table of Contents

List of Abbreviations

APS	Ammonium persulfate
ARF	Alternate reading frame
ATM	ataxia telangiectasia mutated
ATR	A-T and Rad3 related
ATP	Adenosine triphosphate
Bax	Bcl-2-associated X protein
CBP	CREB binding protein
Cdc	cell division cycle
CDK	cyclin dependent kinases
CKI	cyclin dependent kinase inhibitor
cDNA	Complementary DNA
DEPC	diethylpyrocarbonate
dNTP	deoxynucleotide triphosphate
DTT	Dithiothreitol
ECL	Enhanced chemiluminescence
EDTA	Ethylenediaminetetraacetic acid
EGTA	Ethylene(oxyethylenenitrilo)tetraacetic acid
EtBr	Ethidium Bromide
FHC	ferritin heavy chain
FOXO	forkhead box subclass family O

GADD	Growth arrest and DNA damage
HEPES	N-(2-hydroxyethyl)piperazine-N'-(2-ethanesulfonic acid)
IκB	Inhibitor of Nf-κB
IKK	IκB Kinase
JNK	Jun-N-terminal kinase
kDa	kilodalton
Mdm	Murine double minute
MnSOD	Manganese Superoxide Dismutase
mRNA	messenger RNA
NF-κB	Nuclear factor kappa B
PAGE	Polyacrylamide gel electrophoresis
PCNA	Proliferating Cell Nuclear Antigen
PCR	Polymerase Chain Reaction
PUMA	p53 upregulated modulator of apoptosis
PVA	Polyvinyl alcohol
PVDF	Polyvinylidene difluoride
RACE	Rapid Amplification of cDNA Ends
RAGE	Receptor for advanced glycation end products
Rb	Retinoblastoma
RNAase	Ribonuclease
ROS	Reactive oxygen species
rRNA	ribosomal RNA
RT-PCR	reverse transcriptase PCR

SDS	Sodium dodecyl sulfate
STAT	signal transducers of activated transcription
TAE	tris-acetate-ethylenediamine tetraacetic acid buffer
TEMED	N,N,N',N'-tetramethylethylenediamine
TBST	Tris-buffered saline Tween-20
Tris	Tris(hydroxymethyl)aminomethane

List of Tables

List of Figures

Chapter 1

GENERAL INTRODUCTION

The wood frog, *Rana sylvatica*, is the primary model animal used for studying vertebrate freeze tolerance. Extensive information has been accumulated on the wood frog to elucidate the molecular biology, biochemistry, and physiology of natural freezing survival (Costanzo *et al.*, 1993; Layne, 1995; Layne *et al.*, 1998). In particular, much recent work in the Storey laboratory has focused on the organ-specific changes in gene expression that are induced by freezing stress. The focus of this thesis is an examination of the role of the Nuclear Factor kappa B (NF-κB) and p53 transcription factor signalling pathways in the control of freeze-responsive gene expression in wood frogs.

Organisms inhabiting all parts of the planet deal with different forms of environmental stress in their day to day activities. One prominent stress that almost all organisms experience is fluctuation in environmental temperature that can range from very hot to very cold. Extremely cold ambient temperatures that fall well below 0°C are common over many areas of the planet, including temperate, polar and alpine environments. Most organisms living in these areas have adaptations that allow them to survive until spring since cold temperatures can be lethal, especially when body fluids freeze. Freezing can cause many problems to a susceptible organism. Intracellular freezing causes death because ice crystal growth damages subcellular architecture and microcompartmentation (Storey and Storey, 2004a). Tissue damage also arises from ice growth through extracellular spaces; for example, ice expansion in the lumen of capillaries can burst delicate blood vessels. Ice growth in extracellular spaces also draws water out of cells by osmosis so that cell volume is greatly reduced, intracellular ionic

strength increases, and compression stress can damage/rupture cell and organelle membranes so that integrity is destroyed after thawing (Storey and Storey, 2004a). Furthermore, freezing is an ischemic event because blood plasma is completely solidified. Cells are completely cut off from the delivery of oxygen and nutrients and also cannot get rid of waste products. Freezing also halts skeletal and cardiac muscle movements and nerve activity (Storey and Storey, 2004a).

Organisms have adapted in many ways to deal with seasonally cold environmental temperatures. Many birds migrate long distances to a warmer climate whereas other kinds of animals migrate short distances by delving underground below the frost line in dens, caves or burrows, or hibernating underwater. Some animals possess their own insulation in the form of fur or feathers. Thermogenesis is also a strategy for winter survival for endothermic hibernators which allows them to maintain their core body temperatures between 0 and 5°C. Most ectotherms cannot do this and have developed cold hardiness strategies to survive when body temperatures fall below 0°C (Storey and Storey, 2004b). Four options for this are anhydrobiosis, vitrification, freeze avoidance, and freeze tolerance. Anhydrobiosis, meaning life without water, involves the cessation of metabolic activity in response to extreme environmental conditions such as desiccation. Vitrification involves the solidification of water into an amorphous glass instead of into crystal form. Both strategies are used mainly by microscopic animals as well as cysts, embryos, eggs, and seeds (Storey and Storey, 2004b). Organisms employing the freeze avoidance strategy use carbohydrate protectants to maintain their bodies in a liquid state by supercooling to temperatures below the equilibrium freezing

point of their body fluids. Many insects and other invertebrates employ this strategy. Finally, organisms can deal with subzero temperatures by carefully regulating ice formation in extracellular fluid spaces of the body while preserving intracellular water in a liquid state. This is known as freeze tolerance (Storey and Storey, 2004b).

Freeze tolerant organisms display a number of adaptations that aid survival. Firstly, they initiate and control extracellular ice crystal formation using ice nucleating agents. They also upregulate blood clotting proteins in order to control any bleeding injuries caused by ice damage that are detected upon thawing. These animals also manage changes in cell structural integrity and volume through the synthesis of high concentrations of sugar or sugar alcohol cryoprotectants. Since blood flow is stopped during freezing, freeze tolerant organisms also need adaptations that allow them to tolerate long term anoxia as well as provide antioxidant defenses to combat oxidative damage over long periods of freezing or resulting from a rapid increase in reactive oxygen species generation when oxygen uptake soars upon thawing. Metabolic rate depression is also key for freezing survival. A coordinated suppression of "optional" energy-expensive cell activities (e.g. protein synthesis, cell cycle, growth, etc.) greatly extends the time that vital processes (e.g. membrane potential, etc.) can be sustained in the frozen state. Heart beat, breathing, muscle movement and nerve activity are also impaired in frozen organisms and other adaptations must be in place to ensure that these functions are restored upon thawing (Storey and Storey, 2004b). Five species of North American frogs are known to be freeze tolerant and employ these strategies during the winter including the wood frog, *R. sylvatica.*

The wood frog is an excellent model for studying vertebrate freeze tolerance since there is much more information on the molecular biology, biochemistry, physiology of wood frog freeze tolerance than on any other reptile/amphibian. Wood frogs are typically 51-70 mm in length, weigh about 5-10 g and are brown/tan in color with a distinct dark eye mask. They are found from Georgia up to Northern Canada and Alaska (Figure 1.1). Wood frogs spend winters on the forest floor under the protective cover of leaves and snow. Although ambient temperatures can reach -30°C or lower above the snowpack, temperatures under the insulating covering of snow typically fall no lower than -5°C. However, wood frogs can freeze whenever body temperature drops below about -0.5°C, the equilibrium freezing point of frog body fluids. Wood frogs can survive frozen many weeks with up to 65-70% of their total body water as extracellular ice (Storey and Storey, 2004a; Costanzo *et al.*, 1993). By starting to freeze at high subzero temperatures (typically -0.5 to -2.0°C), wood frogs initiate slow and controlled ice formation that allows the animal maximum time to activate mechanisms for freezing survival. There are three main ways that ice can start to form on and inside the wood frog. The first is nucleation via skin contact with environmental ice that initiates ice propagation through the body (Storey and Storey, 2004a). Secondly, ice nucleating bacteria present on the skin or in the gut can seed crystallization at about -2°C, thereby limiting the extent of supercooling (Layne, 1995). Finally, ice nucleating proteins present in the blood of wood frogs potentially assist the spread of ice throughout the interior of the wood frog (Storey and Storey, 2004a). Wood frogs produce a sugar cryoprotectant, glucose, from huge reserves of glycogen that are stored in the liver during summer/autumn feeding. During

freezing, high cryoprotectant levels minimize the reduction in cell volume caused by dehydration as water leaves cells to join growing extracellular ice masses. Glucose levels in wood frog blood and core organs can reach concentrations of 300 mM during freezing compared to 1-5mM in unfrozen frogs (Storey and Storey, 1984, 1986). Glucose is present in highest concentrations in the liver and heart, and lowest levels in skeletal muscle and skin (Storey, 1987); this is because glucose moves outward from the liver at the same time as ice propagates inward from the periphery (Storey and Storey, 2004a). Freezing also prevents oxygen from reaching organs and wastes from being removed and therefore wood frogs must be able to survive without oxygen for long periods of time (Layne *et al.*, 1998). To do this they rely on endogenous glycogen as their main fuel for energy production via glycolysis and also depress their metabolic rate to minimize ATP needs (Storey and Storey, 2004a). Oxidative damage from reactive oxygen species is also a danger during reperfusion events. Wood frogs have two strategies of antioxidant defense: the first is to maintain high constitutive activities of antioxidant enzymes in many organs and the second is to modify the activities of some enzymes in response to freezing (Joanisse and Storey, 1996). Various freezing induced changes in gene and protein expression impart selective advantages that aid the wood frog in surviving the rigors of freezing stress.

Previous studies done in the Storey lab have identified many freeze responsive genes in the wood frog using cDNA screening. For example, cDNA array screening identified glucose transporter 4 (important for cryoprotectant uptake), antioxidants thioredoxin and glutathione-S-reductase, iron and metal binding proteins ferritin and

metallothionein, and the receptor for advanced glycation end products (RAGE) (which could be involved in preventing glycation damage to proteins during freezing) as being upregulated in wood frog heart during freezing (Storey, 2004a, 2004b). Other studies have also identified several transcription factors that participate in mediating various freeze-responsive changes in gene expression in wood frog organs (Du, 2005; DeCroos, 2003; Bouffard, 2007; McNally, 2002)

A transcription factor is a protein that binds to DNA and regulates gene expression. Usually, a transcription factor is responsible for managing a group of genes that are activated under a particular stress. Every transcription factor has a DNA binding domain as well as a domain that is responsible for transcriptional activity through interaction with the essential transcription machinery. Transcription factors can also contain a ligand-binding domain if the presence of a ligand is necessary to activate DNA binding. A dimerization domain is also present within most transcription factors to allow formation of required homodimers or heterodimers for DNA binding. Transcription factors can also contain nuclear localization sequences that allow transcription factors to penetrate the nuclear pores (Willmore, 2004). This is important since many transcription factors are found in the cytoplasm under normal conditions until they are activated and then move into the nucleus where DNA binding occurs. Transcription factors can also be activated in a number of ways including via phosphorylation or acetylation of key serine, threonine, tyrosine, and lysine residues as well as by dissociation of inhibitory proteins bound to the inactive transcription factor. Transcriptional regulation and coordination are key in providing functional organisation to metabolism (Storey, 2008). Parallels can be

drawn between transcription factors activated as a result of a particular stress and the proteins produced by their target genes. Gene expression data obtained by DNA microarray studies can be corroborated by assessing transcription factor activity. This can be done by assessing total protein levels of a particular transcription factor as well as the relative amount of the transcription factor that is phosphorylated or acetylated. Assessment of the nuclear versus cytoplasmic distribution of a transcription factor can also be a good indicator of transcription factor activity (Storey, 2008).

Objectives:

This thesis is based on findings from previous technical work using commercially available scanning tools that used array technology to analyze entire genomes and transcriptomes. The results of heterologous DNA array screening with 19K human gene chips (University of Toronto MicroArray centre; http://www.uhnres.utoronto.ca/facilities/microarray.htm) and of Panomics TranSignal transcription factor array screening that assessed over 200 transcription factors (http://www.panomics.com/) were used as a starting point for this work. Analysis of gene chips compared mRNA populations from control versus 4 hour frozen frogs. The Panomics arrays identified several transcription factors that were highly upregulated in tissues of frozen frogs. These included NF-κB and p53. The 19K gene chips indicated a wide variety of genes that were freeze upregulated including some transcription factors, among them both NF-κB and p53. Thus, two different array screening methods were consistent in indicating potential roles for NF-κB and p53 in freezing survival but, because heterologous gene

screening was used, the results from this study cannot be considered definitive without further validation. However, this information from array screening provided excellent presumptive data for the involvement of these transcription factors in wood frog freeze tolerance. Therefore, I proposed that these two transcription factors, NF-κB and p53, are activated in response to freezing in wood frog organs and lead to specific upregulation of selected downstream genes whose protein products contribute to freezing survival.

Both Western blotting and PCR technologies were applied to explore the expression and regulation of NF-κB and p53 in response to freezing by wood frog tissues. Furthermore, after demonstrating that these signal transduction pathways were activated by freezing, the responses of selected downstream genes that are known to be targets of these two transcription factors were evaluated. Upregulation of these downstream genes further supported the importance of the NF-κB and p53 signaling pathways to freezing survival. Chapter 3 investigates the role of p53 mediated cell cycle arrest as a mechanism of metabolic rate depression during freezing stress, whereas Chapter 4 explores the responses to freezing stress by the transcription factor, NF-κB, and two antioxidant gene targets under its control (ferritin heavy chain and MnSOD) in the wood frog, *Rana sylvatica*, in response to freezing stress.

Figure 1.1: Geographical range of the wood frog, *Rana sylvatica*

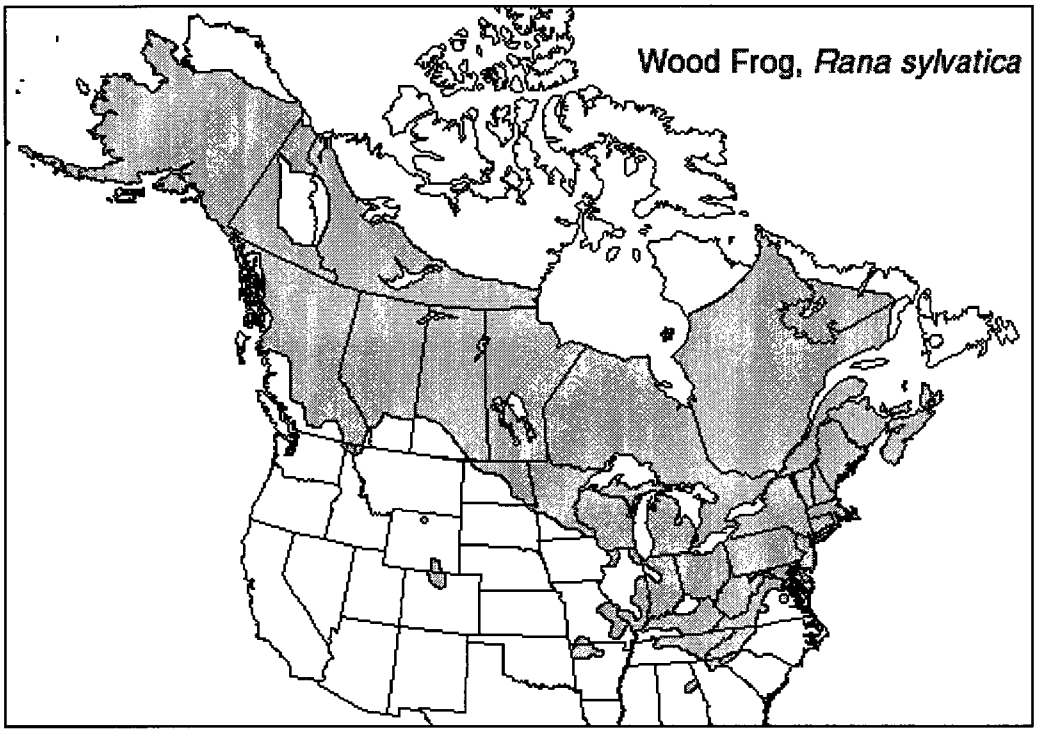

http://en.wikipedia.org/wiki/File:Rana-sylvatica_Range.gif

Chapter 2

MATERIALS AND METHODS

Animal experiments:

Male wood frogs, *Rana sylvatica*, were collected from breeding ponds in the Ottawa area. The frogs were washed in a tetracycline bath and were kept in plastic containers of damp sphagnum moss at 5°C for 1-2 weeks before use. Control frogs were taken from this condition. For freezing exposure, wood frogs were transferred to plastic containers lined with damp paper towels and placed inside a -2.5°C incubator. Ice formation on the papers towels allowed for rapid and uniform seeding of frog body fluids once body temperature dropped below -0.5°C. At these temperatures, freezing begins within 45 minutes as seen in previous experiments (Storey and Storey, 1985). After the initial cooling, frogs were exposed to freezing for 4 or 24 hours. All frogs (control + 2 experimental conditions) were sacrificed by pithing and dissected within 30 to 90 seconds by a team of 5-6 people. Tissues sampled included liver, brain, heart, kidney, and skeletal muscle. All were flash frozen in liquid nitrogen and stored in a -80°C freezer. Protocols for the care, experimentation, and euthanasia of wood frogs were approved by the Carleton University Animal Care Committee in agreement with the Canadian Council on Animal Care guidelines.

Western blotting:

Isolation of total soluble protein

Samples of approximately 500 mg of frozen tissue were placed in 1 mL of homogenization buffer (20 mM Tris-base, 150 mM NaCl, 1 mM EDTA, 1 mM EGTA, 1 mM NaF, 10 mM ß-glycerophosphate, 1% v/v Triton X-100 and 1 mM phenylmethylsulfonyl fluoride) and immediately homogenized using a Polytron homogenizer. Samples were centrifuged at 10,000 x g and 4°C for 15 minutes. The

supernatant was removed and soluble protein concentration was determined. This was repeated for four or five independent samples of each experimental condition.

Isolation of nuclear extracts

Nuclear extracts were prepared using a protocol similar to the one used by Dignam *et al.* (1983). Aliquots of approximately 0.5 g of frozen tissue were weighed and then 500 µL of homogenization buffer [10 mM HEPES, pH 7.9, 10 mM KCl, 10 mM EDTA, 10 mM DTT and 10 µl of protease inhibitor cocktail (Sigma)] was added to each. Tissues were disrupted using a Dounce homogenizer. The nuclei were pelleted with a 10 minute centrifugation at 8000 x g and the supernatant containing the cytoplasmic extract was transferred to a separate tube. Pellets were washed with homogenization buffer and resuspended in 150 µL of extraction buffer (20 mM HEPES, pH 7.9, 400 mM NaCl, 1 mM EDTA, 10% v/v glycerol, 10 mM DTT, and 1.5 µl protease inhibitor cocktail). The pellets were then placed on a rocker for 1 hour at a slow speed. After centrifugation at 10,000 x g for 10 minutes, the supernatants containing the nuclear extracts were collected. This was done for four independent samples for control, 4 hour frozen, and 24 hour frozen conditions. Protein concentrations in both the cytoplasmic and nuclear fractions were determined using the Bio-Rad assay. Confirmation that the cytoplasmic and nuclear fractions were well separated was done by running 20 µg aliquots of both fractions on an SDS-PAGE gel, followed by Western blotting using an anti-histone H3 antibody (Cell Signaling) diluted at 1:1000 v:v and an anti-rabbit secondary antibody (BioShop) diluted at 1:8000 v:v. Bands for histone H3 (a nuclear marker) were found only in the nuclear extracts (data not shown).

Measurement and dilution of proteins

The Coomassie blue dye binding method was used to determine soluble protein concentrations using the Bio-Rad prepared reagent with bovine serum albumin as the standard (BioRad, Hercules, CA). The reagent was diluted 5-fold and typically aliquots of protein extracts were diluted 20 to 80-fold, both with distilled water, before assay. Microplate wells typically contained 10 µl of diluted protein and 190 µl of reagent. Color development occurred over 10 minutes and then samples were read at 595 nm using a microplate reader. The protein concentrations in the original extracts were then adjusted to a constant value for all samples by addition of small amounts of homogenization buffer; e.g. most extracts for standard Western blotting were adjusted to 10 µg/µL. Aliquots of tissue extracts were then diluted 1:1 v/v with 2X SDS-PAGE sample buffer (100 mM Tris-HCl pH 6.8, 4% w/v SDS, 20% v/v glycerol, 0.4% w/v bromophenol blue) with 10% v/v fresh 2-mercaptoethanol added. These were then boiled for 5 min and stored at -20°C. The final protein concentration in samples used for most standard Western blotting as well as nuclear and cytoplasmic extracts was 5 µg/µL.

SDS-PAGE electrophoresis

SDS-polyacrylamide gels (8, 10 or 12% acrylamide, 0.4 M Tris pH 8.8, 0.1% w:v SDS, 0.1% w:v APS, 0.04% v:v TEMED) were prepared with 5% upper stacking gels (5% acrylamide, 0.13 M Tris pH6.8, 0.1% w:v SDS, 0.1% w:v APS, 0.1% v:v TEMED). Each gel had 20 µg of soluble protein loaded in each well along with 3 µg of Kaleidoscope prestained molecular mass ladder (Fermentas) in one well in order to estimate the size of the proteins. The proteins were separated for 45 minutes at 180V

using SDS-PAGE running buffer (25 mM Tris base, 190 mM glycine, 0.1% w/v SDS). Following electrophoresis, proteins were transferred to polyvinylidene difluoride (PVDF) membrane (Millipore) by wet transfer with transfer buffer (25 mM Tris pH 8.5, 192 mM glycine, 20% v:v methanol) at 4°C for 90 minutes at 160 mA. After transfer, membranes were blocked either with 2.5% w:v non-fat dried milk dissolved in Tris buffered saline containing Tween-20 (TBST: 20 mM Tris base, 140 mM NaCl, 0.05% v/v Tween-20) or with 1μg/mL polyvinyl alcohol (PVA) depending on the protein to be detected. Membranes were then incubated overnight incubation at 4°C with primary antibody diluted with TBST and a small amount of sodium azide. Subsequently, the membranes were washed a few times with TBST and then incubated with either anti-rabbit or anti-goat secondary antibody conjugated to horseradish peroxidase. Usually, anti-rabbit secondary antibody (Bioshop) was diluted at 1:8000 v/v and applied for 40 minutes followed by 2 x 10 minute washes with 0.05% v/v TBST. The anti-goat secondary (Santa Cruz) was diluted at 1:4000 v/v and applied for 20 minutes followed by 2 x 10 minute washes with 0.05% v/v TBST. Tables 2.1 and 2.2 list the primary antibodies used as well as their dilutions, secondary antibodies and other conditions of their use. Signal was detected by the enhanced chemiluminescence system (ECL). Bands were visualized using a ChemiGenius Bioimaging system (Syngene, MD, USA) and band intensities were analyzed using the associated Gene Tools software (www.syngene.com). One ECL band was quantified per membrane and this band was verified by a positive mammalian control and a standard protein molecular weight ladder. Information on the amino acid sequence of the epitope recognized by a particular primary antibody was obtained from the literature for different animal species. These sequences were aligned and found to be

highly conserved. Similar results were found with several of the primary antibodies used. Membranes were then stained with Coomassie blue (0.25% w/v brilliant blue, 7.5% v/v acetic acid, 50% v/v methanol) for 15 minutes and destained with destain solution (17% v/v acetic acid, 50% v/v methanol) for 5 minutes in order to verify equal loading of proteins in the lanes. Coomassie bands were quantified by boxing a group of several bands in an area that excluded the band of interest using the Gene Tools software (www.syngene.com). Data were normalized by taking the ECL values and dividing them by Coomassie values.

RT-PCR

RNA isolation and test of purity

In order to prevent contamination by RNAases, all materials and solutions were treated with 0.1% v/v diethylpyrocarbonate (DEPC) and were autoclaved before use. Trizol® solution (Invitrogen) was used to isolate total RNA from tissues. Approximately 100 mg of frozen tissue was homogenized in 1 mL of Trizol using a Polytron homogenizer. The addition of 200 µL of chloroform followed. Samples were centrifuged at 10 000 x g for 15 minutes at 4°C. The upper aqueous phase containing total RNA was separated and transferred to a tube which contained 2-propanol. The RNA was allowed to precipitate for 10 minutes at room temperature. The samples were then centrifuged at 12 000 x g for 15 minutes at 4°C. The RNA pellet was washed with 1 mL 70% ethanol and then centrifuged again at 12 000 x g for 5 minutes. The pellet was isolated and air dried for approximately 10 minutes and then resuspended in 60 µL of DEPC treated water. Four independent samples were extracted for control and 24 hour

frozen groups for each tissue. RNA purity was assessed by determining the 260/280 ratio. RNA quality was also checked by electrophoretic separation of 2 or 3 μg of total RNA from each sample on 1.5% agarose gels containing ethidium bromide (EtBr). The presence of two bands corresponding to the 28S and 18S ribosomal RNA (rRNA) indicated that the RNA was acceptable. Alpha-tubulin exon spanning primers confirmed the absence of genomic DNA contamination as the primers yielded only one band of expected size after PCR amplification as opposed to two bands which would suggest genomic DNA contamination.

Gene specific primer design

Oligonucleotide primers were designed and synthesized for ferritin heavy chain, GADD45α, and 14-3-3σ protein. Primers were designed by selecting nucleotide sequences for the genes of interest from NCBI Genbank for species that were as closely related to *Rana sylvatica* as possible. Human, mouse, African clawed frogs (*Xenopus laevis* and *Xenopus tropicalis*), and zebrafish mRNA sequences were used. The sequences were opened in DNAMAN 4.1.1.1 (Lynnon Biosoft) and were used to create a multiple sequence alignment in order to find regions that were highly conserved as well as consensus sequences to use for primer design. The consensus sequences were loaded into Primer Designer (Scientific and Educational Software) to create both forward and reverse gene specific primers. Primers for the housekeeping gene, alpha-tubulin, were also designed and alpha-tubulin was amplified from all samples and used to normalize the expression of the genes of interest. Primers were made by Sigma Genosys and were

received in dry powdered form. Stock solutions having concentrations of 0.3 nmol/μL in DEPC water were prepared from the dried primers and were stored at -20°C until use.

First strand cDNA synthesis and polymerase chain reaction

Isolated total RNA was used to synthesize complementary DNA (cDNA). About 3 μg of RNA was diluted with DEPC water to a final volume of 10 μL. A 1μL aliquot of 200 ng/μL oligo-dT (5'-TTTTTTTTTTTTTTTTTTTTTTV-3'; V = A, G, or C) (Sigma Genosys) was added to each sample which formed a hybrid with the poly A tails of mRNA. This hybrid was incubated in an Eppendorf thermocycler at 65°C for 5 minutes and then chilled on ice. A master mix containing 4μL 5X first strand buffer, 2μL 10 mM DTT, 1 μL dNTPs, and 1 μL reverse transcriptase enzyme Superscript II (all from Invitrogen) was then added to all samples to a final volume of 19 μL. Samples were then incubated in the Eppendorf thermocycler at 42°C for 45 minutes. The cDNA products were serially diluted (10^{-1} and 10^{-2}) and stored at -80°C until required for PCR.

The amplification of selected genes of interest from the cDNA samples was done using the polymerase chain reaction (PCR). Each PCR reaction contained 15 μL of DEPC water, 0.5 μL of 10X PCR buffer (Invitrogen), 1.75 μL 50 mM $MgCl_2$ (Invitrogen), 1.25 μL of forward and reverse primer mixture (Sigma Genosys), 0.5 μL 10 mM dNTPs, and 1 μL of Taq polymerase (Invitrogen) for a total of 25 μL. The PCR reaction consisted of an initial denaturation step of 4 minutes at 94°C, followed by 40 cycles of 94°C for 45 seconds (denaturation), 53-66°C (optimum annealing temperature) for 45 seconds, and 72°C for 45 seconds (elongation). The final step was an elongation step at 72°C for 4 minutes. Optimum annealing temperatures for the genes amplified

were: 53.2°C, 53.2°C, 65.8°C, 53.0°C for ferritin heavy chain, 14-3-3σ, GADD45α, and α-tubulin, respectively. The PCR products were separated on 1.5% agarose gels containing 0.01% v/v EtBr. The gel was prepared by adding 3 g of agarose (Bioshop) to 200 mL of 1X TAE buffer (5X stock TAE buffer contained 242 g Tris base, 57.1 mL concentrated glacial acetic acid, 100 mL of 0.5 M EDTA in 1L water, adjusted to pH 8.5). The mixture was heated in the microwave and cooled until slightly warm to the touch. A 2 uL aliquot of EtBr (10 mg/mL) was then added and the solution was poured onto a gel casting apparatus and allowed to solidify. A 10 μL amount of PCR product was then mixed with 3 μL of DNA loading buffer (0.25% xylene cyanol FF, 70% v:v glycerol in ddH_2O), loaded on the solidified gel and electrophoresed in 1X TAE buffer for 30 minutes at 100V. Band intensities were quantified using the Syngene and the associated GeneTools software (Syngene, MD, USA) and normalized against the corresponding intensity of α-tubulin bands amplified from the same sample.

PCR products were sent for sequencing to confirm that they encoded the gene of interest. Sequencing was done by DNA Landmarks. Sequences were analyzed by BLASTN (http://www.ncbi.nlm.nih.gov/blast) in order to verify that they were correct.

The forward and reverse primers used for PCR amplifications are listed below:

Ferritin heavy chain forward 2, 5' – GACTGCGARGCYGCCATCAA – 3'
Ferritin heavy chain reverse 2, 5' - TTG TCR AAC AGG TAC TCG CC – 3'
GADD45a forward 2, 5' – AAYGTGGACCCMGAYAACGT – 3'
GADD45a reverse 2, 5' - TCA YCG CTC IGG SAG GTT RA – 3'

14-3-3σ forward 1, 5' – GACATGGCMRCCTKCATGAA – 3'

14-3-3σ reverse 2, 5' - TCK GCG ATG GCC TCR TCA AA – 3'

The above primers produced fragment sizes for Ferritin HC F2R2, GADD45a F2R2, 14-3-3σ F1R2 of approximately 453 base pairs (bp), 313 bp, 525 bp, respectively.

PCR was optimized by trying different numbers of cycles and performing serial dilutions in order to ensure that quantification was being done in the log phase of each corresponding PCR reaction. Ultimately, 40 cycles of PCR and cDNA diluted tenfold was deemed appropriate.

Statistics

Western blotting: Differences between normalized control values (n=4 or 5 independent samples) and normalized experimental values for 4 hour frozen samples (n=4 independent samples) or 24 hour frozen samples (n=4 or 5 independent samples) were evaluated for statistical significance using the Student's t-test with $P<0.05$ accepted as statistically significant. For nuclear extracts, normalized values for control, 4 hour and 24 hour frozen frogs were compared (n=4 independent samples for each).

PCR: Differences between normalized control values (n=8-11 independent samples) and normalized 24 hour frozen values (n=7-10 independent samples) were evaluated for statistical significance using the Student's t-test, $p<0.05$.

Table 2.1: Antibodies used in NF-κB western blotting and their experimental conditions

Primary Ab & dilution	**Primary Ab time**	**Blocking**	**Secondary Ab**	**Size**	**Company**
anti-p50 (1:5000)	overnight	2.5% milk for 15 min	anti-rabbit (1:8000)	~50 kDa	Cell Signaling
anti-p65 (1:5000)	overnight	2.5% milk for 15 min	anti-rabbit (1:8000)	~65 kDa	Cell Signaling
anti-phospho-p65 ser 536 (1:1000)	overnight	2.5% milk for 15 min	anti-rabbit (1:8000)	~65 kDa	Cell Signaling
anti-phospho-IkB ser 32 (1:1000)	overnight	2.5% milk for 15 min	anti-rabbit (1:8000)	~40 kDa	Cell Signaling
anti-Ferritin HC (1:1000)	overnight	1 ug/mL PVA for 1 min	anti-goat (1:4000)	~21 kDa	Santa Cruz
anti-MnSOD (1:1000)	overnight	No blocking	anti-rabbit (1:8000)	~26 kDa	Stressgen

Table 2.2: Antibodies used in p53 western blotting and their experimental conditions

Primary Ab & dilution	**Primary Ab time**	**Blocking**	**Secondary Ab**	**Size**	**Company**
anti-p53 (1:1000)	overnight	2.5% milk for 15 min	anti-rabbit (1:8000)	~53kDa	Cell Signaling
anti-phospho-p53 ser 6 (1:1000)	overnight	2.5% milk for 15 min	anti-rabbit (1:8000)	~53kDa	Cell Signaling
anti-phospho-p53 ser 9 (1:1000)	overnight	2.5% milk for 15 min	anti-rabbit (1:8000)	~53kDa	Cell Signaling
anti-phospho-p53 ser 15 (1:1000)	overnight	2.5% milk for 15 min	anti-rabbit (1:8000)	~53kDa	Cell Signaling
anti-phospho-p53 ser 20 (1:1000)	overnight	2.5% milk for 15 min	anti-rabbit (1:8000)	~53kDa	Cell Signaling
anti-phospho-p53 ser 37 (1:1000)	overnight	2.5% milk for 15 min	anti-rabbit (1:8000)	~53kDa	Cell Signaling
anti-phospho-p53 ser 46 (1:1000)	overnight	2.5% milk for 15 min	anti-rabbit (1:8000)	~53kDa	Cell Signaling
anti-phospho-p53 ser 392 (1:1000)	overnight	2.5% milk for 15 min	anti-rabbit (1:8000)	~53kDa	Cell Signaling
anti-acetyl-p53 lys 373 (1:1000)	overnight	2.5% milk for 15 min	anti-rabbit (1:8000)	~53kDa	Upstate Cell Signaling Solutions
anti-acetyl-p53 lys 382 (1:1000)	3 days	2.5% milk for 15 min	anti-rabbit (1:8000)	~53kDa	Cell Signaling
anti-p21 (1:1000)	overnight	2.5% milk for 15 min	anti-rabbit (1:8000)	~21kDa	Santa Cruz
anti-phospho-p21 ser 146 (1:1000)	overnight	2.5% milk for 15 min	anti-rabbit (1:8000)	~21kDa	Santa Cruz
anti-Mdm2 (1:1000)	overnight	2.5% milk for 15 min	anti-rabbit (1:8000)	~90kDa (~60kDa cleavage product)	Santa Cruz
anti-Gadd45α (1:1000)	overnight	2.5% milk for 15 min	anti-rabbit (1:8000)	~18kDa	Santa Cruz
anti-14-3-3σ (1:1000)	3 days	2.5% milk for 15 min	anti-goat (1:4000)	~30kDa	Santa Cruz
anti-p19ARF	Overnight	2.5% milk for 15 min	anti-rabbit (1:8000)	~19kDa	Novus Biologicals

Chapter 3

REGULATION OF P53 IN WOOD FROG LIVER AND SKELETAL MUSCLE

Introduction

To date, cell cycle arrest as a mechanism of metabolic rate depression has not been studied to any great extent (Storey and Storey, 2007). It could be predicted that many cell types in an organism experiencing hypometabolism would halt their cell cycle. The wood frog, *Rana sylvatica*, may adopt this strategy as one of the many that it employs during prolonged freezing periods. One transcription factor in particular plays a major role in cell cycle arrest is p53. An initial study using a transcription factor array showed enhanced DNA binding by p53 in liver extracts from frozen frogs as compared to control frogs, thereby suggesting that p53 is freeze responsive and that genes under its control may be upregulated to enhance freeze tolerance (Storey, 2008).

The p53 transcription factor is known to stimulate expression of genes involved in cell cycle arrest, apoptosis, and DNA repair. The p53 pathway is activated by many stressors including DNA damage and hypoxia (Levine *et al.*, 2006). Under normal conditions, p53 is held inactive by its inhibitor, Mdm2, that binds to p53 and mediates its transportation to the cytosol where it is ubiquitinated and degraded by the proteasome (Malkin, 2001; Bose and Ghosh, 2007). However, under stress conditions, p53 is stabilized and the amount of p53 in the nucleus rises dramatically as the interaction between p53 and Mdm2 is inhibited. Stabilization of p53 is a frequent response to a myriad of different stresses including DNA damage, metabolic changes, hypoxia, and cold shock (Malkin, 2001; Ashcroft and Vousden, 1999). Next, p53 is rendered transcriptionally active by phosphorylation and acetylation by kinases and acetylases.

Downstream genes activated by p53 include those involved in cell cycle/growth arrest and DNA repair such as p21, Gadd45α and 14-3-3σ (figure 3.1) as well as those involved in apoptosis such as Bax and PUMA. Cell cycle arrest as a result of p53 induction can occur at the G1/S or G2/M checkpoints (Malkin, 2001).

The human p53 protein contains 393 amino acids and consists of five highly conserved domains including a transactivation domain located at the N-terminal. This site is also the place where Mdm2 binds to p53 and keeps it inactive under normal conditions. The N-terminal region contains many serine residues including serine 6, 9, 15, 20, 37, and 46; these are phosphorylated under various stresses. The C-terminal is responsible for controlling specific DNA binding by p53 (Steegenga *et al.*, 1996). It contains two serines (one of which is serine 392) that are phosphorylated and three lysines (including 373 and 382) that are acetylated under stress conditions (Appella and Anderson, 2001). A list of the molecular/cellular outcomes of phosphorylation at different sites on p53 is found in Appendix A (Bode and Dong, 2004).

There are many different ways in which Mdm2-mediated inhibition can be disrupted so that p53 can be stabilized. Two such mechanisms are posttranslational modifications to p53 and Mdm2 as well as inhibition of Mdm2 activity (Brooks and Gu, 2003; Moll and Petrenko, 2003). The p53 protein can be phosphorylated at many different sites including serine 6, 9, 15, 20, 37, 46, and 392 and most of these phosphorylations interfere with the binding interaction between p53 and Mdm2 (Meek, 1998). The most commonly phosphorylated sites are serine 15, 20, 37, and 46 (Lavin and

Gueven, 2006). Phosphorylation of p53 at many of these key serines especially serine 15 and 20 leads to the dissociation of Mdm2 from p53 which exposes the p53 transactivation domain (Lakin and Jackson, 1999; El-Deiry, 1998).

Acetylation of p53 at specific lysine residues including lys 373 and lys 382 also leads to p53 stabilization (Lakin and Jackson, 1999). It is known that the p53 protein is ubiquitinated and acetylated on similar sites and this suggests that acetylation of p53 may outcompete ubiquitination of p53 under stress conditions (Brooks and Gu, 2003). Acetylation of p53 also leads to its transcriptional activation.

Another mechanism that exists to stabilize p53 does not involve post-translational modification of p53. Instead, a protein called p19ARF is activated and expressed under stress and blocks the interaction between p53 and Mdm2 by binding directly to Mdm2 at a site different from that where Mdm2 normally binds to p53 (Brooks and Gu, 2003). Due to this p19ARF-Mdm2 interaction, p53 breakdown is prevented. The protein p19ARF carries out its action by sequestering Mdm2 into the nucleolus which stops p53 from being exported from the nucleus and being degraded. The action of p19ARF prevents Mdm2 from ubiquitinating p53 by hindering the ubiquitin ligase activity of Mdm2 (Ashcroft and Vousden, 1999; Sherr, 2006).

Stabilization of p53 is the key first step in the p53 pathway in response to various stresses, but p53 must also be transcriptionally activated in order to turn on its downstream genes and effect a proper response. Activation of p53 occurs by various

phosphorylation and acetylation events. There are two main mechanisms that are responsible for p53 activation, one at the N-terminus and one at the C-terminus (El-Deiry, 1998). Phosphorylation of p53 leads to elevated p53 levels and increased transcriptional activity. Phosphorylation of p53 at the N-terminal at multiple serine sites leads to p53 stabilization. DNA binding activity is then activated by the phosphorylation and acetylation cascade of p53 at the C-terminus (Appella and Anderson, 2001; El-Deiry, 1998; Colman *et al.*, 2000).

Acetylation of lysine residues at the carboxyl terminus, in particular at lysine 373 and 382, has been found to activate p53 sequence-specific DNA binding by increasing the affinity of p53 for DNA (Brooks and Gu, 2003). In addition to a higher amount of DNA binding, acetylation also positively affects the interactions between p53 and its transcriptional co-activators (eg. CBP/p300) through attraction of these to promoter regions and subsequent target gene activation (Brooks and Gu, 2003). Phosphorylation of p53 at serine 15 leads to increased binding of p53 to p300 (Appella and Anderson, 2001).

p53 activation can lead to cell cycle arrest at the G1/S and G2/M checkpoints by turning on genes such as the cyclin dependent kinase inhibitor p21 as well as growth arrest and DNA damage alpha (GADD45α) and 14-3-3σ (Shu *et al.*, 2007). The cyclin dependent kinase inhibitor (CKI) p21 is part of the Cip/Kip family of CKIs (Dotto, 2000). CKIs regulate the cyclin-cyclin dependent kinases (CDKs) that in turn regulate the cell cycle by inhibiting their kinase activity (El-Deiry, 1998). Cyclin-CDK complexes are important for cell cycle progression as they phosphorylate the retinoblastoma (Rb)

protein and allow it to be released from E2F transcription factors. E2F can then transcribe S phase genes that allow cells to pass from G1 to S phase (Ju *et al.*, 2006). The p21 protein interacts with two of these complexes, cyclin D1/CDK 4,6 and cyclin E/Cdk2. These interactions lead to a build up of hypophosphorylated Rb which is able to tightly bind E2F and prevent it from transcribing the genes necessary to make the transition into S phase. The p21 protein can also bind to PCNA, a supporting factor of DNA polymerase δ that is necessary for DNA repair, and halt DNA replication thereby stopping the cell cycle at G1/S, S, and G2/M (Ju *et al.*, 2006). p21 has also been reported to act at the G2/M checkpoint. Levels of p21 increase again during G2 phase after going down in S phase (Taylor and Stark, 2001). The p21 protein can be posttranslationally modified via phosphorylation on threonine 145 and serine 146. Phosphorylation at these sites is responsible for decreased binding of p21 to PCNA. Phosphorylation at both sites also plays a role in the stability of p21; both increased and decreased p21 stability have been reported (Li *et al.*, 2002; Child and Mann, 2006).

Another target gene of p53 during cell cycle arrest is GADD45α which encodes a 165 amino acid protein with a molecular weight of 18 kDa (Zhan, 2005). It is part of the GADD45 gene family which consists of GADD45α, GADD45ß, and GADD45γ (Lierbermann and Hoffman, 2007). GADD45α acts on the G2/M checkpoint in the cell cycle, specifically on the cdc2/cyclin B complex (Jin *et al.*, 2003). Cdc2 is the cyclin dependent kinase needed to make the transition into mitosis and it must be bound to cyclin B1 in order to carry out its function (Taylor and Stark, 2001). Under stress conditions, GADD45α binds to cdc2 which causes the removal of cyclin B1 from the

cdc2/cyclinB1 complex. Cyclin B1 is then exported to the cytoplasm where it is degraded (Zhan, 2005). Cdc2 kinase activity is inhibited and cells are arrested at the G2/M checkpoint and cannot proceed into the mitotic phase of the cell cycle.

Another target of p53 is the gene for the 14-3-3σ protein, one of the 7 isoforms of the 14-3-3 family. Among these, the sigma family member has three amino acids that make it unique (Lee and Lozano, 2006). For cdc2 to bring about mitosis, it must be transported into the nucleus through a process that involves binding to cyclin B1 (Taylor and Stark, 2001). Under stress conditions, 14-3-3σ acts by binding to the cdc2/cyclin B1 complex and sequestering it in the cytoplasm, leading to G2 arrest (Hermeking and Benzinger, 2006). Another function of 14-3-3σ is as a positive regulator of p53 stability and as an enhancer of p53 transcriptional activity (Taylor and Stark, 2001; Lee and Lozano, 2006).

The present chapter focuses on the response of the p53 transcription factor during natural freezing in the wood frog, *Rana sylvatica*, and its role in arresting the cell cycle when frogs transition into the frozen state.

Figure 3.1. The p53 signaling pathway leading to cell cycle arrest. Under normal conditions, p53 is held inactive by Mdm2 which transports it into the cytoplasm where it is ubiquitinated and degraded. Under stress conditions, p53 is posttranslationally modified and rendered stable and transcriptionally active. The interaction between p53 and Mdm2 is inhibited. The amount of p53 in the nucleus can then increase dramatically and p53 is able to transcribe a number of target genes including p21, Gadd45a, and 14-3-3σ. These proteins are responsible for cell cycle arrest at various points in the cell cycle.

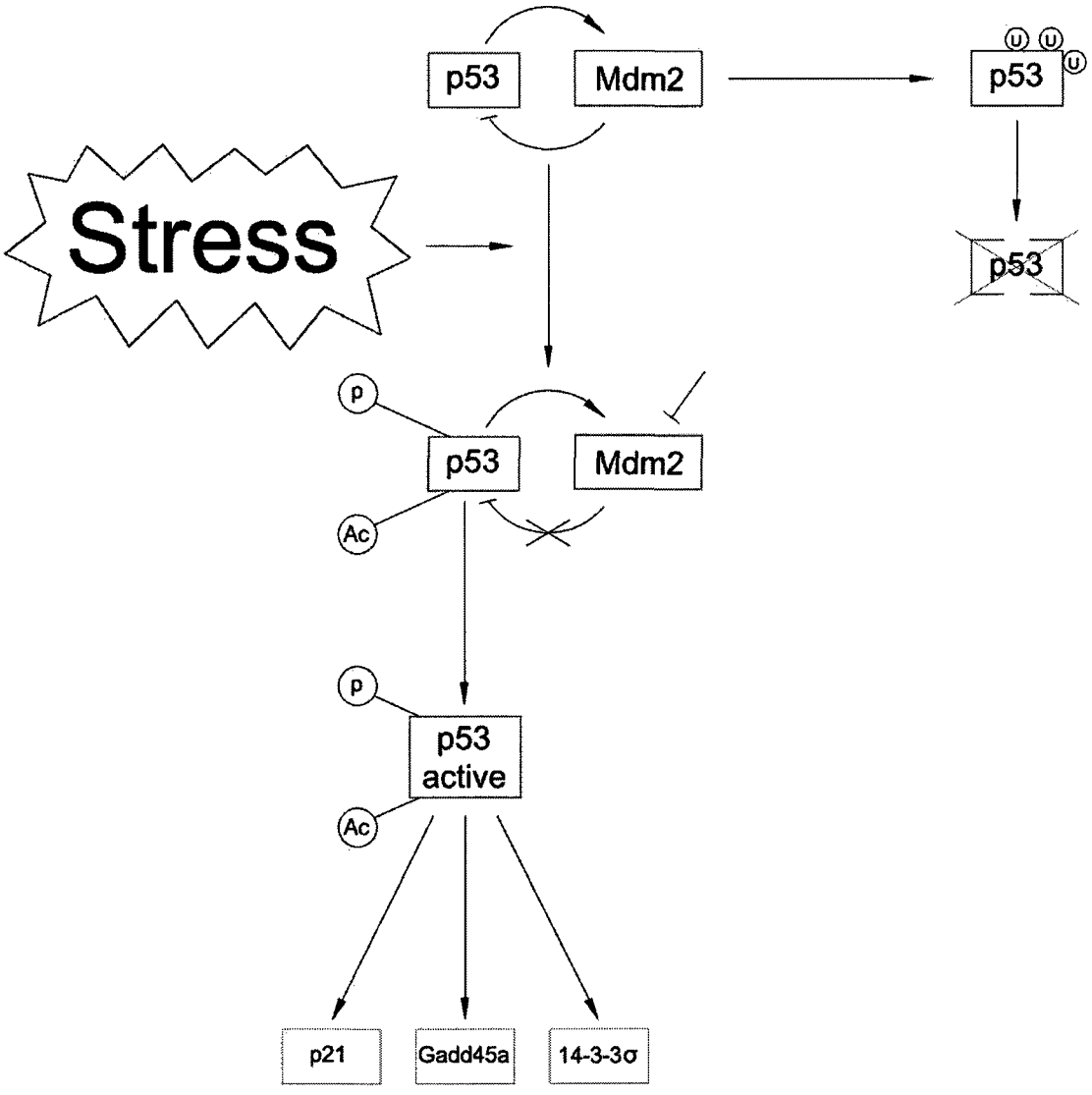
p53
Mdm2
p53
Stress
p53
p
p53
Mdm2
Ac
p
p53
active
Ac
p21
Gadd45a
14-3-3σ
Growth / cell
cycle arrest

Results

Effect of freezing on p53

Membranes were probed with antibodies that detected total p53 protein as well as antibodies that detected specific phosphorylated or acetylated residues on the protein. All antibodies crossreacted with single bright bands at about 53 kDa, the expected molecular mass of the vertebrate p53 protein. Figure 3.2 shows p53 levels in liver and skeletal muscle of wood frogs comparing controls (5°C acclimated) with animals given 4 hours or 24 hours of freezing exposure at -2.5°C. In wood frog liver, levels of total p53 protein increased significantly by 2.1 fold after 4 hours freezing exposure and remained high at 1.7 fold above controls after 24 hours of freezing (Figure 3.2A). In skeletal muscle, total p53 levels were also elevated significantly in frozen frogs by 1.6 fold and 1.5 fold after 4 and 24 hours, respectively (Figure 3.2B).

The p53 protein can be phosphorylated on multiple serine residues and antibodies are available that target different phosphorylated peptides on the protein. The effect of freezing on the relative amount of phosphorylation at seven different sites was assessed and, in general, the amount of phosphorylation increased at all sites in response to freezing in both liver and muscle. For liver, significant increases in p53 phosphorylation after 4 hours of freezing were as follows: serine 6 (1.8 fold), serine 9 (1.7 fold), serine 15 (1.9 fold), serine 20 (1.5 fold), serine 37 (1.7 fold), serine 46 (1.8 fold), and serine 392 (1.6 fold). After 24 hours of freezing the level of phosphorylation remained significantly elevated at six loci as compared with controls: serine 6 (1.5 fold), serine 9 (1.5 fold), serine 15 (1.2 fold), serine 20 (1.3 fold), serine 37 (1.7 fold), and serine 46 (1.7 fold).

However, the amount of phospho-Ser 15 was strongly reduced as compared with the peak value at 4 hours and phospho-Ser 392 content was lowered to a level that was not significantly different from the control.

The relative amount of phosphorylation on different sites of wood frog skeletal muscle p53 also increased significantly after 4 hours of freezing: serine 6 (1.7 fold), serine 9 (1.5 fold), serine 15 (1.6 fold), serine 20 (1.6 fold), serine 37 (1.4 fold), serine 46 (1.6 fold), and serine 392 (1.8 fold). After 24 hours of freezing, phosphorylation of the protein remained high, with significantly increased amounts relative to controls of: serine 6 (1.8 fold), serine 9 (1.4 fold), serine 15 (1.8 fold), serine 20 (1.9 fold), serine 37 (1.5 fold), serine 46 (1.6 fold), and serine 392 (1.4 fold).

The p53 protein is also modified by acetylation on selected lysine residues. In liver, the relative amounts of acetylation on lysine 373 and lysine 382 both increased significantly after 4 hours of freezing by 2.4 and 1.5 fold, respectively (Figure 3.2A). However, after 24 hours of freezing, acetylation levels were reduced again to levels that were not significantly different from controls. In skeletal muscle a similar pattern was seen for lysine 373 acetylation; levels increased significantly by 1.7 fold after 4 hours of freezing but were reduced again to control levels after 24 hours frozen (Figure 3.2B). By contrast, acetyl-p53 lysine 382 content in muscle was significantly increased over control values after both 4 and 24 hours of freezing by 1.6 fold and 1.8 fold, respectively.

Effect of freezing on Mdm-2 and p19ARF proteins

Mdm-2 is a protein that binds to and blocks the N-terminal transactivation domain of p53 and thereby represses p53 transcriptional activity. p19ARF is a protein that binds directly to Mdm-2 and thereby prevents Mdm-2 binding to p53; therefore, p19ARF provides a phosphorylation-independent stabilization mechanism for p53. The anti-Mdm-2 rabbit polyclonal antibody crossreacted with two bands in wood frog tissue extracts, one at ~90 kDa which represents the full size protein and another at ~60 kDa which represents the known cleavage product. The anti-p19ARF rabbit polyclonal antibody yielded one band at ~19kDa.

Figure 3.3A shows that protein levels of Mdm-2 decreased significantly after both 4 hours of freezing (to 38% of control values) and 24 hours of freezing (40% of control) in wood frog liver. Mdm-2 levels in skeletal muscle also decreased significantly during freezing, falling to 57% of control values by 4 hours of freezing and to 40% of the control after 24 hours of freezing.

Figure 3.3B shows that p19ARF protein levels remained unchanged in the liver after 4 hours of freezing then rose significantly by 1.7 fold after 24 hours of freezing. There were no significant changes in p19ARF in wood frog skeletal muscle after 4 hours or 24 hours of freezing. Total p19ARF levels may be less important to p53 regulation than the amount of p19ARF in the nucleus. Nuclear extracts were prepared from wood frog tissues and Figure 3.3C shows the relative amounts of p19ARF in the nuclear fraction alone. There was no significant change in the nuclear distribution of p19ARF in

wood frog skeletal muscle in response to freezing. However, nuclear levels of p19ARF increased significantly in wood frog liver, rising by 1.7 fold after 4 hours and further increasing to 2.1 fold greater than control values after 24 hours freezing.

Protein levels of p21, phosphorylated p21, 14-3-3σ, and GADD45α at 4 hours and 24 hours freezing

Protein levels of three genes that are regulated by p53 were assessed to determine if they were up- or down-regulated during freezing stress. The antibodies used for all three proteins showed good cross-reaction with the frog proteins in both liver and muscle with bands detected at the expected molecular masses of ~21 kDa for p21, 30 kDa for 14-3-3σ, and 18 kDa for GADD45α.

Freezing exposure had a strong effect on p21 total protein levels in wood frog liver (Figure 3.4A). After 4 hours of freezing, p21 protein levels had increased significantly by 2.3 fold and remained high at 2.6 fold above control values after 24 h freezing. In skeletal muscle p21 content was 2.0 fold higher that control values after 4 h freezing but levels were reduced again after 24 h to a value that was not significantly different from controls. The p21 protein can be phosphorylated on serine 146 which leads to changes in stability. Hence, the relative phosphorylation level of the protein is a good indicator of p21 activity. Figure 3.4B shows that the relative amount of phosphorylated p21 Ser 146 increased significantly after 4 hours of freezing in both liver (1.8 fold) and skeletal muscle (1.3 fold). Phosphoprotein content increased even more in liver after 24

hours freezing (to 2.4 fold above control) but decreased significantly in skeletal muscle falling to 70% of the control value.

Protein levels of 14-3-3σ increased significantly after 4 hours of freezing in both wood frog liver (1.6 fold) and skeletal muscle (1.5 fold) (Figure 3.5A). Levels remained high in both tissues after 24 hours of freezing, being 1.3 fold higher than control levels in both tissues.

After 4 hours of freezing, protein levels of GADD45α increased markedly in liver by 2.8 fold and also rose 1.5 fold in skeletal muscle (Figure 3.5B). After 24 hours of freezing, muscle levels were about the same (1.7 fold above control) but liver levels were reduced from the 4 hour value although still significantly higher (1.4 fold) than controls.

Movement of p53 into the nucleus

Transcription factors carry out their actions in the nucleus. Therefore, it is of interest to see how much of the p53 transcription factor is in the nucleus under freezing stress. Nuclear distributions of p53, phosphorylated p53, and acetylated p53 were analyzed in wood frog liver and muscle by immunoblotting. Figure 3.6 analyzes this.

Figure 3.6A shows that total p53 protein in the nucleus increased significantly in wood frog liver after 4 hours of freezing (1.3 fold over control values) and remained high after 24 hours of freezing (1.4 fold). Similarly, in wood frog skeletal muscle, nuclear

levels of p53 increased significantly by 1.5 fold after 4 hours of freezing and rose to 1.7 fold higher than controls after 24 hours of freezing (Figure 3.6B).

In general, the nuclear levels of the various phosphorylated p53 forms also rose during freezing. In wood frog liver after 4 hours of freezing, significant increases occurred in the nuclear content of all of the phosphorylated forms of p53. As compared with controls these were: serine 6 (1.6 fold), serine 9 (1.6 fold), serine 15 (1.3 fold), serine 20 (1.4 fold), serine 37 (1.2 fold), serine 46 (1.4 fold), and serine 392 (1.15 fold) (Figure 3.6A). After 24 hours of freezing, the amounts of some forms remained elevated as compared with controls: serine 6 (1.5 fold), serine 9 (1.3 fold), serine 20 (1.4 fold), and serine 37 (1.3 fold). However, the content of other phospho-forms (Ser 15, Ser 46, Ser 392) decreased to levels that were not significantly different from control values. In wood frog skeletal muscle, the amounts of all phosphorylated forms of p53 also increased significantly in the nucleus after 4 hours of freezing. As compared with controls, the increases were: serine 6 (2.5 fold), serine 9 (1.4 fold), serine 15 (1.4 fold), serine 20 (1.6 fold), serine 37 (2.4 fold), serine 46 (1.9 fold), and serine 392 (2.2 fold) (Figure 3.6B). After 24 hours of freezing, the nuclear amounts of several of these were largely unchanged, showing elevations compared with controls of: serine 9 (1.5 fold), serine 15 (1.4 fold), serine 20 (1.5 fold), and serine 46 (1.6 fold). However, the relative nuclear amounts of two forms were reduced as compared with 4 hours freezing although still elevated as compared with controls: serine 6 (1.7 fold) and serine 392 (1.5 fold). Furthermore, the content of serine 37 was reduced again to control levels.

Significant increases in the amount of acetylated p53 in the nucleus also occurred in skeletal muscle. The relative amount of acetylated lysine 373 was significantly elevated after 4 hours and 24 hours of freezing (2.1 and 1.6 fold respectively) (Figure 3.6B). The content of acetylated lysine 382 in nuclear extracts of muscle was also significantly increased after 4 hours of freezing by 1.4 fold but returned to control levels in 24 hour frozen frogs. However, there were no significant changes in the amount of acetylated p53 in nuclear extracts of liver at either freezing time.

Transcript levels of 14-3-3σ and GADD45α

To determine if the increase in protein levels of 14-3-3σ and GADD45α during freezing was actually due to transcriptional upregulation of the genes encoding these proteins, mRNA transcript levels of these two genes were measured using RT PCR in wood frog skeletal muscle and liver. PCR products derived from the primer sets used for each gene were sequenced and then a sequence comparison in BLASTN confirmed that the products encoded segments of 14-3-3σ or GADD45α. Figure 3.7A shows an example of the amplification of 14-3-3σ from a dilution series of cDNA prepared from liver and muscle. Alpha-tubulin was similarly amplified from the same samples and used to normalize 14-3-3σ transcript levels. The 10^{-1} dilution was chosen for quantification. Figure 3.7B shows that 14-3-3σ transcript levels in liver were significantly increased by 2.09 fold in 24 hour frozen frogs as compared with control. However, there was no change in transcript levels in skeletal muscle.

Figure 3.8 shows data for GADD45α mRNA levels. Again, as for 14-3-3σ, mRNA transcript levels of GADD45α were elevated significantly by 2.64 fold in liver of 24 hour frozen wood frogs (Figure 3.8B). However, GADD45α transcripts in skeletal muscle did not change between control and frozen.

Analysis of 14-3-3σ and GADD45α sequences

The amplified product from wood frog skeletal muscle obtained using 14-3-3σ primers was sequenced and compared to the Genbank database found on the National Center for Biotechnology Information website. The nucleotide and deduced amino acid sequences can be seen in Figure 3.9. The partial wood frog sequence was composed of 488 nucleotides and the deduced protein sequence contained 162 amino acids. A comparison of the wood frog 14-3-3σ nucleotide sequence to those of African clawed frog, chicken, mouse, and human 14-3-3σ sequences can be seen in part A of Appendix B. The homology tree shows that wood frog 14-3-3σ nucleotide sequence shared 69% identity with the African clawed frog sequence and 62% identity with the chicken, mouse, and human sequences (Appendix B, part B).

Appendix B also shows a comparison of the 14-3-3σ amino acid sequences of the five vertebrate species. The 162 amino acid residues of the 14-3-3σ protein retrieved for the wood frog represented 63-65 % of the full length sequence for the African clawed frog, human and mouse proteins (247-256 amino acids). The wood frog amino acid sequence showed high identity with the other vertebrate sequences. The wood frog amino acid sequence shared 79% identity with the African clawed frog amino acid sequence,

and 71% identity with the chicken, human, and mouse amino acid sequences (Appendix B, part D).

The amplified product from wood frog skeletal muscle that was obtained using GADD45α primers was sequenced and compared to the Genbank database found on the National Center for Biotechnology Information website. The nucleotide and deduced amino acid sequences are shown in (Figure 3.10). The partial wood frog sequence contained 264 nucleotides and the deduced protein sequence was 88 amino acids. A comparison of the wood frog GADD45α nucleotide sequence to the African clawed frog, western clawed frog, chicken, human and zebrafish GADD45α sequences is shown in Appendix C. The homology tree shows that wood frog GADD45α shared 84% identity with the African clawed frog sequence, 86% identity with the western clawed frog sequence, 60% identity with the chicken and human sequences, and 56% identity with the zebrafish sequence (Appendix C, part B).

Appendix C also shows a comparison of the amino acid sequences of the six vertebrate species. The 88 amino acid residues of the GADD45α protein retrieved for the wood frog represented 53-56 % of the full length sequences of the other species (156-165 amino acids). Again the wood frog sequence showed very high identity with the other vertebrate sequences. The wood frog amino acid sequence shared 89% identity with the African clawed frog and western clawed frog amino acid sequences, and 72% identity with the chicken, human, and zebrafish amino acid sequences (Appendix C, part D).

Figure 3.2

Western blot analysis demonstrating the effects of short and long term freezing on total p53 protein levels as well as the content of phosphorylated p53 and acetylated p53 in wood frog skeletal muscle and liver.

A) Levels of total p53 protein, phospho-p53, and acetyl-p53 in wood frog liver under three conditions: controls (5°C acclimated), 4 hours or 24 hours freezing exposure at -2.5°C. Representative western blots show total p53 content and p53 phosphorylated at multiple serine residues or acetylated at multiple lysine residues. Peptide antibodies detected phosphorylation at specific sites: Ser 6, Ser 9, Ser 15, Ser 20, Ser 37, Ser 46, or Ser 392. Other peptide antibodies detected acetylated residues at Lys 373 or Lys 382. An equal amount of protein (20 μg) was loaded into each lane. Bar graphs show normalized mean values (± SEM, n=4-5 independent determinations).

* - Significantly different from the corresponding control value as determined by the Student's t-test, $P<0.05$.

B) Levels of total p53 protein, phospho-p53, and acetyl-p53 in wood frog skeletal muscle under three conditions: controls (5°C acclimated), 4 hours or 24 hours freezing exposure at -2.5°C. Other information as in part A.

A)

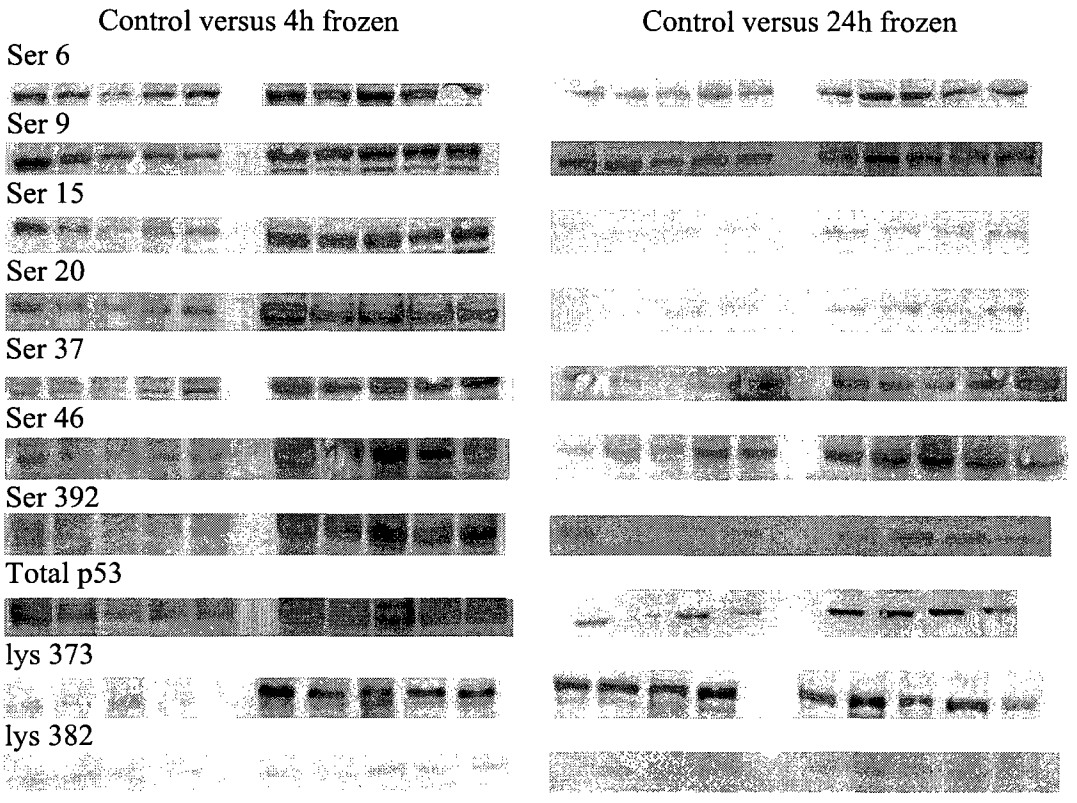
Control versus 4h frozen
Control versus 24h frozen
Ser 6
Ser 9
Ser 15
Ser 20
Ser 37
Ser 46
Ser 392
Total p53
lys 373
lys 382

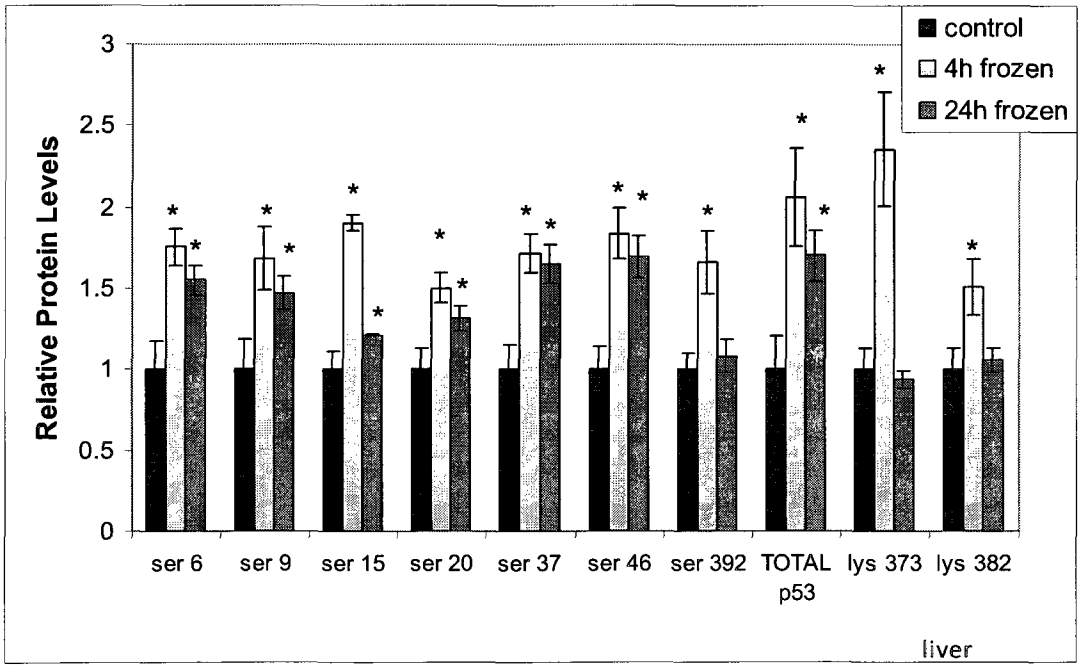
control
4h frozen
24h frozen
Relative Protein Levels
3
2.5
2
1.5
1
0.5
0
ser 6
ser 9
ser 15
ser 20
ser 37
ser 46
ser 392
TOTAL p53
lys 373
lys 382
liver

B)

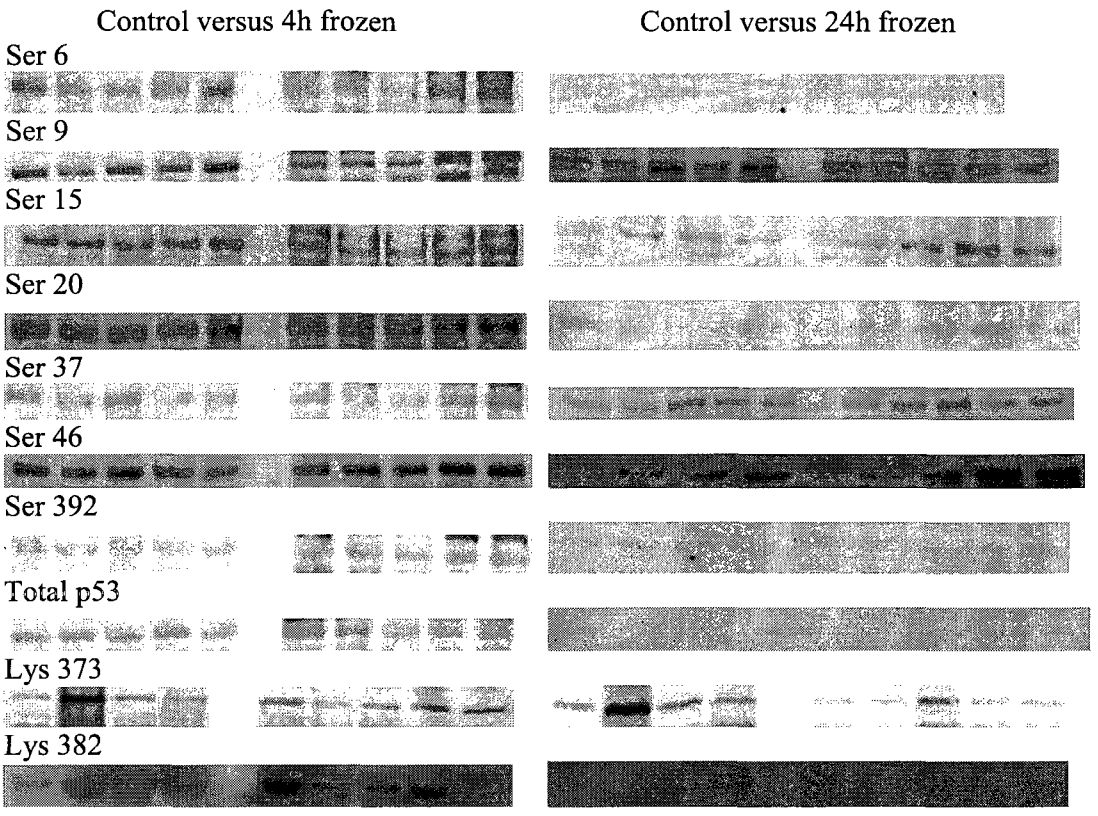
Control versus 4h frozen
Control versus 24h frozen
Ser 6
Ser 9
Ser 15
Ser 20
Ser 37
Ser 46
Ser 392
Total p53
Lys 373
Lys 382

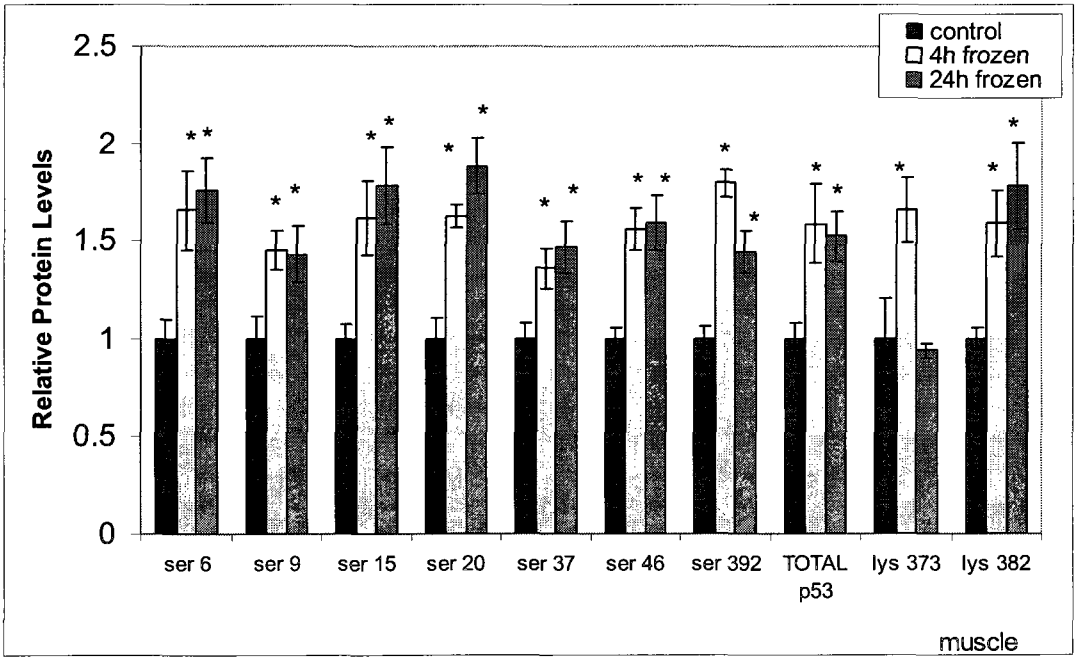
control
4h frozen
24h frozen
Relative Protein Levels
2.5
2
1.5
1
0.5
0
ser 6
ser 9
ser 15
ser 20
ser 37
ser 46
ser 392
TOTAL p53
lys 373
lys 382
muscle

Figure 3.3

Western blot analysis demonstrating the effects of short term and long term freezing on the levels of Mdm-2 and p19ARF proteins in wood frog skeletal muscle and liver.

A) Mdm-2 protein levels in skeletal muscle and liver. Representative Western blots show Mdm-2 levels in control (5°C acclimated), 4 hour freezing (-2.5°C) and 24 hour freezing (-2.5°C) groups. Bar graphs show normalized mean values (± SEM, n=4-5 independent determinations) for Mdm2 levels.

* - Significantly different from the corresponding control value as determined by the Student's t-test, $P<0.05$.

B) p19ARF total protein levels in wood frog skeletal muscle and liver. Other information as in part A.

C) Nuclear content of p19ARF in wood frog skeletal muscle and liver. Other information as in part A.

A)

Control versus 4h frozen liver

Control versus 24h frozen liver

Control versus 4h frozen muscle

Control versus 24h frozen muscle

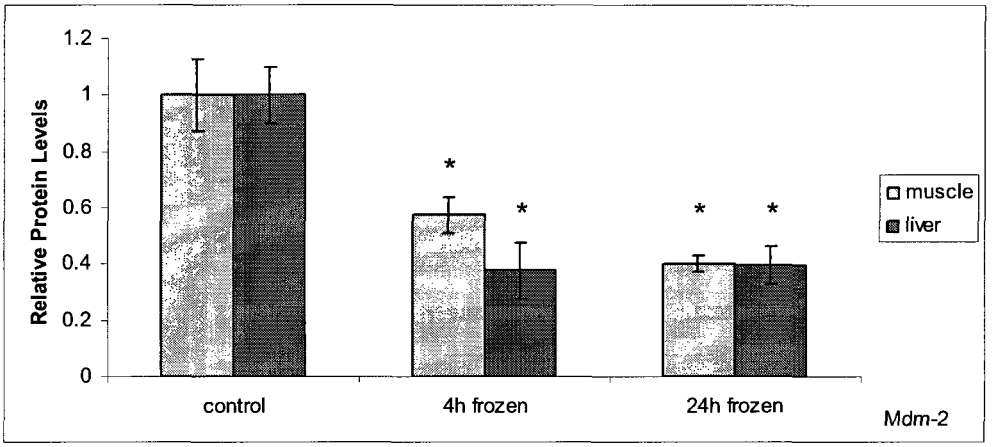

B)

Control versus 4h and 24h frozen liver

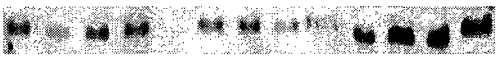

Control versus 4h and 24h frozen muscle

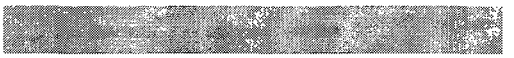

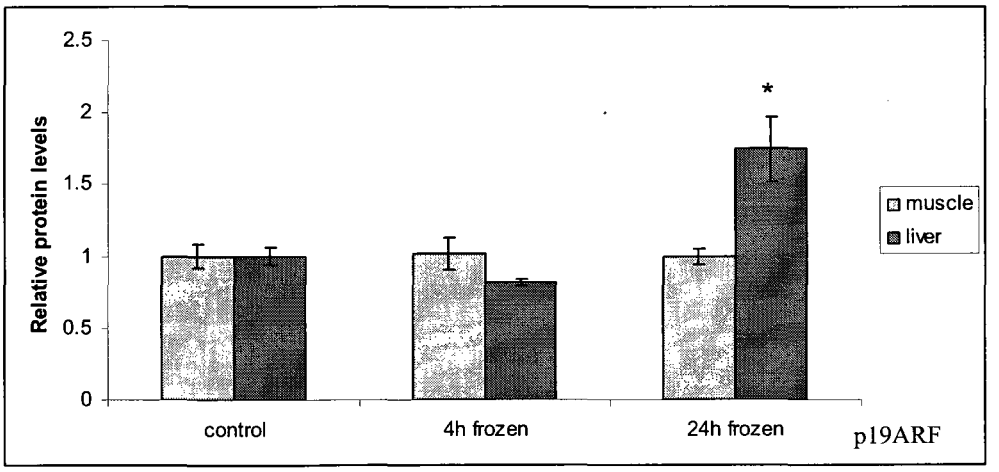

C)

Control versus 4h and 24h frozen liver

Control versus 4h and 24h frozen muscle

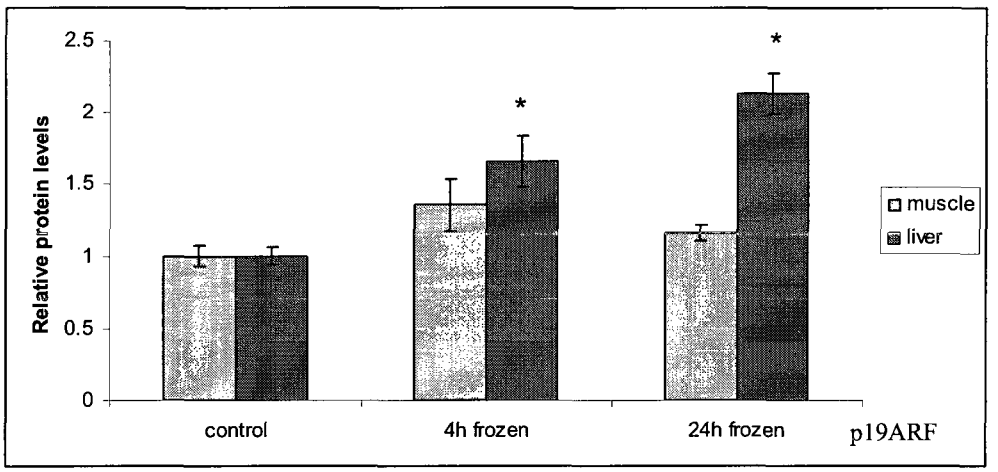

Figure 3.4

Western blot analysis demonstrating the effects of short term and long term freezing on the p21 protein and its phosphorylated form in wood frog skeletal muscle and liver

A) Total p21 protein levels in skeletal muscle and liver. Western blots show p21 levels in tissues from control (5°C), 4 hours freezing (-2.5°C) and 24 hours freezing (-2.5°C) conditions. Bar graphs depict normalized mean values (± SEM, n=4-5 independent determinations).

* - Significantly different from the corresponding control value as determined by the Student's t-test, $P<0.05$.

B) Relative amount of p21 phosphorylated on Ser146 in wood frog skeletal muscle and liver under the three experimental conditions. Other information as in part A.

A)

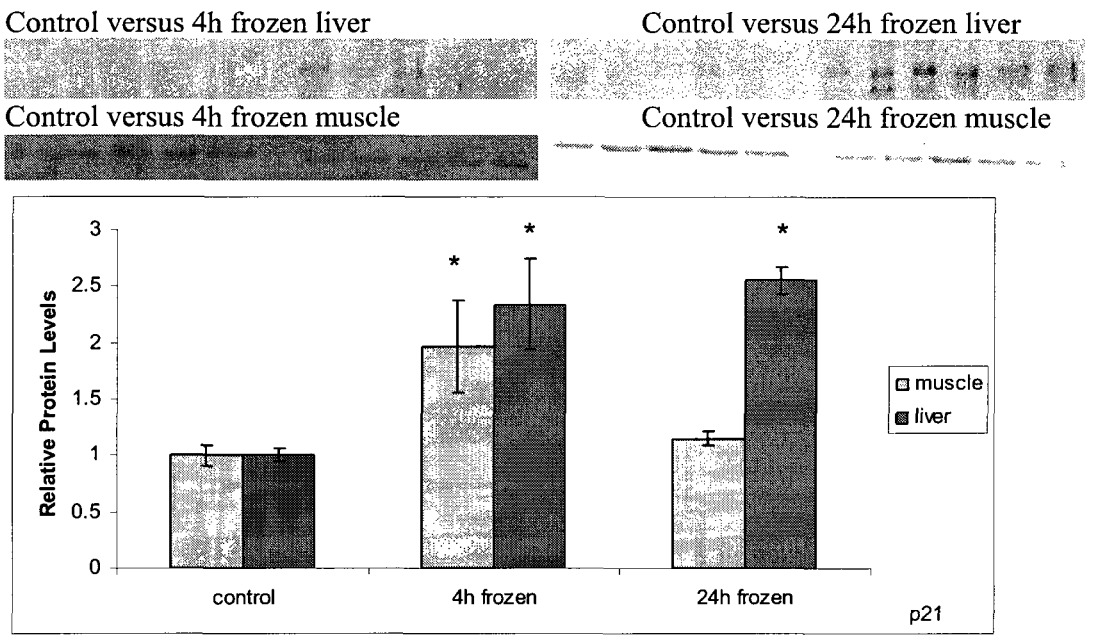
Control versus 4h frozen liver
Control versus 24h frozen liver
Control versus 4h frozen muscle
Control versus 24h frozen muscle
Relative Protein Levels
3
2.5
2
1.5
1
0.5
0
control
4h frozen
24h frozen
muscle
liver
p21

B)

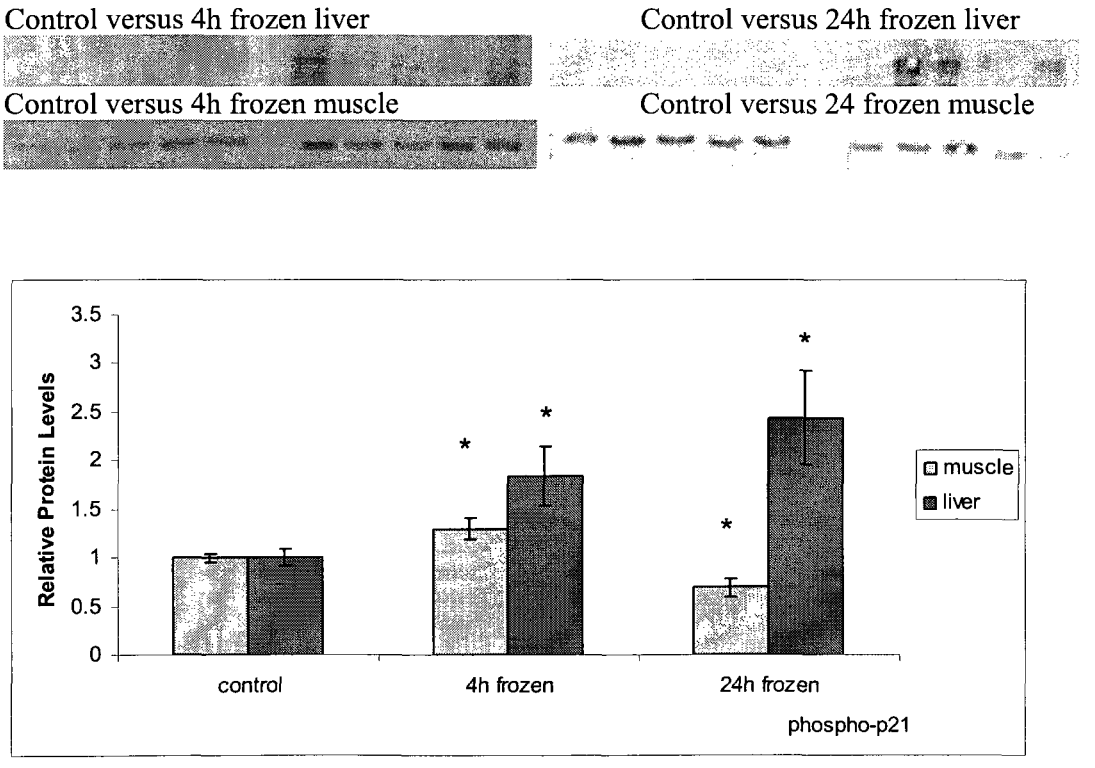
Control versus 4h frozen liver
Control versus 24h frozen liver
Control versus 4h frozen muscle
Control versus 24 frozen muscle
Relative Protein Levels
3.5
3
2.5
2
1.5
1
0.5
0
control
4h frozen
24h frozen
muscle
liver
phospho-p21

Figure 3.5

Western blot analysis demonstrating the effects of short term and long term freezing on the 14-3-3σ and GADD45α protein levels in wood frog skeletal muscle and liver.

A) 14-3-3σ protein levels in wood frog skeletal muscle and liver. Western blots show 14-3-3σ levels in wood frog skeletal muscle and liver for control (5°C), 4 hours freezing (-2.5°C) and 24 hours freezing (-2.5°C) conditions. Bar graphs depict normalized mean values (± SEM, n=4-5 independent determinations).

* - Significantly different from the corresponding control value as determined by the Student's t-test, $P<0.05$.

B) GADD45α protein levels in wood frog skeletal muscle and liver. Other information as in part A.

A)

Control versus 4h frozen liver

Control versus 24h frozen liver

Control versus 4h frozen muscle

Control versus 24h frozen muscle

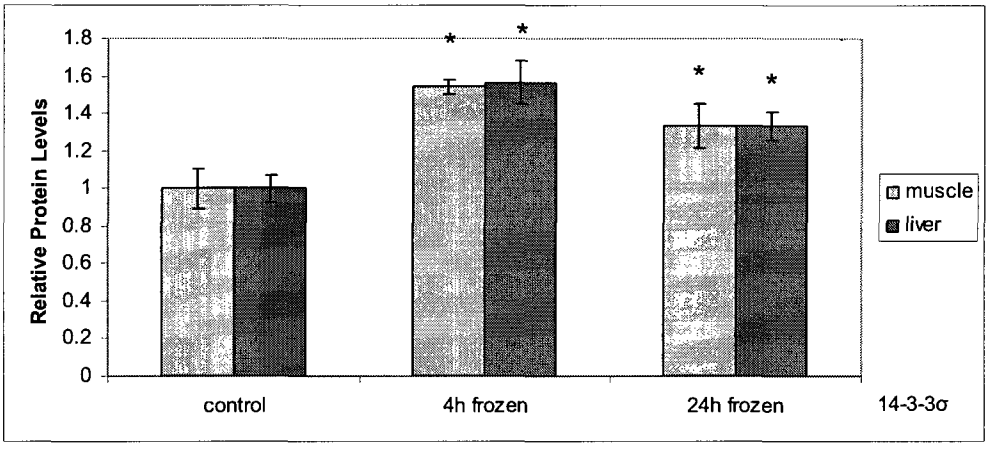

B)

Control versus 4h frozen liver

Control versus 24h frozen liver

Control versus 4h frozen muscle

Control versus 24h frozen muscle

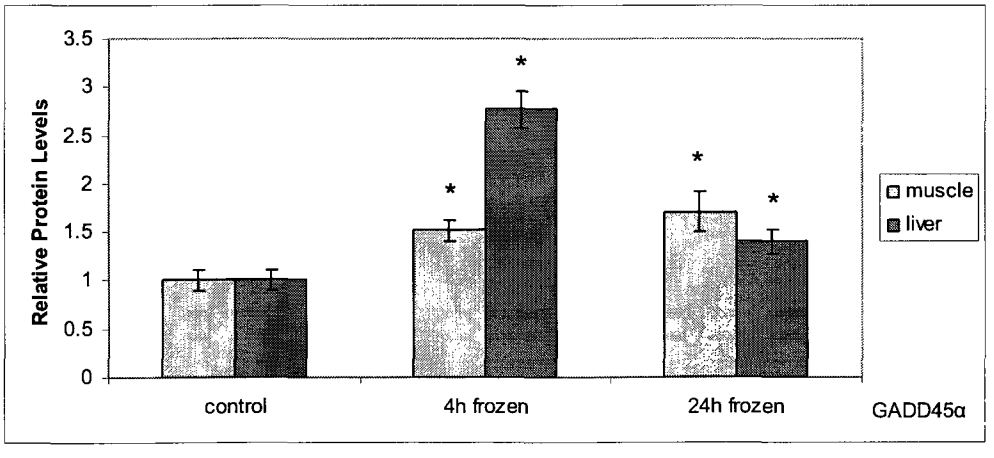

Figure 3.6

Western blot analysis of the nuclear distribution of the p53 protein as well as its phosphorylated and acetylated forms during freezing in wood frog skeletal muscle and liver.

A) Nuclear distributions of p53, phospho-p53, and acetyl-p53 proteins in wood frog liver. Representative western blots show nuclear distributions of total p53, phospho-p53 ser 6, phospho-p53 ser 9, phospho-p35 ser 15, phospho-p53 ser 20, phospho-p53 ser 37, phospho-p53 ser 46, phospho-p53 ser 392, acetyl-p53 lys 373, and acetyl-p53 lys 382 for control (5°C), 4 hours freezing (-2.5°C) and 24 hours freezing (-2.5°C) conditions. An equal amount of protein (20μg) was loaded into each lane. Histograms show normalized mean values (± SEM, n=4-5 independent determinations).

* - Significantly different from control value as determined by Student's t-test, $P<0.05$.

B) Nuclear distributions of p53, phospho-p53, and acetyl-p53 proteins in wood frog skeletal muscle. Other information as in part A.

A)

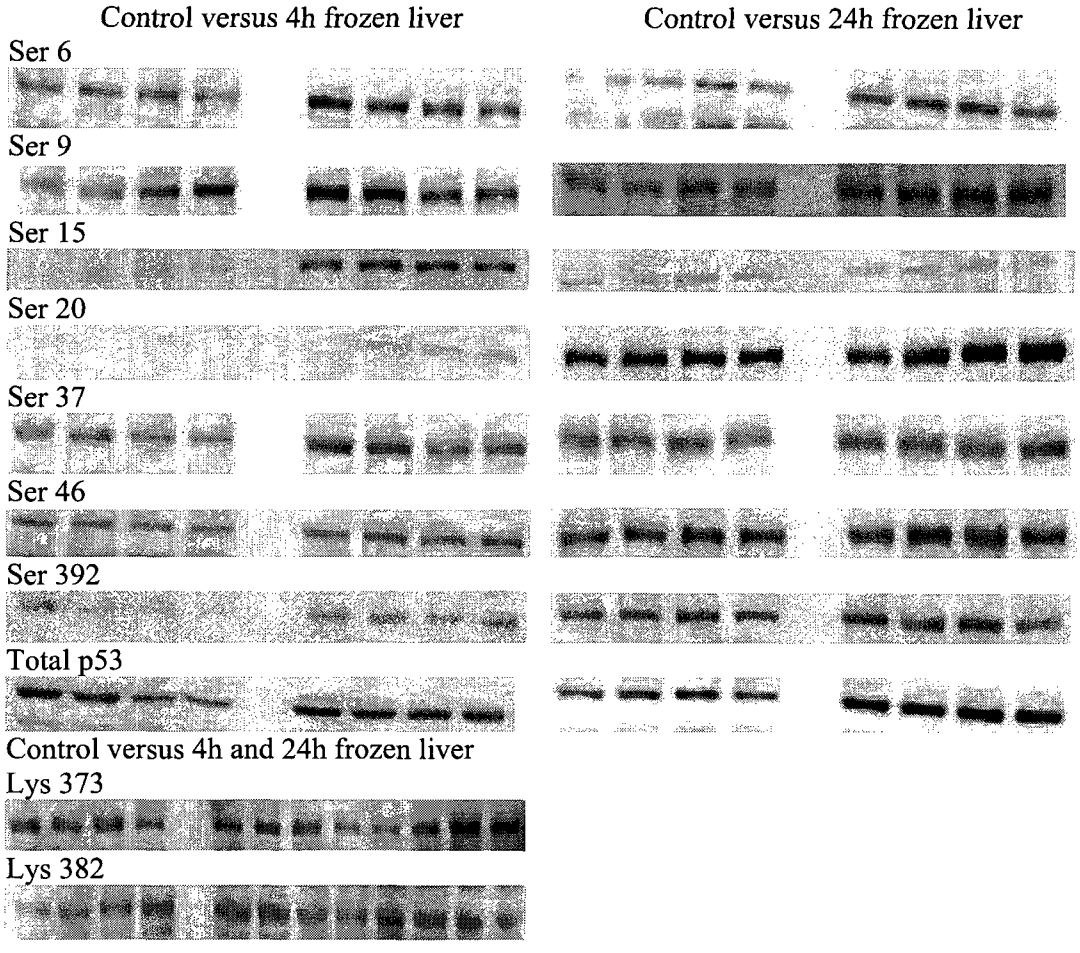
Control versus 4h frozen liver
Control versus 24h frozen liver
Ser 6
Ser 9
Ser 15
Ser 20
Ser 37
Ser 46
Ser 392
Total p53
Control versus 4h and 24h frozen liver
Lys 373
Lys 382

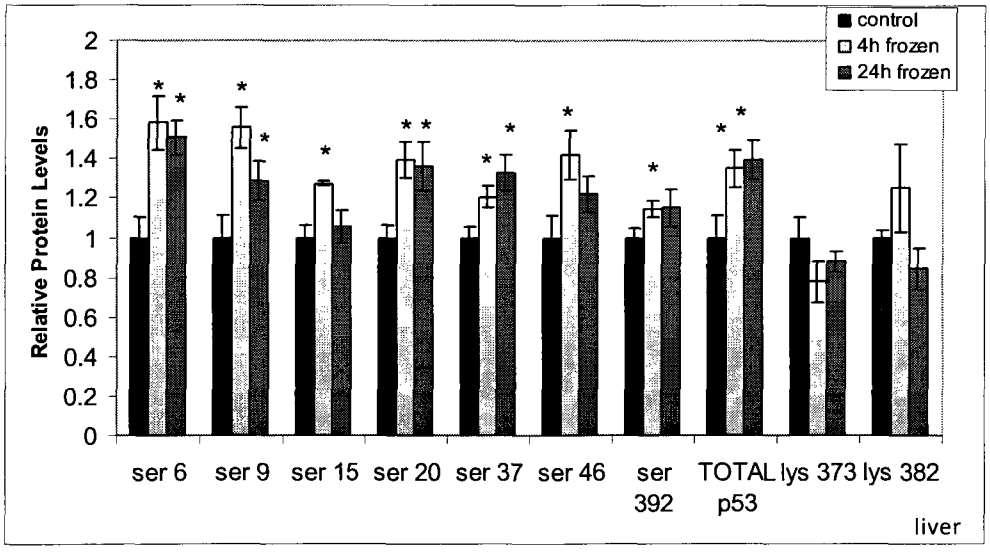
control
4h frozen
24h frozen
Relative Protein Levels
2
1.8
1.6
1.4
1.2
1
0.8
0.6
0.4
0.2
0
ser 6
ser 9
ser 15
ser 20
ser 37
ser 46
ser 392
TOTAL p53
lys 373
lys 382
liver

B)

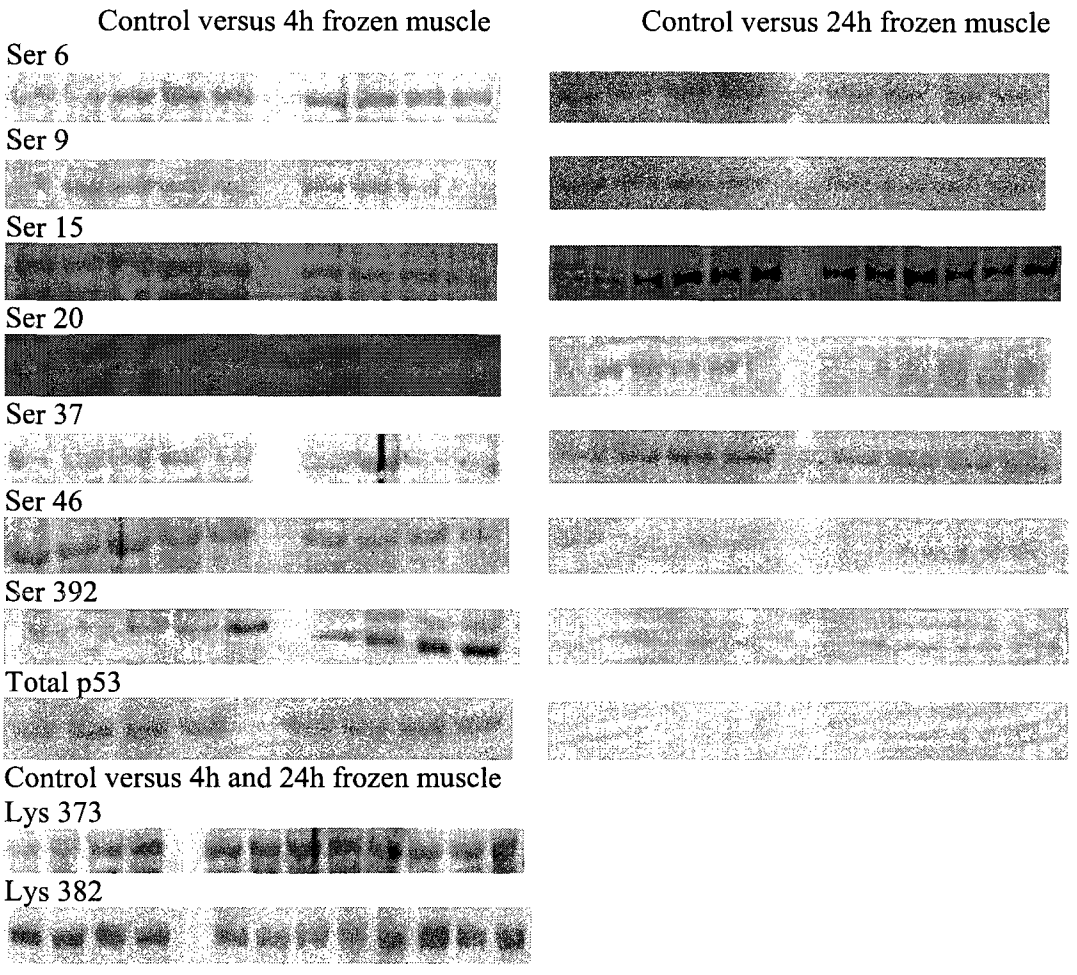
Control versus 4h frozen muscle
Control versus 24h frozen muscle
Ser 6
Ser 9
Ser 15
Ser 20
Ser 37
Ser 46
Ser 392
Total p53
Control versus 4h and 24h frozen muscle
Lys 373
Lys 382

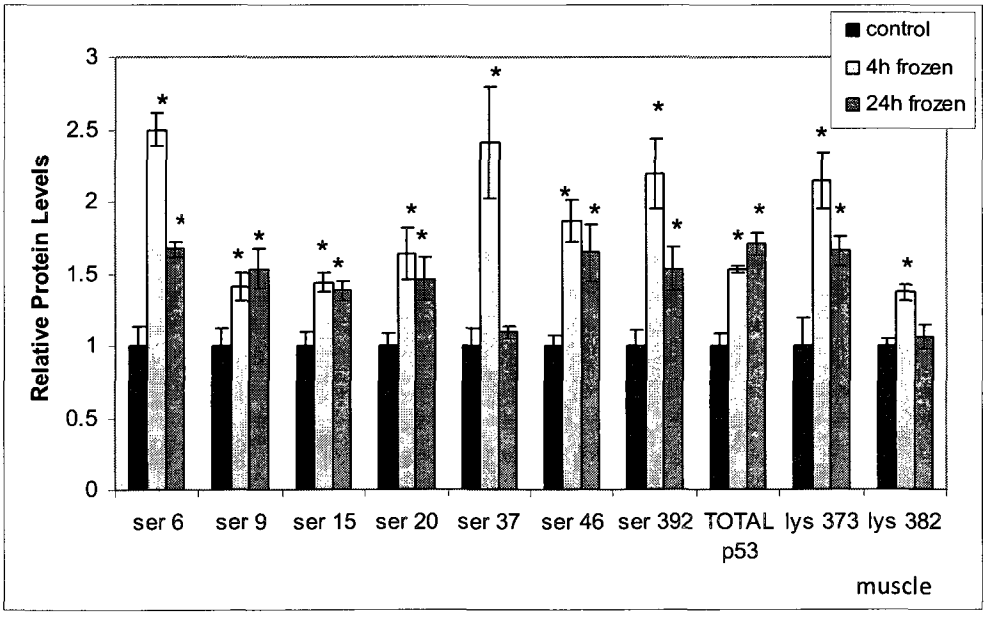
control
4h frozen
24h frozen
Relative Protein Levels
0
0.5
1
1.5
2
2.5
3
ser 6
ser 9
ser 15
ser 20
ser 37
ser 46
ser 392
TOTAL p53
lys 373
lys 382
muscle

Figure 3.7

Transcript levels of 14-3-3σ in wood frog muscle and liver.

A) Expression of 14-3-3σ and α-tubulin in a serial dilution of muscle and liver cDNA from control and 24 hour frozen samples. The figure shows a representative example. PCR product levels of 14-3-3σ were normalized against the corresponding α-tubulin levels for the same sample since previous studies had shown that α-tubulin product levels did not change between control and frozen state. The 10^{-1} dilution level was used for quantification.

B) Histogram showing relative 14-3-3σ transcript levels in muscle and liver from control and 24 hours frozen wood frogs as determined by RT-PCR. Data are normalized means ± SEM, at least n=4 independent determinations.

* - Significantly different from control value as determined by Student's t-test, $P<0.05$.

A)

14-3-3σ liver control versus frozen 10^{-1} dilution

14-3-3σ muscle control versus frozen 10^{-1} dilution

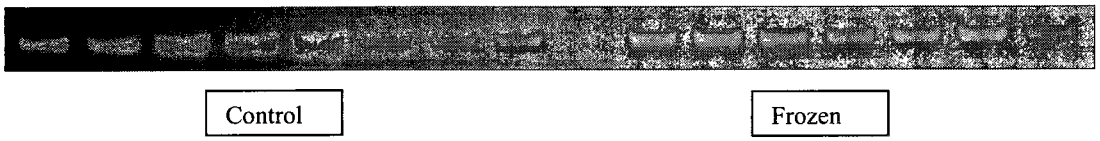

α-tubulin liver control versus frozen 10^{-1} dilution

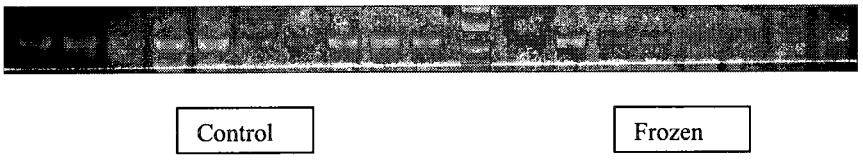

α-tubulin muscle control versus frozen 10^{-1} dilution

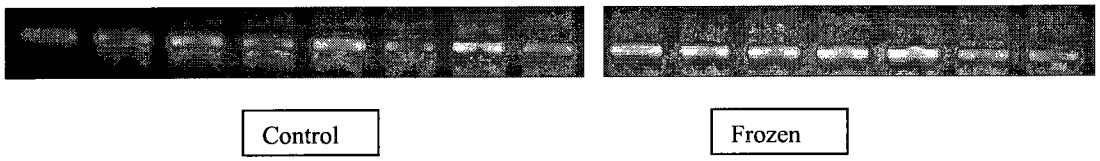

B)

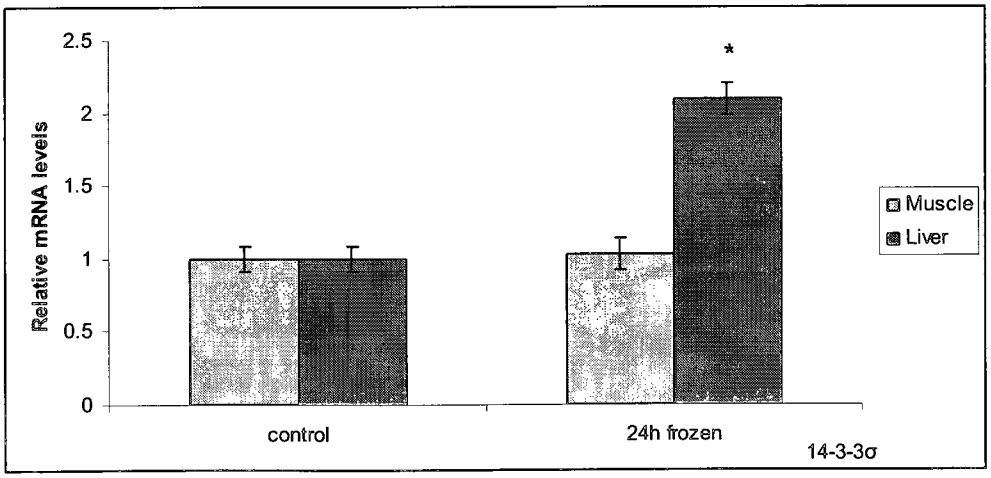

Figure 3.8

Transcript levels of GADD45α in wood frog muscle and liver

A) Expression of GADD45α and α-tubulin in a serial dilution of muscle and liver cDNA from control and 24 hour frozen samples. The figure shows a representative example. PCR product levels of GADD45α were normalized against the corresponding α-tubulin levels for the same sample since previous studies had shown that α-tubulin product levels did not change between control and frozen state. The 10^{-1} dilution level was used for quantification.

B) Histogram shows relative GADD45α transcript levels in muscle and liver of control and 24 hour frozen wood frogs as determined by RT-PCR. Data are normalized means ± SEM, at least n=4 independent determinations.

* - Significantly different from control value as determined by Student's t-test, $P<0.05$.

A)

GADD45α liver control versus frozen 10^{-1} dilution

GADD45α muscle control versus frozen 10^{-1} dilution

α-tubulin liver control versus frozen 10^{-1} dilution

α-tubulin muscle control versus frozen 10^{-1} dilution

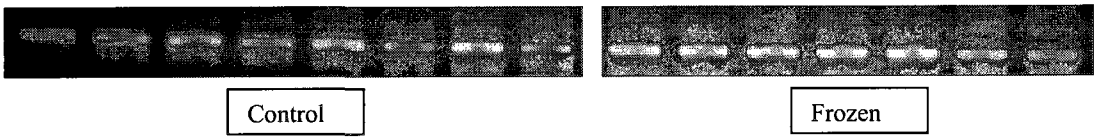

B)

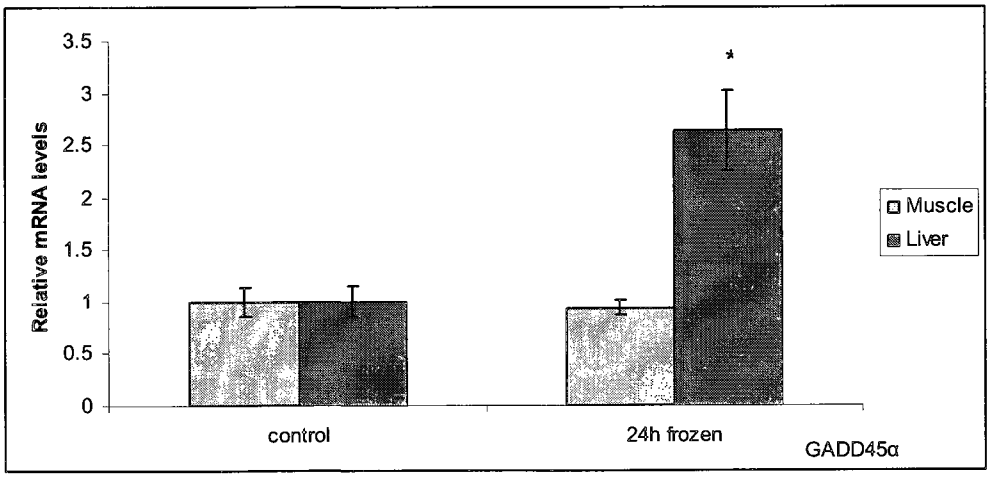

Figure 3.9

Partial mRNA sequence and corresponding amino acid sequence of wood frog skeletal muscle 14-3-3σ. A total of 448 nucleotide residues were retrieved and coded for 162 amino acids.

```
1          AGAAGGAACCTTCTTTCTGTTGCTTACAAGAATGTGGTTGGAGCAAGGAGGTCTTCTTGG
1           R  R  N  L  L  S  V  A  Y  K  N  V  V  G  A  R  R  S  S  W

61         AGGGTCATTTCCAGCATTGAGCAGAAGTCAGGTGAATCGGAAAAGAAGCTGCAATTGACT
21          R  V  I  S  S  I  E  Q  K  S  G  E  S  E  K  K  L  Q  L  T

121        AAAGAATACCGGGAGAAAATAGAGTGCGAGCTCAAGAGTGTTTGTGACACGGTTTTGGAT
41          K  E  Y  R  E  K  I  E  C  E  L  K  S  V  C  D  T  V  L  D

181        CTGCTTAAGGATTTCTTAATTCCTAAAGCCACGCAACCAGAGTGCAAAGTATTTTACCTG
61          L  L  K  D  F  L  I  P  K  A  T  Q  P  E  C  K  V  F  Y  L

241        AAGATGAAAGGGGACTATTACCGATACCTTTCAGAGGTGGCGAAGGATACTGAGAGAACT
81          K  M  K  G  D  Y  Y  R  Y  L  S  E  V  A  K  D  T  E  R  T

301        GAGACAATAGACCTCTCACAACAAGCTTATCAAGAAGCATTTGACATCAGCAAGGAGAAA
101         E  T  I  D  L  S  Q  Q  A  Y  Q  E  A  F  D  I  S  K  E  K

361        ATGCAGCCAACCCACCCCATCCGCTTGGGCTTAGCCCTAAATTTTTCCGTATTCTATTAT
121         M  Q  P  T  H  P  I  R  L  G  L  A  L  N  F  S  V  F  Y  Y

421        GAAATTCTTAATAGCCCAGAAAAGGCTTGTTCACTGGCAAAGACTGCATTTGACGAGGCC
141         E  I  L  N  S  P  E  K  A  C  S  L  A  K  T  A  F  D  E  A

481        ATCGCCGA
161         I  A
```

Figure 3.10

Partial mRNA sequence and corresponding amino acid sequence of wood frog skeletal muscle GADD45α A total of 264 nucleotide residues were retrieved and coded for 88 amino acids.

```
1          GCTCTACAGATTCACTTCACTCTGATCCAGGCTTTCTGCTGCGAGAATGACATCAACATC
1           A  L  Q  I  H  F  T  L  I  Q  A  F  C  C  E  N  D  I  N  I

61         CTGAGAGTGAGCAACATGAGCCGGCTGGCTGAGATCCTGGGCGGCTCTGACAAGCCGGGA
21          L  R  V  S  N  M  S  R  L  A  E  I  L  G  G  S  D  K  P  G

121        GAACCTGCCGACCTGCATTGTATTCTAATCAACAACCCGCACGCTTCTCAGCTAAAGGAT
41          E  P  A  D  L  H  C  I  L  I  N  N  P  H  A  S  Q  L  K  D

181        CCCGCCATCAACAAAGTGAGCAACTTCTGCAAAGAGAGCCGCTACCTGGATCAGTGGGTT
61          P  A  I  N  K  V  S  N  F  C  K  E  S  R  Y  L  D  Q  W  V

241        CCCGTGATCAACCTGCCCGAGCGA
81          P  V  I  N  L  P  E  R
```

Discussion

Organisms expend a lot of energy during growth and it makes sense that entry into a hypometabolic state in response to stress would have consequences for activities including cell proliferation, growth, and development, all of which rely on the cell cycle (Storey and Storey, 2007). However, cell cycle arrest as a component of metabolic rate depression in stressed animals has yet to be explored extensively. Selected organs of wood frogs such as liver, intestine or skin would likely have a substantial rate of cell turnover normally and these in particular may show marked cell cycle arrest as a response to freezing (Storey and Storey, 2007). The wood frog, *Rana sylvatica*, undergoes prolonged periods of freezing during cold winters, and is able to survive with minimal damage when it thaws in the spring. During freezing, blood plasma freezes completely and this means that oxygen and nutrients cannot be delivered to organs, and wastes cannot be removed; hence all cells experience hypoxia/anoxia and ischemia (Storey and Storey, 2004a). Wood frog body temperatures are also below 0°C during freezing, which itself equates to low metabolic rates. Since freezing can last for long periods of time, and since cells are completely cut off from oxygen each cell must have enough fuel reserves and also be able to generate enough energy anaerobically in order to carry out the essential metabolic reactions needed to survive (Storey and Storey, 2004a). Cells in frozen animals cannot maintain normal rates of metabolic activity and as such several mechanisms are called upon to repress metabolic activity (Storey and Storey, 2004a). It is quite conceivable that one such mechanism used by the wood frog during long periods of freezing stress is cell cycle arrest. Data generated from DNA array screening and Panomics transcription factor array screening of liver extracts from control and frozen

wood frogs identified several transcription factors that showed enhanced DNA binding during freezing (Storey, 2008). The amount of a transcription factor bound to DNA is the ultimate evidence that the particular transcription factor is active (Storey, 2008). One transcription factor in particular that showed enhanced DNA binding in liver of frozen animals was p53. This transcription factor has many different actions, one of which stands out: its ability to stimulate the expression of genes involved in cell cycle arrest including p21, GADD45α, and 14-3-3σ. p53 is known to be activated by metabolic changes (Prives and Hall, 1999). The present study examined the major proteins involved in the p53 pathway leading to cell cycle arrest.

The p53 polypeptide consists of five highly conserved domains including a transactivation domain located at the N terminal. The N-terminal is the site that allows p53 to recruit the machinery needed to activate target genes (Prives and Hall, 1999). This is also the site where Mdm2 binds to p53 and keeps it inactive under normal conditions. The N-terminal contains many serines including serine 6, 9, 15, 20, 37, and 46 which are phosphorylated in responses to various stresses. The C-terminal is responsible for controlling the specific DNA binding by p53 (Steegenga *et al.*, 1996). The C-terminal contains two serines one of which is serine 392 and three lysines including lys 373 and 382 which are phosphorylated and acetylated under stress (Appella and Anderson, 2001).

In order to transcribe target genes, p53 must first be stabilized and activated. Phosphorylation at key serine residues of p53 in the transactivation domain including Ser 6, 9, 37, 46, and especially Ser 15 and 20 leads to dissociation of the inhibitor protein

Mdm2 from p53 since the interaction between the two proteins is disrupted. This stabilizes p53 and exposes its transactivation domain (Lakin and Jackson, 1999; El-Deiry, 1998). Acetylation of p53 at many lysine residues including lys 373 and lys 382 can also lead to p53 stabilization (Lakin and Jackson, 1999). It is known that the p53 protein is ubiquitinated and acetylated on similar sites and this suggests that acetylation of p53 may outcompete ubiquitination of p53 under stress conditions (Brooks and Gu, 2003). Stabilization of p53 is the key first step in the p53 pathway in response to various stresses, but p53 must also be transcriptionally activated in order to turn on its downstream genes and effect a proper response.

Activation of p53 is effected by various phosphorylation and acetylated events. There are two main mechanisms that are responsible for p53 activation, one at the N-terminal and one at the C terminal (El-Deiry, 1998). Phosphorylation of p53 leads to elevated p53 levels and an increased amount of transcriptional activity. Phosphorylation of p53 at the N terminal at multiple serine sites including serine 6, 9, 15, 20, 37, and 46 leads to the phosphorylation and acetylation of p53 at the C terminus and subsequent activation of p53 via a cascade. (Appella and Anderson, 2001; El-Deiry, 1998). Acetylation of lysine residues at the carboxyl terminus, in particular lysine 373 and lysine 382, has been found to activate p53 sequence-specific DNA binding by increasing the affinity of p53 for DNA (Brooks and Gu, 2003). In addition to a higher amount of DNA binding, acetylation also positively affects the interactions between p53 and its transcriptional co-activators (eg. CBP/p300) through attraction of these to promoter regions and subsequent target gene activation (Brooks and Gu, 2003).

The data shows that in wood frog liver, total p53 levels increased significantly by 2.1 fold after 4 hours of freezing and stayed elevated when freezing was prolonged to 24 hours. This provided the initial indication that p53 is activated by freezing stress. Significant increases in p53 phosphorylation at multiple sites further supported this idea. Enhanced phosphorylation of N-terminal serines 6, 9, 15, 20, 37, and 46 was seen after 4 hours of freezing exposure (Figure 3.2). Intensive phosphorylation at the N-terminal region indicates that p53 is activated after 4 hours of freezing because phosphorylation at these residues leads to Mdm-2 being dissociated from p53 so that the p53 transactivation domain is exposed. Significant increases in p53 phosphorylated at serine 392 were also observed after 4 hours of freezing (Figure 3.2) which suggests that the p53 activation cascade was initiated. Phosphorylation of most of these sites was still high after 24 hours of freezing (Figure 3.2). However, the amount of phosphorylated p53 at serine 15 was reduced after 24 hours and the amount of phosphorylated p53 Ser 392 had returned to control values. Overall, however, there was still strong evidence that p53 remained activated after 24 hours of freezing in wood frog liver.

Significant increases in liver p53 acetylation on lysines 373 and 382 after 4 hours of freezing also suggested that p53 is activated at 4 hours of freezing (Figure 3.2).

An increase in acetylation of lysine residues at the carboxyl terminus in particular lysine 373 and lysine 382 indicates an activation of p53 sequence-specific DNA binding since it increases the affinity of p53 for DNA. However, after 24 hours of freezing, acetylation levels were reduced to levels not significantly different from controls.

Increased acetylation of p53 corresponds to a higher affinity of p53 for DNA which implies that genes under p53 control would be upregulated.

The data show a similar story in wood frog skeletal muscle. Total p53 protein levels were significantly elevated by 1.6 fold after 4 hours and remained high after 24 hours (Figure 3.2). A higher amount of p53 in freezing muscle again suggests p53 activation. Similar to wood frog liver, the amounts of N- and C-terminal phosphorylated p53 increased significantly after 4 hours in muscle and most remained elevated after 24 hours (Figure 3.2). These findings provide strong evidence for p53 activation in wood frog skeletal muscle since phosphorylation at the N-terminal corresponds to decreased Mdm2 binding as well as stabilization of p53. Phosphorylation of p53 at the C-terminal serine 392 also strongly suggests activation of p53 via the activation cascade. Significant increases in acetylation of p53 at lysine 373 after 4 hours and at lysine 382 after both 4 and 24 hours also occurred in wood frog muscle and also provides strong evidence for p53 activation by freezing (Figure 3.2).

Nuclear levels of p53 in wood frog liver and skeletal muscle were also assessed since transcription factors must be resident in the nucleus to carry out their actions. Significant increases in nuclear p53 levels after both 4 and 24 hours of freezing in both tissues (Figure 3.6) provides strong evidence that p53 is transcriptionally active and transcribing downstream genes. Nuclear levels of phosphorylated p53 were also significantly elevated after 4 hours of freezing in both tissues (Figure 3.6) which further supports p53 as being transcriptionally active. Nuclear levels of phosphorylated p53 after

24 hours of freezing showed some significant increases but others decreased to values not different from controls (Figure 3.6). For example, in wood frog liver, key serine 15 nuclear levels were not significantly different from controls. However, nuclear levels of another important serine, serine 20, were significantly elevated compared to controls suggesting a reduced but still active p53 transcriptional activity after 24 hours compared to 4 hours freezing. It is probable that different Ser residues are responding to different protein kinases and therefore the elevated levels of particular phosphorylated residues in the nucleus might occur because a particular kinase is especially important in responding to freezing stress. The N-terminal amino acids of p53 contain the sites that are most highly phosphorylated. A number of protein kinases phosphorylate p53, including ataxia-telangiectasia mutated (ATM), A-T and Rad3 related (ATR), the checkpoint kinases Chk1 and Chk2, casein kinase 1α, the Jun-N-terminal kinase (JNK) and p38 (Lavin and Gueven, 2006; Meek, 1998). From the data in figure 3.6, a number of phosphorylated residues are elevated in the nucleus in both wood frog liver and muscle, suggesting that these kinases play a role in responding to freezing stress. For example, elevated levels of the serine 37 residue in the nucleus of wood frog liver and muscle suggest a possible role for p38 in freezing response.

Data on acetylation of p53 in the nuclear compartment are also interesting since nuclear levels of lysine 373 and lysine 382 in muscle were significantly elevated after 4 hours of freezing but only lysine 373 remained elevated after 24 hours. Also of note, no significant changes in amount of acetylated p53 in nuclear extracts of liver for either lysine 373 or 382 were observed (Figure 3.6). This data suggests a higher transcriptional

activity of p53 in skeletal muscle compared to wood frog liver. High fold changes in amounts of nuclear p53 phosphorylated at serines 6, 9, 37, and 392 in wood frog liver and muscle after 4 hours of freezing could signify that these residues are important to mediating freeze responsive gene expression by p53.

Another key protein to examine during freezing stress is the inhibitor of p53, Mdm2. Under normal conditions, Mdm2 binds to p53 at the N-terminal and thus masks the transactivation domain of p53 (El-Deiry, 1998). Under stress conditions, phosphorylation of p53 disrupts the binding of Mdm2 and this leads to Mdm2 degradation. Figure 3.3 shows that in both wood frog skeletal muscle and liver, Mdm2 protein levels decreased significantly after 4 hours of freezing exposure and remained significantly lower after 24 hours. This indicates that the Mdm2 protein has been removed from p53 during freezing stress and that p53 has been activated. Therefore, these data correlate well with the observed enhanced phosphorylation levels of residues in the N-terminal domain of p53.

Another mechanism that exists to stabilize p53 involves the p19ARF protein. This protein is activated and expressed under stress and blocks the interaction between p53 and Mdm2 by binding directly to Mdm2 (at a site different from the p53 binding site) (Brooks and Gu, 2003). This prevents p53 from being targeted for degradation due to binding by Mdm2. The protein p19ARF carries out its action by sequestering Mdm2 into the nucleolus and this stops p53 from being exported from the nucleus and being degraded. It acts to preventing Mdm2 from ubiquitinating p53, which would mark it for

degradation by the proteasome, by hindering the ubiquitin ligase activity of Mdm2 (Ashcroft and Vousden, 1999). There were no significant changes in p19ARF protein levels or in its nuclear distribution in wood frog skeletal muscle during freezing (Figure 3.3B and 3.3C). However, p19ARF protein levels are significantly increased in wood frog liver after 24 hours of freezing and nuclear p19ARF levels increased significantly after 4 hours of freezing and rose further after 24 hours (Figure 3.3B and 3.3C). Therefore, these data show organ-specific control of p53 by p19ARF and, in liver, indicate that the action of p19ARF in inhibiting Mdm2 provides an additional mechanism of p53 regulation in response to freezing. Liver has a very major role in the overall cryoprotection of the whole frog since it is responsible for the synthesis and export of both the low molecular weight cryoprotectant, glucose, and selected plasma proteins that aid freezing survival. Hence, it is not surprising that added layers of p53 control mechanisms are present in liver.

The transcription factor p53 can upregulate the expression of a number of genes that in turn control cell cycle arrest. Three of the downstream targets of p53 that are involved in cell cycle arrest were analyzed in the present study. These are p21, a potent cell cycle inhibitor that can halt the cell cycle at the G1/S and G2/M checkpoints, and GADD45α and 14-3-3σ both of which arrest the cell cycle at the G2/M checkpoint, although by slightly different mechanisms. The data showed that p21 levels were significantly increased in wood frog skeletal muscle and liver after 4 hours (Figure 3.4A). Levels remained high in liver after 24 h frozen but returned to control levels in skeletal muscle. These data suggest that p21 expression is upregulated by p53 in wood frog liver

and that p21 could be important in cell cycle arrest in response to freezing in wood frogs. This proposal is further supported by the fact that levels of phosphorylated p21 also rose significantly in both liver and skeletal muscle after 4 hours of freezing and remained high after 24 hours of freezing in wood frog liver (Figure 3.4B). Phosphorylation of p21 at serine 146 has been reported to increase stability of p21 (Li *et al.*, 2002; Child and Mann, 2006).

Protein levels of 14-3-3σ increased significantly after 4 hours of freezing in wood frog liver and skeletal muscle and remained significantly high after 24 hours of freezing in both tissues (Figure 3.5A). GADD45α showed the same pattern (Figure 3.5B). These data suggests an important role for both 14-3-3σ and GADD45α in G2 arrest in frog organs as the animal transitions into the frozen state. Levels of 14-3-3σ and GADD45α mRNA transcripts were also assessed in wood frog muscle and liver. Freeze responsive significant increases were observed for both gene products in wood frog liver after 24 hours of freezing (Figures 3.7 and 3.8). This provides further evidence that p53-mediated gene upregulation occurs during freezing leading to enhanced transcription and translation of 14-3-3σ and GADD45α that are important regulators of cell cycle arrest. The upregulation of these two proteins as well as p21 at both the transcriptional and translational levels during freezing also demonstrates that cell cycle arrest is an important part of freeze responsive metabolic rate depression.

Structural analysis of wood frog 14-3-3σ and GADD45α sequences

An analysis of wood frog 14-3-3σ nucleotide and amino acid sequences revealed that 14-3-3σ shares a high identity with both the African clawed frog and selected endothermic vertebrates, namely chicken, mouse, and humans. It shares 69% identity with the African clawed frog nucleotide sequence and 62% identity with the other vertebrate sequences (Appendix B part B). The wood frog 14-3-3σ showed 3 unique substitutions at residues that were fully conserved in the other four species. Two are serine substitutions for alanine and one a cysteine substitution for serine (at residues 19, 91 and 75 of the wood frog sequence, respectively; these are in bold underline in Appendix B, part C). Since the other four species are either warm-blooded (chicken, human, mouse) or live in warm environments (African clawed frog), these unique substitutions to wood frog 14-3-3σ protein might make general conformational changes that could aid protein function at low temperatures. Alternatively, the serine substitutions would offer additional potential sites for phosphorylation control of wood frog 14-3-3σ. The cysteine substitution may maintain a disulfide bond that is needed for protein conformation. Both frog species contained 4 cysteine residues in the 14-3-3σ sequence (ie. 2 potential S-S bonds) whereas the mammalian sequences have only 2 cysteines. The cysteine at residue 55 of the wood frog sequence is conserved in all species (= Cys 94 of clawed frog) and Cys 150 in wood frog sequence is also conserved in the clawed frog sequence (= Cys 189 of clawed frog). However, the wood frog sequence also shows cysteines at residues 48 and 75 of its sequence whereas the African clawed frog has cysteines in different places at residues 134 and 237 of its sequence. The wood frog 14-3-3σ amino acid sequence shares 79% identity with the African clawed frog amino acid

sequence and 71% identity with sequences from other vertebrates (Appendix B part D). Based on these results, it is probable that the wood frog 14-3-3σ protein contains the same functional domains and also carries out the same functions as the 14-3-3σ proteins from other species.

An analysis of the GADD45α nucleotide and amino acid sequences reveals that GADD45α also shares a high identity with both Xenopi, as well as the chicken, human, and zebrafish sequences. The wood frog GADD45α nucleotide sequences shares 84% identity with the African clawed frog sequence, 86% identity with the western clawed frog sequence, 60% identity with the chicken and human sequences, and 56% identity with the zebrafish sequence (Appendix C, part B). The wood frog GADD45α amino acid sequences shares 89% identity with the African clawed frog and western clawed frog amino acid sequences, and 72% identity with the chicken, human, and zebrafish amino acid sequences (Appendix C, part D). Analysis of the wood frog partial amino acid sequence revealed only one unique substitution at residue 63 where an isoleucine is substituted for a leucine in all other species. As with wood frog 14-3-3σ, it is probable that the wood frog GADD45α protein contains the same functional domains and also carries out the same functions as the GADD45α proteins from other species.

Conclusion

The data collected from the present analysis of skeletal muscle and liver from 4 hour and 24 hour frozen wood frogs suggested strong activation of the p53 transcription factor and subsequent upregulation of three of its known target genes: p21, 14-3-3σ, and

GADD45α. Protein levels of the p53 inhibitor protein, Mdm2, that were significantly reduced under stress, and an upregulation of p19ARF in wood frog liver all further support the idea that during freezing, the p53 pathway is activated in order to arrest the cell cycle in wood frog organs as part of metabolic rate depression. The evidence is strong for an activation of p53 in the wood frog after 4 hours of freezing, and a less pronounced effect after 24 hours of freezing. This argues that p53 action is needed most during the transition period when tissues are freezing, ice is accumulating, cryoprotective measures are being put in place, and cellular metabolism is being suppressed (ie. the 4 hour sampling time) whereas by 24 hours when ice accumulation is maximal (up to 70% of total body water) and the transition to the hypometabolic state is complete, some features of p53 activation may be reversed back towards the control situation. Further studies are needed in order to confirm these findings.

Chapter 4

REGULATION OF NF-KB IN WOOD FROG LIVER AND SKELETAL MUSCLE

Introduction

Oxidative damage in wood frogs is always a threat during freezing and thawing and as such wood frogs must have in place various mechanisms to prevent undue damage by reactive oxygen species (ROS) (Storey and Storey, 2004). One pathway of interest that is known to be activated by free radicals is NF-κB; indeed, previous transcription factor profiling studies have found strong evidence that NF-κB and target genes of NF-κB play a role in response to freezing (Storey, 2008).

Nuclear factor-κB (NF-κB) is a transcription factor that plays a role in cellular responses to stimuli such as stress, free radicals, UV, and bacterial/viral antigens. It regulates the immune response to infection. Incorrect regulation can cause cancer and some autoimmune diseases. It is composed of 5 protein subunits: NF-κB1 (p50), NF-κB2 (p52), RelA (p65), RelB, and c-Rel (Kumar *et al.*, 2004; Tergaonkar, 2006). The p50-p65 heterodimers and the p50 homodimers are important in transcriptional activation. Under normal conditions, NF-κB is present in an inactive state; therefore protein synthesis is not needed for its activation. IκB (inhibitors of NF-κB) proteins mask nuclear localization signals of NF-κB proteins and keep them in an inactive state in the cytoplasm by their ankyrin repeats. The ankyrin repeats on the IκB proteins interact with the C-terminus of the NF-κB Rel homology domain and prevent nuclear translocation of NF-κB (Wegener and Krappmann, 2008). NF-κB can be activated by two different pathways, the classical (or canonical) pathway which involves rapid degradation of IκB proteins, and the alternative pathway which involves activation of p52/RelB heterodimers

via p100 (Ahmed and Li, 2008; Wietek and O'Neill, 2007). Usually, NF-κB is activated through the classical pathway (figure 4.1). In canonical NF-κB activation, NF-κB complexes are activated through the action of the IκB kinase (IKK). IKK phosphorylates two serine residues, serine 32 and serine 36, in the IκB regulatory domain (Ravi and Bedi, 2004). IκB proteins that are phosphorylated dissociate from NF-κB and are subsequently ubiquitinated at selected lysine residues which then targets them for degradation by the proteosome. After IκB proteins have been degraded, NF-κB is then able to enter the nucleus and turn on the expression of certain genes that have DNA binding sites for NF-κB in their promoter. NF-κB also turns on the expression of its own repressor, IκBα, which re-inhibits NF-κB via an auto feedback loop that involves IκBα moving into the nucleus and stopping NF-κB expression of target genes by moving it back into the cytoplasm (Ahmed and Li, 2008). This results in oscillating levels of NF-κB activity.

Although activation of NF-κB takes place as a result of IκB phosphorylation, NF-κB subunits can also be phosphorylated. Optimal NF-κB activation involves phosphorylation of the NF-κB subunits such as p65 in their transactivation domains. Phosphorylation of p65 augments its transactivation potential (Viatour *et al.*, 2005).

NF-κB activation leads to the expression of many target genes. Two target genes of NF-κB that are typically activated under stress conditions are the heavy chain of ferritin and manganese superoxide dismutase (MnSOD). Both play a role in protecting

animals from damage by ROS and provide a mechanism for the antioxidant activity of NF-κB.

Ferritin is a 450 kDa iron storage protein that is composed of 24 subunits of two types, a heavy chain subunit of ~21 kDa and a light chain of 19 kDa (Orino and Watanabe, 2008). The heavy chain is a ferroxidase, which acts to convert free iron in the form of Fe(II) to the non-toxic form of Fe(III) that is stored in the mineral core of ferritin whereas the light chain subunits are responsible for modifying the protein environment so as to sequester more iron by iron nucleation (Orino and Watanabe, 2008; Knovich *et al.*, 2009). Iron is a critical trace element that all organisms utilize for many cellular functions such as metabolism, oxygen transport, and energy production. Too much iron is toxic to cells because excess free iron in the form of Fe(II) catalyzes the formation of reactive oxygen species, namely the hydroxyl radical, via the Fenton reaction ($Fe^{2+} + H_2O_2 \rightarrow Fe^{3+} + OH^- + OH^{\cdot}$) which is very damaging to DNA and proteins (Orino and Watanabe, 2008; Knovich *et al.*, 2009). One mechanism by which organisms cope with excess iron is through the action of the ferritin protein.

Manganese superoxide dismutase (MnSOD) is an enzyme found in the mitochondrion that has a molecular weight of ~26 kDa. The scavenger enzyme catalyzes the neutralization reaction of superoxide (O_2^-) to form O_2 and H_2O_2 (hydrogen peroxide) (Bubici *et al.*, 2004). Superoxide radicals can arise from the electron transport chain when electrons leak out from complexes I and III and reduce molecular oxygen (Ji *et al.*, 2007). Superoxide radicals are toxic to the cell and, although they can spontaneously

dismute to oxygen and hydrogen peroxide, they can react even faster with other targets to produce other toxic compounds such as hydroxyl radicals and peroxynitrite. SOD enzymes such as MnSOD are able to outcompete all other harmful reactions of superoxide, and therefore play a critical role in antioxidant defense in almost all cells exposed to oxygen.

The present study focuses on the responses to freezing stress by the transcription factor, NF-κB, and two antioxidant gene targets under its control (ferritin H chain, MnSOD) in tissues of the wood frog, *Rana sylvatica*.

Figure 4.1: NF-kB classical signaling pathway leading to activation of downstream genes. In the absence of stress, IkB proteins mask nuclear localization signals of NF-kB proteins and keep them in an inactive state in the cytoplasm by their ankyrin repeats. NF-kB complexes are activated through the activation of the IkB kinase (IKK). IKK phosphorylates two serine residues in an IkB regulatory domain. This tags the IkB proteins for degradation by the proteosome. NF-kB is then able to enter nucleus and turn on the expression of certain genes that have DNA binding sites for NF-kB whose activation leads to a particular response.

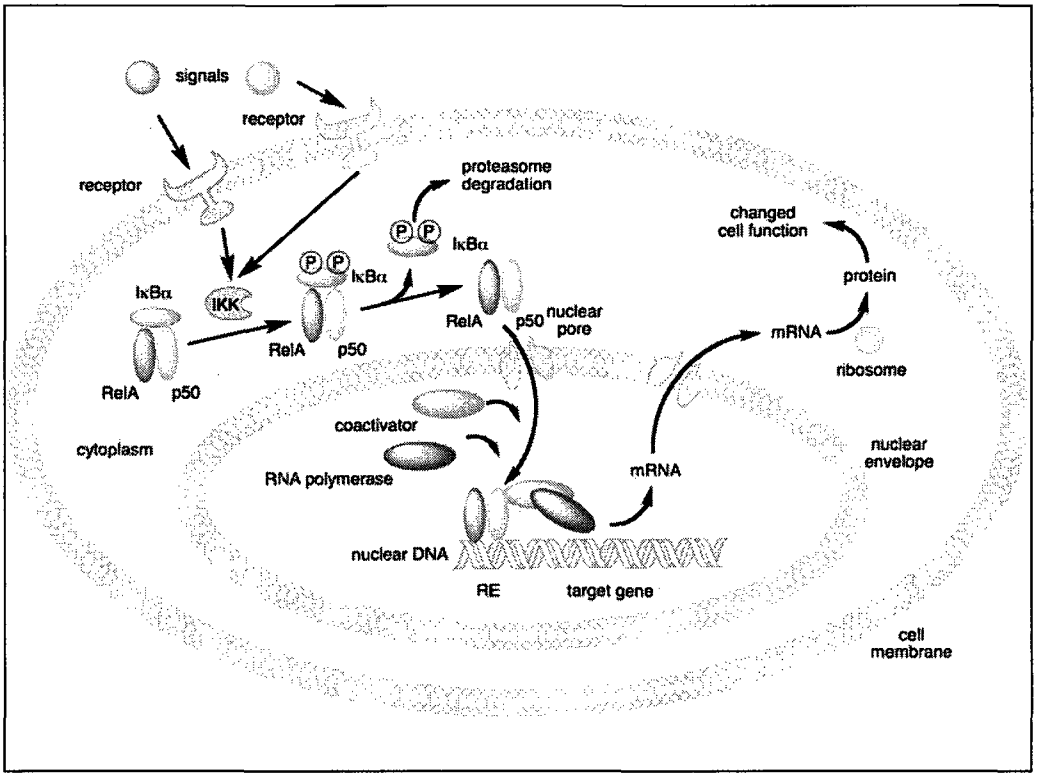

www.Wikipedia.org

Results

Effect of freezing on levels of NF-κB subunits p50, p65 and phosphorylated p65

Membranes probed with antibodies raised against total p50 or p65 protein or against the peptide containing the phosphorylated (ser 536) residue on p65 showed strong single bands at around 50 kDa, 65 kDa, and 65 kDa, respectively, with samples from both liver and skeletal muscle of wood frogs.

Figure 4.2A shows representative Western blots for the p50 subunit of NF-κB in liver and muscle along with histograms depicting mean protein levels (± SEM, n=4-5 independent determinations) in the two organs from control (5°C acclimated), 4 hour and 24 hour frozen (at -2.5°C) frogs. Protein levels of p50 increased significantly in both wood frog liver and skeletal muscle by 1.7 fold and 1.9 fold, respectively, after 4 hours of freezing. Levels remained high after 24 hours of freezing; values for liver and skeletal muscle were 2.2- and 1.4-fold higher and significantly different from controls.

Protein levels of the NF-κB p65 subunit showed a similar pattern to that seen for p50 (Figure 4.2B). Levels were significantly increased after 4 hours of freezing in both liver (1.4 fold) and skeletal muscle (2.2 fold). Protein levels remained elevated after 24 hours of freezing in both liver (1.7 fold) and skeletal muscle (2.1 fold), as compared with controls.

Phosphorylation of the NF-κB subunit p65 on Ser 536 leads to enhanced transactivation potential of the NF-κB transcription factor. In skeletal muscle, protein levels of phosphorylated p65 showed no change after 4 hours of freezing but decreased significantly after 24 hours of freezing (to 68% of control value) (Figure 4.2C). Protein levels of phosphorylated p65 increased significantly by 1.8 fold in wood frog liver after 4 hours of freezing but returned to levels similar to control after 24 hours of freezing.

Effect of freezing on levels of phosphorylated IκB in wood frog organs

The inhibitor protein, IκB, binds to NF-κB and prevents it from moving into the nucleus; however, when phosphorylated on Ser32, IκB dissociates from NF-κB so that the latter can translocate into the nucleus to activate gene expression. Hence, the relative amount of phospho-IκB Ser32 provides a good indication of the activity state of NF-κB. The rabbit polyclonal anti-phospho-IκB antibody crossreacted with a strong single band at the expected molecular mass for this protein of ~40 kDa.

In liver, protein levels of phosphorylated IκB increased significantly by 1.5 fold after 4 hours of freezing but by 24 hours levels were reduced again to values that were not significantly different from controls (Figure 4.3). In skeletal muscle, a different pattern was seen. Levels of phospho-IκB were significantly reduced after 4 hours of freezing (to 63% of control values) but a strong increase was observed after 24 hours (levels were 1.4-fold higher than control values).

Protein levels of Ferritin Heavy Chain and Manganese Superoxide Dismutase (MnSOD) after 4 and 24 hours freezing

Given that the above data for NF-κB and IκB suggest activation of the transcription factor during freezing, levels of two downstream genes under NF-κB were next analyzed to see if they were up-regulated during freezing stress.

Figure 4.4A shows data for ferritin heavy chain levels in wood frog liver and muscle. Membranes probed with antibodies recognizing the heavy chain of ferritin crossreacted with a bright strong single band at about 21 kDa, consistent with the known size of this protein in other vertebrates. In wood frog skeletal muscle, protein levels of ferritin had increased significantly after both 4 hours (1.7 fold) and 24 hours (2.2 fold) of freezing. In liver, protein levels rose significantly after 4 hours of freezing by 1.5 fold but were reduced again after 24 hours to levels not significantly higher than controls.

Figure 4.4B shows comparable data for MnSOD. Membranes probed with anti-MnSOD showed a bright band at the expected molecular mass of ~26 kDa. Protein levels of MnSOD increased significantly in wood frog liver (1.3 fold) and skeletal muscle (1.4 fold) after 4 hours of freezing. A similar trend was observed after 24 hours of freezing as levels remained high in both liver (1.2 fold) and skeletal muscle (1.5 fold), as compared with controls.

Movement of NF-κB into the nucleus

Movement of transcription factors into the nucleus is essential for their action in up-regulating gene transcription. Hence, the relative amount of NF-κB that is in the nucleus is a good indicator of whether or not genes under its control are up-regulated during freezing stress. Nuclear distributions of p50 and p65 were examined in wood frog liver and muscle by western blotting.

Figure 4.5A shows that a significant increase in nuclear levels of p50 occurred after 4 hours of freezing in both liver (1.4 fold) and skeletal muscle (1.4 fold) as compared with the nuclear content of the protein in control frogs. Nuclear levels of p50 also remained significantly elevated after 24 hours of freezing in both liver (2.2 fold) and skeletal muscle (1.6 fold).

An examination of the nuclear levels of p65 revealed a similar pattern to that seen for p50. A significant increase in nuclear p65 content occurred after 4 hours of freezing in both liver (1.9 fold) and skeletal muscle (1.8 fold) (Figure 4.5B). Nuclear levels of p65 remained high after 24 hours of freezing, being 2.1 fold higher in liver and 2.8 fold higher in skeletal muscle than control values.

Nuclear levels of phosphorylated p65 (Ser 536) remained unchanged by either short (4 hours) or long (24 hours) term freezing in either tissue (Figure 4.5 C).

Transcript levels of Ferritin Heavy Chain

Figure 4.6 shows that mRNA levels of wood frog skeletal muscle ferritin heavy chain remain constant after 24 hours of freezing compared to control conditions. However, freezing triggered a significant 2.1 fold increase in mRNA levels of ferritin heavy chain in wood frog liver.

Analysis of Ferritin Heavy Chain sequences

The amplified product obtained using ferritin heavy chain primers was sequenced and compared to the Genbank database found on the National Center for Biotechnology Information website. The nucleotide sequence contained 307 residues (Figure 4.7) and represented about 40-48 % of the full vertebrate sequence which contains 646-770 nucleotide residues depending on the species. Part A of Appendix D shows a comparison of the wood frog ferritin heavy chain nucleotide sequence to that of the bullfrog, Asiatic toad, African clawed frog, western clawed frog, chicken, mouse, and human sequences. The partial wood frog nucleotide sequence showed strong similarity with the sequences from other vertebrates, particularly with other amphibians. Indeed, the homology tree shows that the wood frog sequence shared 91% nucleotide identity with the bullfrog sequence, 82% identity with the Asiatic toad sequence, 78% identity with the African clawed frog and western clawed frog sequences and 61% identity with the chicken, mouse, and human sequences (Appendix D, part B).

The partial wood frog sequence coded for 102 amino acids (Figure 4.7). Part C of Appendix D shows a comparison of the amino acid sequences of the eight vertebrate species and again the wood frog sequence showed very high identity with the other vertebrate sequences. The wood frog amino acid sequence shared 89% identity with the African clawed frog, western clawed frog and Asiatic toad amino acid sequences, and 70% identity to the bullfrog, chicken, human, and mouse amino acid sequences (Appendix D, part D).

Figure 4.2.

Western blot analysis demonstrating the effects of short term and long term freezing on the levels of p50 and p65 NF-kB subunits as well as phosphorylated p65 (Ser 536) in wood frog skeletal muscle and liver.

A) NF-kB p50 subunit protein levels in wood frog skeletal muscle and liver. Representative western blot shows p50 protein levels in tissues from control (5°C), 4 hours frozen (-2.5°C) and 24 hours frozen (-2.5°C) frogs. An equal amount of protein (20 μg) was loaded into each lane.

Bar graphs depict normalized mean values (± SEM, n=4-5 independent determinations) for p50 protein levels. * - Significantly different from the corresponding control value as determined by Student's t-test, $P<0.05$.

B) NF-kB p65 subunit protein levels in wood frog skeletal muscle and liver. Other information as in A above.

C) Relative levels of phosphorylated-p65 (Ser 536) in wood frog skeletal muscle and liver. Other information as in A above.

A)

Control versus 4h frozen liver

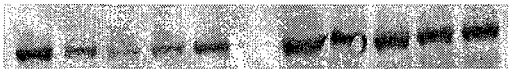

Control versus 24h frozen liver

Control versus 4h frozen muscle

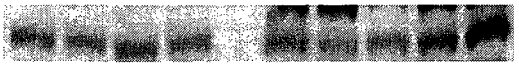

Control versus 24h frozen muscle

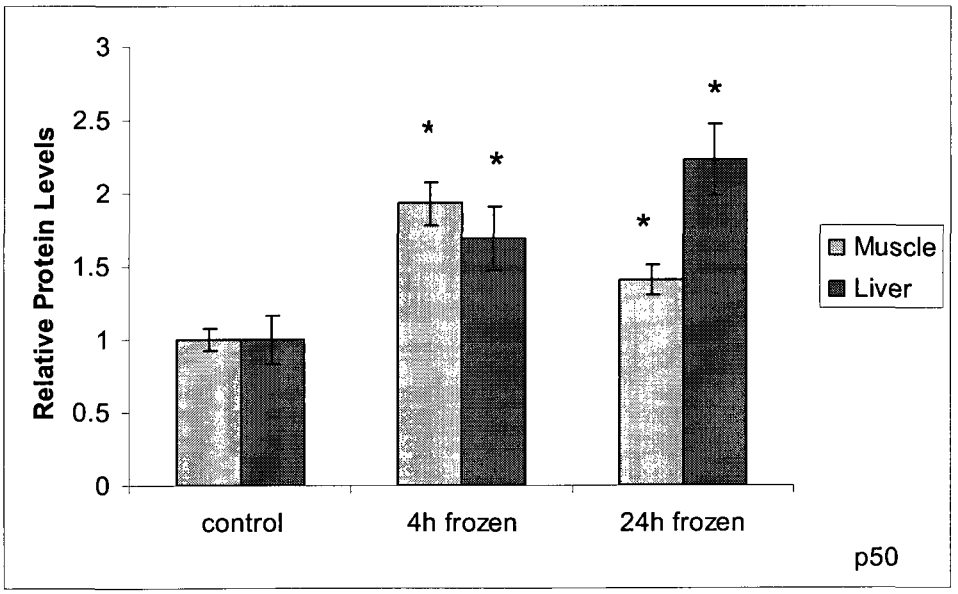

B)

Control versus 4h frozen liver

Control versus 24h frozen liver

Control versus 4h frozen muscle

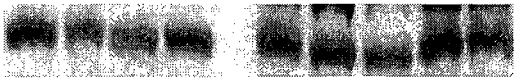

Control versus 24h frozen muscle

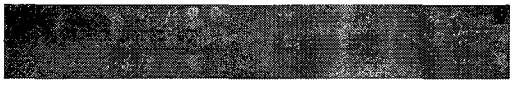

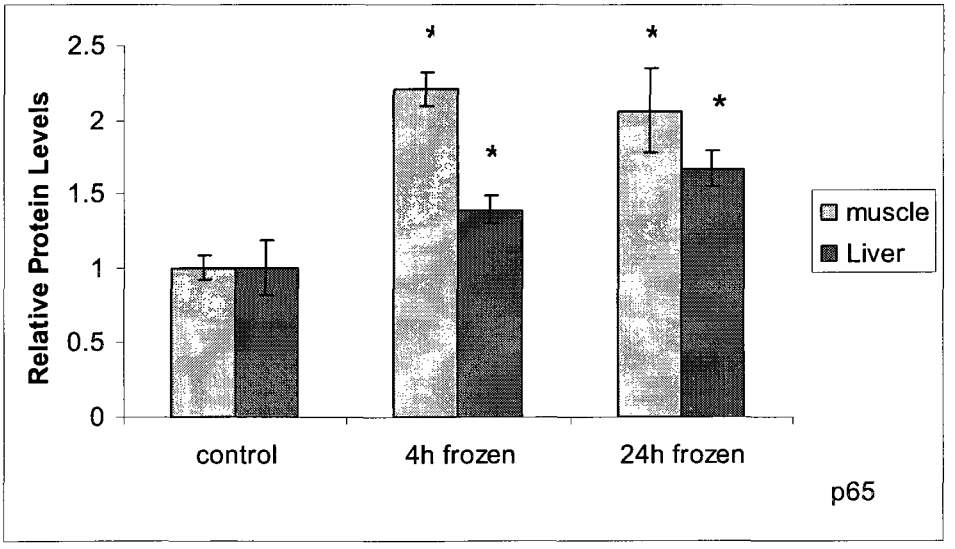

C)

Control versus 4h and 24h frozen liver

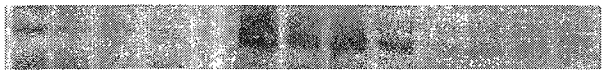

Control versus 4h and 24h frozen muscle

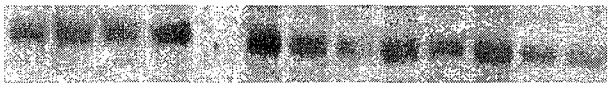

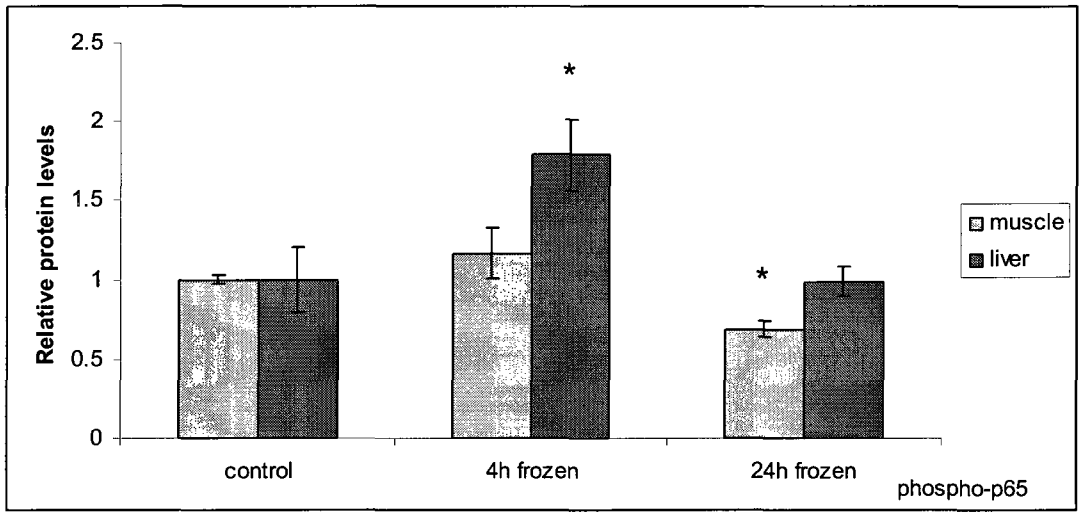

Figure 4.3.

Western blot analysis demonstrating the effects of short and long term freezing on the relative content of phosphorylated IkB (Ser32) protein in wood frog skeletal muscle and liver.

Western blots show phospho-IkB levels in skeletal muscle and liver of control (5°C acclimated), 4 hour and 24 hour frozen (-2.5°C) frogs. An equal amount of protein (20 μg) was loaded into each lane.

Bar graphs depict normalized mean values (± SEM, n=4-5 independent determinations) for phospho-IkB levels in liver and muscle of control, 4 hour and 24 hour frozen frogs.

* - Significantly different from the corresponding control value as determined by Student's t-test, $P<0.05$.

Control versus 4h and 24h frozen liver

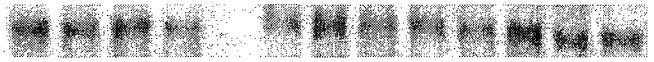

Control versus 4h and 24h frozen muscle

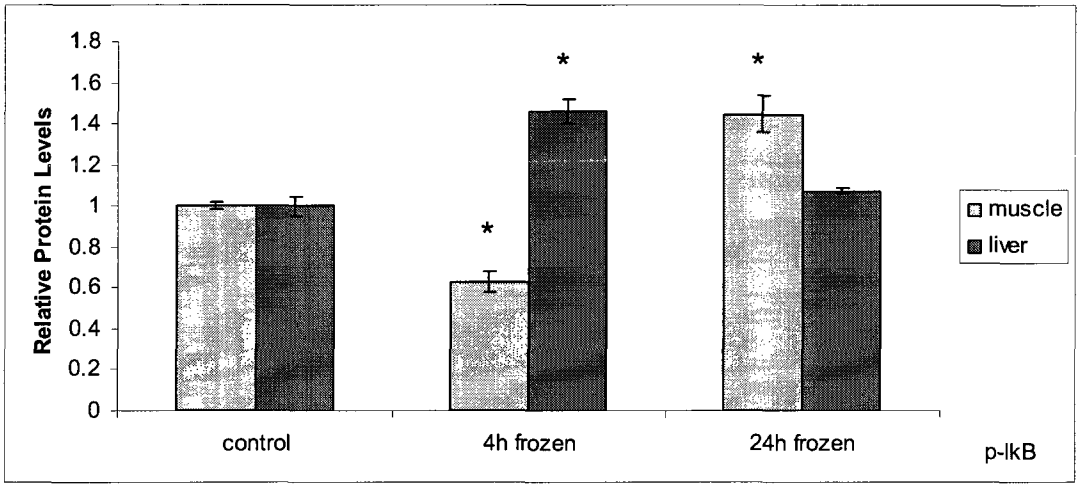

Figure 4.4.

Western blot analysis demonstrating the effects of short term and long term freezing on the protein levels of two downstream targets of NF-kB action: ferritin heavy chain and manganese superoxide disumutase (MnSOD) in wood frog skeletal muscle and liver.

A) Ferritin heavy chain protein levels in skeletal muscle and liver.

Western blots show relative levels of ferritin heavy chain in wood frog skeletal muscle and liver for control (5°C acclimated), 4 hour and 24 hours frozen (at -2.5°C) frogs. An equal amount of protein (20 μg) was loaded into each lane.

Bar graphs depict normalized mean values (± SEM, n=4-5 independent determinations) of ferritin heavy chain levels under the three experimental conditions.

* - Significantly different from control value as determined by Student's t-test, $P<0.05$.

B) MnSOD protein levels in wood frog skeletal muscle and liver.

Other information as in A above.

A)

Control versus 4h and 24h frozen liver

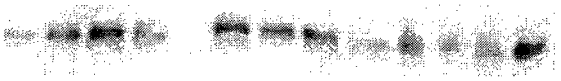

Control versus 4h and 24h frozen muscle

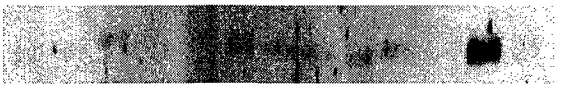

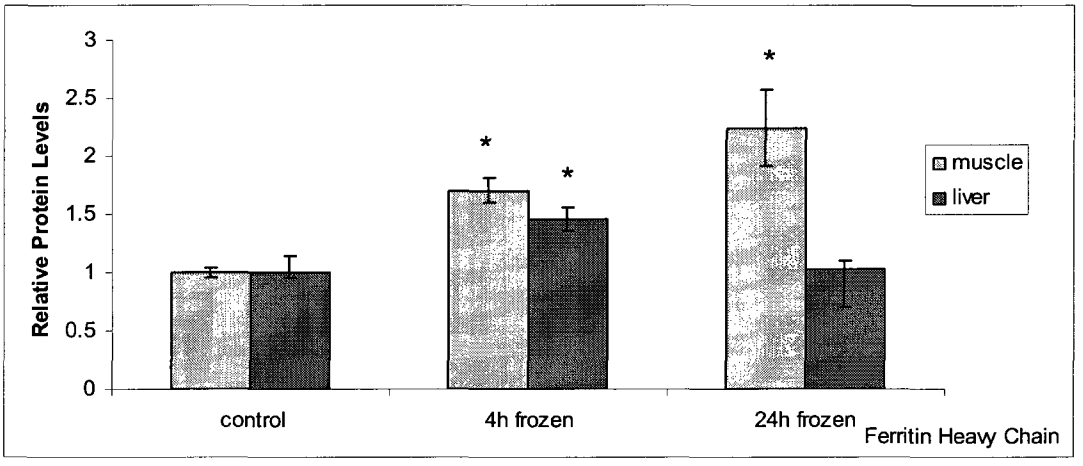

B)

Control versus 4h frozen liver

Control versus 24h frozen liver

Control versus 4h frozen muscle

Control versus 24h frozen muscle

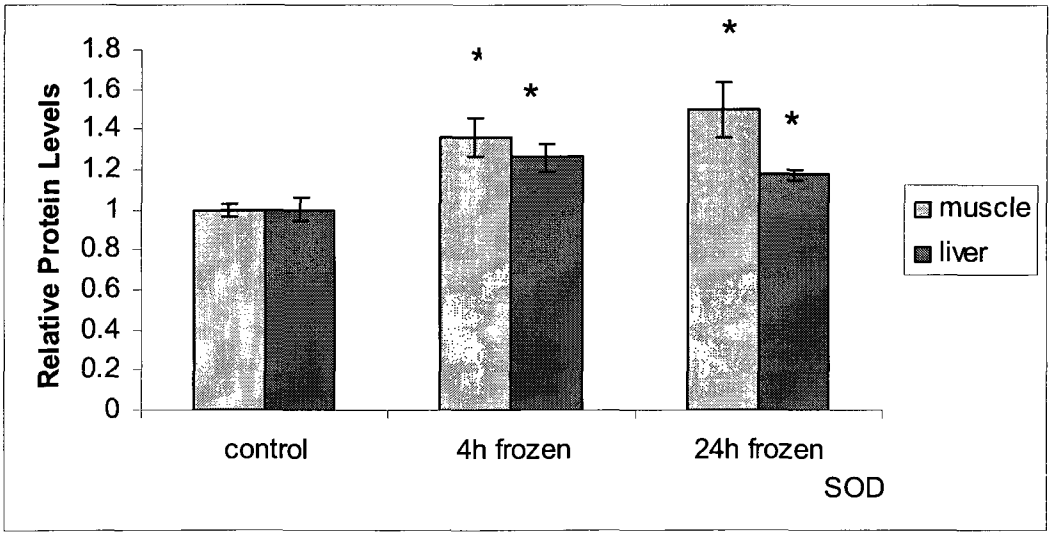

Figure 4.5.

Western blot analysis depicting the nuclear distribution of the NF-kB p50 and p65 subunit proteins as well as the amount of phosphorylated p65 during short term and long term freezing in wood frog skeletal muscle and liver.

A) Nuclear distribution of p50 protein in wood frog skeletal muscle and liver.

Representative western blots show nuclear distributions of p50 for control (5°C), 4 and 24 hours freezing (-2.5°C). Equal amount of protein (20 μg) were loaded into each lane.

Bar graphs depict normalized mean values (± SEM, n=4-5 independent determinations) for nuclear distributions of p50 protein.

* - Significantly different from control value as determined by Student's t-test, $P<0.05$.

B) Nuclear distributions of p65 protein in wood frog skeletal muscle and liver.

Other information as in A above.

C) Nuclear distributions of phosphorylated-p65 (Ser 536) protein in wood frog skeletal muscle and liver.

Other information as in A above.

A)

Control versus 4h frozen liver

Control versus 24h frozen liver

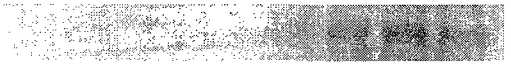

Control versus 4h frozen muscle

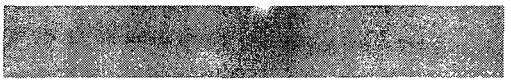

Control versus 24h frozen muscle

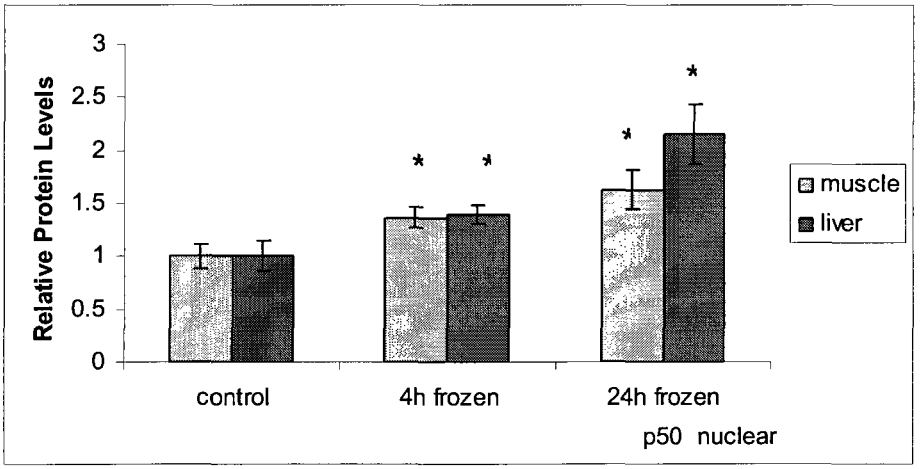

B)

Control versus 4h frozen liver

Control versus 24h frozen liver

Control versus 4h frozen muscle

Control versus 24h frozen muscle

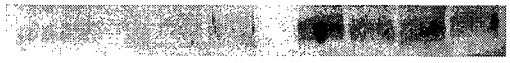

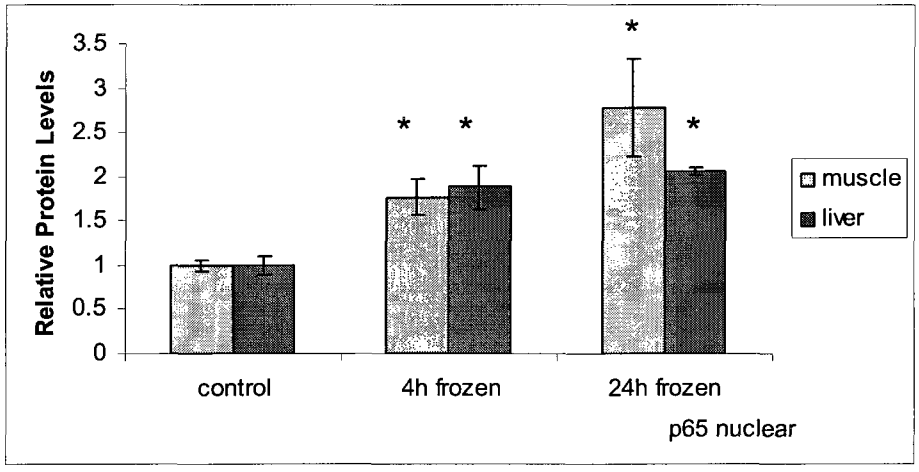

C)

Control versus 4h and 24h frozen liver

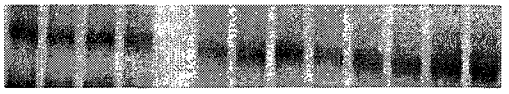

Control versus 4h and 24h frozen muscle

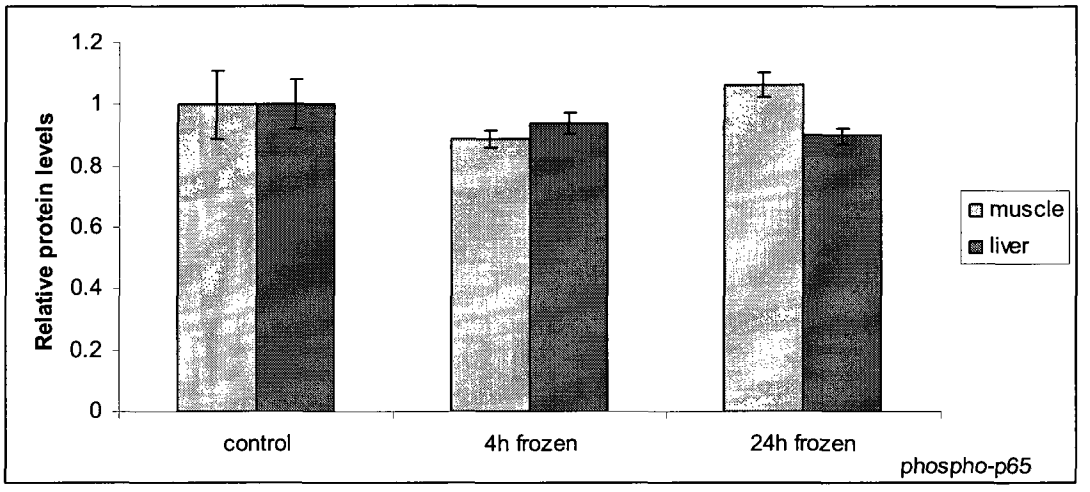

Figure 4.6.

Transcript levels of Ferritin Heavy Chain in wood frog muscle and liver

A) Expression of α-tubulin and ferritin heavy chain in a serial dilution of muscle and liver cDNA from control and 24 hour frozen samples. The figure shows a representative example. PCR product levels of ferritin heavy chain were normalized against the corresponding α-tubulin levels for the same sample since previous studies had shown that α-tubulin product levels did not change between control and frozen state. The 10^{-1} dilution level was used for quantification.

B) Relative ferritin heavy chain transcript levels in muscle and liver of control and 24 hours frozen wood frogs determined by RT-PCR. Histogram shows mean ± SEM, at least n=4 independent determinations. * - Significantly different from the corresponding control value as determined by the Student's t-test, $P<0.05$.

A)

Ferritin Heavy Chain liver control versus frozen 10^{-1} dilution

Ferritin Heavy Chain muscle control versus frozen 10^{-1} dilution

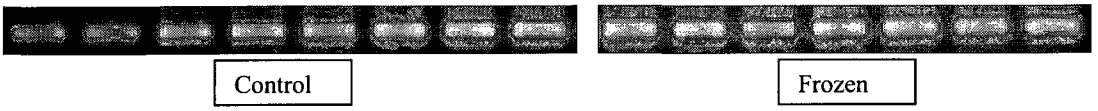

α-tubulin liver control versus frozen 10^{-1} dilution

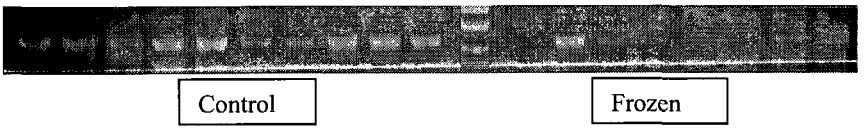

α-tubulin muscle control versus frozen 10^{-1} dilution

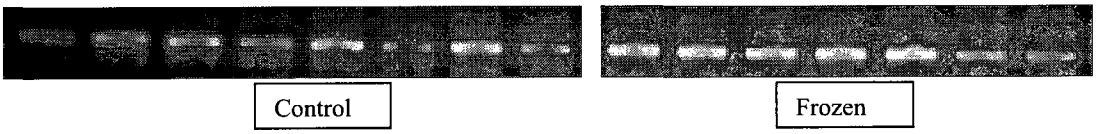

B)

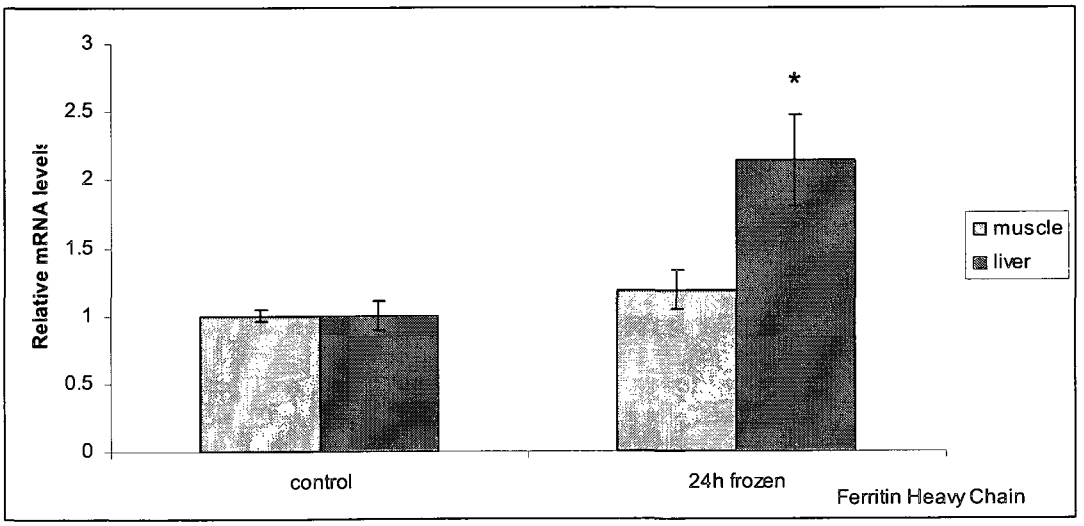

Figure 4.7.

Partial mRNA sequence and corresponding translated amino acid sequence of wood frog ferritin heavy chain.

```
1          GAAATATCAAAACAAGCGTGGGGGACGCGTTGTCCTGCAGGACGTCAAGAAACCAGAGCG
1            K  Y  Q  N  K  R  G  G  R  V  V  L  Q  D  V  K  K  P  E  R

61         TGATGAATGGGGTAACACCCTGGATGCCATGCAGGCTGCTCTGCAGCTGGAAAAGACCGT
21           D  E  W  G  N  T  L  D  A  M  Q  A  A  L  Q  L  E  K  T  V

121        GAATCAGGCTCTTCTGGACCTGCACAAGCTGGCATCTGACAAAGTTGACCCCCATCTGTG
41           N  Q  A  L  L  D  L  H  K  L  A  S  D  K  V  D  P  H  L  C

181        TGATTTCCTGGAAACGGAATACCTGGAGGAACAGGTGAAGGATATTAAACACTTTGGAGA
61           D  F  L  E  T  E  Y  L  E  E  Q  V  K  D  I  K  H  F  G  D

241        TTACATCACCAACCTGAAACGCCTTGGGCTGCCCGAGAACGGCATGGGCGAGTACCTGTT
81           Y  I  T  N  L  K  R  L  G  L  P  E  N  G  M  G  E  Y  L  F

301        CGACAAA
101          D  K
```

Discussion

Reactive oxygen species present a serious problem to organisms as they can cause extensive damage to DNA, proteins, and lipids (Storey and Storey, 2007). All organisms are equipped with mechanisms to combat oxidative stress. Previous studies have found elevated antioxidant defenses in organisms that depress their metabolic rate for extended periods of time, including freeze tolerant species (Hermes-Lima *et al.*, 2001; Hermes-Lima and Zenteno-Savín, 2002). In the wood frog, *Rana sylvatica*, the problem presented by ROS is two-fold. During freezing, oxygen cannot be delivered to organs. Upon thawing, oxygen is suddenly reintroduced and can cause a rapid burst of ROS generation leaving to massive damage to cells, tissues and whole organs. Furthermore, the wood frog accumulates very high concentrations of glucose as a cryoprotectant to allow freezing survival. Glucose can be oxidized which can lead to the formation of free radicals and as such presents another problem for the wood frog to cope with in terms of oxidative damage (Storey and Storey, 2007). Wood frogs have many mechanisms they employ in order to deal with the threats of oxidative damage including activation of transcription factors and upregulation of antioxidant enzymes in anticipation of reperfusion events. One potential transcription factor that is activated under freezing stress in wood frogs to enhance antioxidant defense in anticipation of reperfusion during thawing is NF-κB. NF-κB is known to be activated in response to oxygen free radicals (Kumar *et al.*, 2004). Data generated from gene chip and Panomics array studies on liver samples from control versus frozen wood frogs identified several transcription factors that showed enhanced DNA binding during freezing, one of which was NF-κB (Storey, 2008). Previous work done by DeCroos (2003) also provided evidence that NF-κB is

activated at the early onset of freezing in the wood frog and suggested that target genes of NF-κB could play a crucial role during freezing. Previous gene screening studies also identified downstream targets of NF-κB that have strong potential to be upregulated during freezing stress (Storey, 2008). Two targets of NF-κB analyzed in this study were ferritin heavy chain and manganese superoxide dismutase; both are involved in antioxidant defense. Ferritin binds free iron and stores it in a non-toxic form (Orino and Watanabe, 2008; Knovich *et al.*, 2009) whereas MnSOD converts superoxide radicals to oxygen and hydrogen peroxide (Bubici *et al.*, 2004). The present study examined major proteins involved in the NF-κB pathway leading to enhanced gene expression of ferritin heavy chain and MnSOD.

Usually, NF-κB is activated via the classical pathway. In this pathway, the p50-p65 heterodimer is the most abundant form of NF-κB (Ahmed and Li, 2008). Total protein levels of p50 and p65 were assessed in wood frog skeletal muscle and liver. In addition, nuclear distributions of p50 and p65 were also assessed. Significant increases in total p50 and p65 were observed after 4 hours of freezing in both skeletal muscle and liver. Levels of p50 and p65 increased even further in wood frog liver after 24 hours but in wood frog skeletal muscle, levels fell somewhat but to values still significantly higher than controls. Total levels of p50 and p65 in the nucleus also rose significantly after 4 hours of freezing and increased even further after 24 hours frozen indicating that NF-κB moved into the nucleus during freezing to transcribe target genes. These data suggest that NF-κB is activated in the wood frog as an early response to freezing and that after 24 hours of freezing, NF-κB is still active.

NF-κB proteins can be targets of phosphorylation. The Rel A (p65) subunit is known to be phosphorylated by a variety of kinases. These phosphorylation events increase the transactivation potential of p65 (Viatour *et al.*, 2005). Levels of p65 phosphorylated at serine 536 were assessed in wood frog skeletal muscle and liver. Protein levels remained constant after 4 hours of freezing and then fell to levels significantly lower than controls after 24 hours of freezing in wood frog skeletal muscle. This data suggests that lower transactivation of p65 in muscle could be possible after long periods of freezing, since most changes take place soon after freezing begins. In wood frog liver, levels of p65 phosphorylated at serine 536 increased significantly after 4 hours of freezing and falling back to values similar to controls after 24 hours suggesting enhanced transactivation of p65 after initial onset of freezing in order to cope with the stress. This provides further evidence for NF-κB activation in wood frog liver after short term freezing.

In order for NF-κB to enter the nucleus and transcribe target genes, it must free itself from its interaction with IκB. This is accomplished by the action of the IκB kinase. IKK phosphorylates IκB in two places, serine 32 and serine 36 (Ravi and Bedi, 2004) and this causes the inhibitor to dissociate from NF-κB. Levels of IκB phosphorylated at serine 32 were assessed in wood frog muscle and liver. Interestingly, a significant decrease was observed after 4 hours of freezing in wood frog skeletal muscle, but by 24 hours of freezing levels increased to a point that they were significantly greater than controls. In wood frog liver, a significant increase in p-IκB was observed after 4 hours but by 24 hours levels had fallen to values not different from controls. These data are

consistent with an activation of NF-κB after long periods of freezing stress in wood frog skeletal muscle while an activation of NF-κB during the early onset of freezing in wood frog liver is likely.

Upon activation, NF-κB moves into the nucleus and transcribes a wide variety of genes. Two genes involved in antioxidant defense are ferritin heavy chain and MnSOD. Ferritin is responsible for storing iron in a non-toxic form. In particular, the heavy chain contains ferroxidase, which converts excess free iron into the non-toxic Fe(III) which is sequestered in the ferritin core (Orino and Watanabe, 2008; Knovich *et al.*, 2009). Excess free iron is a problem for cells because it can catalyze the formation of highly damaging ROS via the Fenton reaction. Protein levels of ferritin heavy chain were assessed in skeletal muscle and liver of wood frogs frozen for 4 hours and 24 hours. A significant increase in ferritin heavy chain in skeletal muscle after 4 hours frozen and an even greater increase after 24 hours suggests an upregulation of ferritin heavy chain in the muscle during freezing. Protein levels increased significantly after 4 hours of freezing in wood frog liver but decreased to values not significantly different from controls after 24 hours. This suggests an activation of antioxidant defenses in the form of ferritin heavy chain at the onset of freezing in wood frog liver. Transcript levels of ferritin were also assessed. Significant increases in transcript levels were observed in wood frog liver after 24 hours of freezing but no significant changes were observed in wood frog muscle. This also presents strong evidence for an upregulation of ferritin heavy chain during freezing in the wood frog. A study done by Bubici *et al.* identified ferritin heavy chain as a key mediator of NF-κB antioxidant activity by means of a gene array-based screen (Bubici *et al.*,

2004). This study provides even more support for the potential upregulation of ferritin heavy chain in the wood frog during freezing, possibly in preparation for the eventual thawing and reperfusion events.

An examination of the wood frog ferritin heavy chain nucleotide and amino acid sequences revealed that ferritin heavy chain shared a high identity with the sequence from a number of amphibians as well as with chicken and mammals. Indeed, the wood frog ferritin heavy chain nucleotide sequence shared 91% identity with the bullfrog sequence, 82% identity with the Asiatic toad sequence, 78% identity with the African and western clawed frog sequences, and 61% identity with the chicken, human, and mouse sequences (Appendix D). The amino acid sequence also showed high identity with other amphibians (89% identity with the Asiatic toad, African clawed frog, and western clawed frog) as well as 70% identity with the other species (Appendix D). Based on this information, it can be inferred that the wood frog ferritin heavy chain protein possesses the same functional domains and also performs the same functions as the ferritin heavy chain proteins from other species.

Another gene involved in antioxidant defense that is known to be regulated by NF-kB is MnSOD. This enzyme has the task of converting toxic superoxide radicals to oxygen and hydrogen peroxide. Bubici *et al.* (2004) also report an upregulation of MnSOD as part of the antioxidant activity of Nf-kB. Protein levels of MnSOD were assessed in wood frog skeletal muscle and liver after 4 hours and again at 24 hours of freezing. A significant increase in MnSOD was seen after 4 hours of freezing in both muscle and liver and levels remained elevated after 24 hours of freezing. This suggests

the possibility that MnSOD is upregulated under freezing stress by NF-kB in the wood frog in preparation for the re-introduction of oxygen during thawing.

Conclusion

An analysis of the NF-κB pathway in wood frog skeletal muscle and liver frozen for 4 hours and 24 hours revealed strong evidence for the upregulation of NF-κB protein subunits p50 and p65, as well as the phosphorylation of the p65 subunit and of the inhibitor protein IκB. Ferritin heavy chain protein levels increased significantly during freezing and transcript levels also increased significantly in wood frog liver suggesting that ferritin heavy chain is actively transcribed possibly as a preparatory mechanism for the eventual reperfusion event during thawing. Significant increases in MnSOD in both wood frog muscle and liver also suggest that MnSOD is another target in the NF-κB activation of antioxidant defenses in the wood frog during freezing in anticipation of the reactive oxygen species generated during reperfusion when the wood frog begins to thaw.

Chapter 5

GENERAL DISCUSSION

The wood frog, *Rana sylvatica*, is the primary model used for studying vertebrate freeze tolerance and much information has been accumulated on the physiological, molecular biological, and biochemical aspects of its ability to freeze completely and suffer minimal damage upon thawing (Storey and Storey, 2004a). Previous cDNA screening studies done in this laboratory gave evidence of putative upregulation of a variety freeze responsive genes in wood frog heart. These included the glucose transporter 4, which is relevant for cryoprotectant uptake, antioxidants thioredoxin and glutathione-S-reductase that suggest anticipatory changes that could defend against oxidative damage during reperfusion, and the receptor for advanced glycation end products (RAGE), which potentially plays a role in limiting protein glycation damage during freezing (Storey, 2004a; Storey, 2004b). Other studies also demonstrated activation of selected transcription factors in wood frog tissues during freezing including signal transducers of activated transcription (STATs) and forkhead box subclass family O (FOXOs) (Du, 2005; DeCroos, 2003; Bouffard, 2007; McNally, 2002).

Array technology was previously used to identify genes and transcription factors that were freeze-induced in frozen wood frogs compared to control frogs. Two such transcription factors identified were nuclear factor kappa B (NF-κB) and p53. This method identified a probable role for NF-κB and p53 in the wood frog during freezing stress, however, the results were not definitive since heterologous gene screening was done. Further studies were needed to provide more conclusive evidence to support these findings. That was the focus of this thesis. Transcription factor activity was assessed by measuring total protein levels as well as the relative content of posttranslationally

modified transcription factor. Nuclear distribution was also used to assess transcriptional activity by NF-κB and p53. Protein and transcript levels of selected downstream genes of the transcription factors of interest were also measured.

The NF-κB transcription factor is involved in cellular responses to stimuli including free radicals (Wietek and O'Neill, 2007). Usually, NF-κB is activated via the classical pathway which involves the phosphorylation and degradation of its inhibitor proteins and translocation of subunits, commonly p50 and p65 heterodimers, into the nucleus where NF-κB can transcribe its many target genes including those responsible for antioxidant defense (Schmitz *et al.*, 2004). Optimal activation of NF-κB involves phosphorylation of its subunits as well as its inhibitory proteins. Phosphorylation of p65 elevates its transactivation potential (Viatour *et al.*, 2005). Total protein levels and nuclear distributions of p50, p65, and phosphorylated p65 were measured in the skeletal muscle and liver of 4 hour and 24 hour frozen wood frogs. Significant increases in both total p50 and p65 and the nuclear content of p50 and p65 in muscle and liver during freezing suggested an activation of the NF-κB pathway at the early onset of freezing in the wood frog. This was further supported by increases in the amount of phosphorylated IkB. Protein levels of the NF-κB target genes ferritin heavy chain (FHC), which is responsible for storing iron in a non-toxic form, and manganese superoxide dismutase (MnSOD), which converts toxic superoxide radicals to oxygen and hydrogen peroxide were also measured in wood frog muscle and liver after 4 hours and 24 hours of freezing. Both play critical antioxidant roles in animals. Transcript levels of FHC were also measured in wood frog muscle and liver after 24 hours of freezing. Significant increases

in FHC protein levels in wood frog muscle at 4 hours and even higher increases after 24 hours provided strong evidence that elevated iron storage capacity contributes to cell protection during freezing. A similar pattern was observed in wood frog liver as significant increases in FHC protein levels were observed after 4 hours of freezing and in FHC transcript levels after 24 hours. It is also possible that ferritin is part of a preventative defensive system in the wood frog which is responsible for minimizing cumulative ROS damage over long periods of inactivity since metabolic depression reduces the ability to mend or restore molecules damaged by ROS (Storey and Storey, 2007). Increases in MnSOD in wood frog skeletal muscle and liver after 4 hours and again at 24 hours suggested that MnSOD is upregulated in the wood frog during freezing as an antioxidant mechanism in preparation for oxidative damage to come with the re-introduction of oxygen during thawing.

The p53 transcription factor is involved in the stimulation of genes involved in cell cycle arrest, among other things. To date, cell cycle arrest as a mechanism of metabolic rate depression has not been studied to any great extent (Storey and Storey, 2007). It is probable that organisms experiencing hypometabolism would halt or strongly suppress the cell cycle (an energy-expensive process) in proliferating, growing and developing cells and tissues. There is a possibility that the wood frog, *Rana sylvatica*, adopts this strategy as one of the many that it employs to reduce energy expenditures and maximize the time that frogs can remain viable during prolonged freezing exposures. Stabilization of p53 is a common response to a number of stresses including DNA damage, metabolic changes, hypoxia, and cold shock (Malkin, 2001; Ashcroft and

Vousden, 1999). Under conditions of stress, p53 is stabilized and activated by phosphorylation and acetylation actions which inhibit the interaction between p53 and its inhibitor protein, Mdm2 (Vogelstein *et al.*, 2000). p53 is then able to trigger transcription of target genes such as p21, GADD45α, and 14-3-3σ which are all involved in cell cycle arrest. Protein levels and nuclear distributions of p53 and several phosphorylated and acetylated forms of p53 were assessed in wood frog muscle and liver after 4 hours and again at 24 hours. Protein levels of Mdm2, p19ARF which prevents Mdm2 from ubiquitinating p53, p21, phosphorylated p21, GADD45α, and 14-3-3σ, and transcript levels of GADD45α and 14-3-3σ were also assessed in wood frog muscle and liver during freezing. Overall, significant increases were observed in protein levels of phosphorylated and acetylated p53 as well as decreased levels of Mdm2 after 4 hours and 24 hours of freezing. Significant increases in p19ARF levels in wood frog liver also provided more evidence for p53 activation. The liver of a wood frog is very important in producing the cryoprotectant glucose as well as plasma proteins that are important in surviving freezing. Therefore, it comes as no surprise that the wood frog liver employs more than one mechanism in order to activate p53 during freezing. Significant increases in the cell cycle inhibitor p21 after 4 hours of freezing in wood frog muscle and liver as well significant increases in the phosphorylation of p21 which acts to stabilize p21 (Li *et al.*, 2002; Child and Mann, 2006) and significant increases in protein and transcript levels of GADD45α and 14-3-3σ which are involved in G2 arrest all taken together strongly suggested that p53 mediated cell cycle arrest was occurring in wood frogs during freezing. This indicates that cell cycle suppression is an important part of freeze responsive metabolic rate depression in the wood frog during freezing.

Summary

An investigation of the antioxidant aspect of the NF-κB transcription factor in the wood frog showed evidence for upregulation of NF-κB and its target genes ferritin heavy chain and MnSOD. Significant increases in protein and transcript levels of ferritin heavy chain in wood frog liver suggested that ferritin heavy chain was being transcribed to scavenge and store free iron and minimize the potential for iron-mediated free radical generation during freeze/thaw. MnSOD protein levels also increased significantly during freezing in wood frog muscle and liver which suggested that MnSOD transcription was activated by Nf-κB during freezing, again in anticipation of the reactive oxygen species generated during the reperfusion events that take place when the wood frog starts to thaw.

An investigation of the p53 transcription factor in the wood frog during short term and long term freezing revealed that p53 was likely responsible for cell cycle arrest during freezing. The wood frog must slow its metabolism since oxygen is cut off from tissues during freezing so energy savings can be made by shutting off energy-expensive activities such as the cell cycle arrest. The data show that p53 was strongly activated after short term freezing in the wood frog which makes sense as this is the time where a shift is taking place from normal conditions to the frozen state; organs are freezing, cryoprotectants are being produced and a depression in cellular metabolism is occurring. A less pronounced p53 activation remained after long term freezing (24 hours) in the wood frog. This is probable since the frog has passed the transition period to a depressed

metabolism and maximum freezing has taken place. Therefore, it would make sense that p53 is less active at this stage of freezing in the wood frog than it is right after freezing is initiated.

Future Directions

To follow up the NF-κB antioxidant defence study, a variety of experiments could be conducted. First of all, it is known that freezing stress in wood frogs includes anoxia and dehydration (Storey and Storey, 2004a). It would be of interest to assess total protein levels and nuclear distributions of the p50 and p65 subunits of NF-κB and total protein levels of ferritin heavy chain and MnSOD of frogs subjected to dehydration versus long term anoxia. Such studies could help to pinpoint the specific stress (anoxia, cell dehydration) that is triggering the NF-κB pathway and lead to a better understanding of the function of the target proteins in freezing survival. It would also be of extreme interest to assess protein levels of p50 and p65 as well as ferritin heavy chain and MnSOD in wood frogs that have thawed for a period of time and therefore have had oxygen reintroduced to their systems and compare this to antioxidant defense preparation during freezing stress. A further increase in target protein levels during thawing could confirm the idea that gene up-regulation during freezing is in anticipation of the need for enhanced levels of the proteins when frogs thaw. NF-κB activity could also be assessed

in other important tissues such as the brain and heart of frozen wood frogs. The ultimate predictor of transcription factor activity is by assessing the amount of a transcription factor that is bound to DNA during stress (Storey, 2008). A DNA binding assay for the p65 subunit of NF-κB could be run where nuclear extracts from control, short term and long term frozen frogs would be assessed to determine the relative amount of p65 binding to the conserved promoter sequence and thereby fully confirm that transcriptional activity of NF-κB is elevated when frogs freeze. Previous studies using cDNA gene chips identified many freeze responsive genes in the wood frog including many that were related to antioxidant defense (Storey, 2004a; Storey, 2004b). Some examples are ferritin light chain, which works with ferritin heavy chain in order sequester free iron and convert it to a non-toxic form, metallothionein, a metal binding protein, and thioredoxin, a low molecular weight peptide reducing agent. Protein and mRNA levels of these genes could be assessed in muscle and liver from control, frozen and thawed frogs via western blotting and RT-PCR in order to determine other proteins involved in antioxidant defense are upregulated in concert with ferritin heavy chain and MnSOD. It would also be interesting to determine the full length nucleotide and corresponding amino acid sequences of wood frog ferritin heavy chain using 5' and 3' RACE PCR. This would allow for a complete comparative study between wood frog ferritin heavy chain protein and the ferritin heavy chain protein in other organisms.

The p53 cell cycle arrest study could be followed up in several ways. Since freezing involves dehydration and anoxia as mentioned above, it would be of interest to assess total protein levels and nuclear distributions of p53 and posttranslationally

modified p53 in dehydrated wood frogs as well as frogs subjected to long term anoxia. Protein levels of Mdm2, p21, GADD45α, and 14-3-3σ would also be measured in dehydrated and anoxic wood frogs. The p53 pathway can be activated by many mechanisms including DNA damage (Caspari, 2000). DNA damage is sensed by many extremely well conserved checkpoint proteins, some of which are kinases (Vogelstein *et al.*, 2000). Examples of these kinases are ataxia telangiectasia mutated (ATM), DNA-dependent protein kinase, Chk1 and Chk2. These kinases are known to phosphorylate p53 in the N terminal region which is significant since the inhibitor Mdm2 binds to the N terminal region as well. Other kinases of interest that phosphorylate p53 at the N terminal are jun-N-terminal kinase (JNK) and p38. Phosphorylation by these kinases leads to dissociation of Mdm2 from p53. It would be of interest to assess activity of these enzymes by kinase assays as well as levels of these kinases by western blotting in muscle and liver of frozen wood frogs and compare them to levels in control frogs. It would also be relevant to examine the activity of the wood frog cell cycle in more detail during freezing. Progression through the cell cycle is tightly regulated by cyclin dependent kinases (CDKs) whose activity is dependent on binding to proteins called cyclins. A number of these interactions allow progression through the cell cycle (Orzaez *et al.*, 2009). Growth factors signal production of cyclin D which binds to CDK4 forming a cyclin-CDK complex. This complex phosphorylates the retinoblastoma (Rb) protein, which is then decoupled from the E2F/Rb interaction. The E2F/Rb interaction prevents E2F from transcribing target genes needed for progression of the cell cycle. Free from Rb, E2F can transcribe genes such as cyclin E and cyclin A. Cyclin E forms a complex with CDK2, which allows cells to move from the G1 phase to the S phase. Later, cyclin

B combines with CDK1, forming a complex that moves cells from G2 to the mitotic phase. There exist two families of CDK inhibitors that work to stop cell cycle progression. The cip/kip family includes p21 (covered in the p53 chapter), p27, and p57. The INK4a/ARF family includes p16 and p19ARF (covered in the p53 chapter). Most of these inhibitors (excluding p19ARF) bind to specific cyclin-CDK complexes, inactivating them and arresting the cell cycle in the G1 phase. A rigorous assessment of protein and transcript levels of the many cyclins and CDKs involved in the cell cycle in frozen wood frogs would no doubt provide valuable insight as to what is going on when the wood frog cell cycle is halted in response to depressed metabolism during freezing. As with Nf-kB, a DNA binding assay for p53 could be run using frozen frog nuclear extracts. These extracts would be assessed for p53 DNA binding activity and the results could further confirm that the p53 transcription factor is activated in the wood frog during freezing. 5' and 3' RACE PCR could also be used to elucidate the full length nucleotide and corresponding amino acid sequences of wood frog GADD45α and 14-3-3σ. As with FHC, this would allow for a complete comparative study between wood frog GADD45α and 14-3-3σ proteins and the comparable proteins in other organisms.

REFERENCES

Ahmed, K. and Li, J. 2008. NF-κB-mediated adaptive resistance to ionizing radiation. *Free Radical Biology & Medicine* 44: 1-13.

Appella, E., and Anderson, C. 2001. Post-translational modifications and activation of p53 by genotoxic stresses. *European Journal of Biochemistry* 268: 2764-2772.

Ashcroft, M., and Vousden, K. 1999. Regulation of p53 stability. *Oncogene* 18: 7637-7643.

Bode, A., and Dong, Z. 2004. Post-translational modification of p53 in tumorigenesis. *Nature Reviews* 4: 793-805.

Bose, I., and Ghosh, B. The p53-MDM2 network: from oscillations to apoptosis. *Journal of Biosciences* 32: 991-997.

Bouffard, M. 2007. Involvement of FOXO transcription factors and glycogen synthase kinase 3 in the freeze tolerance capability of the wood frog, *Rana sylvatica* M.Sc. thesis, Dept of Chemistry, Carleton University.

Brooks, C., and Gu, W. 2003. Ubiquitination, phosphorylation and acetylation: the molecular basis for p53 regulation. *Current Opinion in Cell Biology* 15: 164-171.

Bubici, C., Papa, S., Pham, C., Zazzeroni, F., and Franzoso, G. 2004. NF-κB and JNK. *Cell Cycle* 3: 1524-1529.

Caspari, T. 2000. Checkpoints: How to activate p53. *Current Biology* 10: R315-R317.

Child, E.S., and Mann, D.J. 2006. The Intricacies of p21 Phosphorylation. *Cell Cycle* 5: 1313-1319.

Colman, M.S., Afshari, C.A., and Barrett, J.C. 2000. Regulation of p53 stability and activity in response to genotoxic stress. *Mutation Research* 462: 179-188.

Costanzo, J.P., Lee, R.E., and Lortz, P.H. 1993. Glucose concentration regulates freeze tolerance in the wood frog *Rana sylvatica. Journal of Experimental Biology* 181: 245-255.

De Croos, J.N.A 2003. Gene and protein regulation in liver of the freeze tolerant wood frog, *Rana sylvatica.* Ph.D. thesis, Dept of Biology, Carleton University.

Dignam, J.D., Lebovitz, R.M. and Roeder, RG. 1983. Accurate transcription initiantion by RNA polymerase II in a soluble extract from isolated mammalian nuclei. *Nucleic Acids Research* 11: 1475-1489.

Dotto, G. 2000. $p21^{WAF1/Cip1}$: more than a break to the cell cycle? *Biochimica et Biophysica Acta* 1471: M43-M56.

Du, J. 2005. Anti-apoptotic and antioxidant defenses in the freeze tolerant wood frog, *Rana sylvatica*. M.Sc. thesis, Dept of Chemistry, Carleton University.

El-Deiry, W. 1998. Regulation of p53 downstream genes. *Seminars in Cancer Biology* 8: 345-357.

Hermeking, H., and Benzinger, A. 2006. 14-3-3 proteins in cell cycle regulation. *Seminars in Cancer Biology* 16: 183-192.

Hermes-Lima M, Zenteno-Savín T. 2002. Animal response to drastic changes in oxygen availability and physiological oxidative stress. *Comperative Biochemistry and Physiology C Toxicology & Pharmacology*. 133(4):537-556).

Hermes-Lima, M., Storey, J.M. and Storey, K.B. 2001. Antioxidant defenses and animal adaptation to oxygen availability during environmental stress. In: Cell and Molecular Responses to Stress (Storey, K.B. and Storey, J.M., eds.), *Vol. 2: Protein Adaptations and Signal Transduction. Elsevier Press*, Amsterdam, pp. 263-287.

Ji, L.L., Gomez-Cabrera, M-C., and Vina, J. 2007. Role of nuclear factor κB and mitogen-activated protein kinase signalling in exercise-induced antioxidant enzyme adaptation. *Applied Physiology, Nutition, and Metabolism* 32: 930-935.

Jin, S., Mazzacurati, L., Zhu, X., Tong, T., Song, Y., Shujian, S., Petrik, K., Rajasekaran, B., Wu, M., and Zhan, Q. 2003. Gadd45a contributes to p53 stabilization in response to DNA damage. *Oncogene* 22: 8536-8540.

Joanisse, D.R., and Storey, K.B. 1996. Oxidative Damage and antioxidants in *Rana sylvatica*, the freeze-tolerant wood frog. *American Journal of Physiology* 271: R545-553.

Ju, Z., Choudhury, A.R., and Rudolph, K.L. 2006. A Dual Role of p21 in Stem Cell Aging. *Annals of the New York Academy of Sciences* 1100: 333-344.

Knovich, M.A., Storey, J.A., Coffman, L.G., Torti, S.V., and Torti, F.M. 2009. Ferritin for the clinician. *Blood Reviews* 23 95-104.

Kumar, A., Takada, Y., Boriek, A., and Aggarwal, B. 2004. Nuclear factor-κB: its role in health and disease. *Journal of Molecular Medicine* 82: 434-448.

Lakin, N., and Jackson, S. 1999. Regulation of p53 in response to DNA damage. *Oncogene* 18: 7644-7655.

Lavin, M., and Gueven, N. 2006. The complexity of p53 stabilization and activation. *Cell Death and Differentiation* 13: 941-950.

Layne, J.R. 1995. Crystallization temperatures of frogs and their individual organs. *Journal of Herpetology* 29: 296-298.

Layne, J.R., Costanzo, J.P., and Lee, R.E. 1998. Freeze duration influences postfreeze survival in the frog *Rana sylvatica*. *Journal of Experimental Zoology* 280: 197-211.

Lee, M-H., and Lozano, G. 2006. Regulation of the p53-MDM2 pathway by 14-3-3 σ and other proteins. *Seminars in Cancer Biology* 16: 225-234.

Levine, A., Hu, W., and Feng, Z. 2006. The P53 pathway: what questions remain to be explored? *Cell Death and Differentiation* 13: 1027-1036.

Li, Y., Dowbenko, D., and Lasky, L.A. 2002. AKT/PKB Phosphorylation of $p21^{Cip/WAF1}$ Enhances Protein Stability of $p21^{Cip/WAF1}$ and Promotes Cell Survival. *Journal of Biological Chemistry* 277: 11352-11361.

Lierbermann, D.A., and Hoffman, B. 2007. Gadd45 in the response of hematopoietic cells to genotoxic stress. *Blood Cells, Molecules, and Disease* 39: 329-335.

Malkin, D. 2001. The role of p53 in human cancer. *Journal of Neuro-Oncology* 51: 231-243.

McNally, J.D. 2002. Response to freeze exposure by the wood frog, *Rana sylvatica*: investigating the freeze induced changes in transcription and translation patterns in heart and liver. Ph.D. thesis, Dept of Chemistry, Carleton University.

Meek, D. 1998. Multisite Phosphorylation and the Integration of Stress Signals at p53. *Cellular Signaling* 10: 159-166.

Moll, U.M., and Petrenko, O. 2003. The MDM2-p53 interaction. *Molecular Cancer Research* 1: 1001-1008.

Orino, K. and Watanabe, K. 2008. Molecular, physiological and clinical aspects of the iron storage protein ferritin. *The Veterinary Journal* 178: 191-201.

Orzáez, M., Gortat, A., Mondragón, L., Bachs, O., and Pérez-Payá, E. 2009. ATP-Noncompetitive Inhibitors of CDK-Cyclin Complexes. *ChemMedChem* 4: 19-24.

Prives, C. and Hall, P. 1999. The P53 Pathway. *Journal of Pathology* 187: 112-126.

Ravi, R. and Bedi, A. 2004. NF-κB in cancer – a friend turned foe. *Drug Resistance Updates* 7: 53-67.

Schmitz, M., Mattioli, I., Buss, H., and Kracht, M. 2004. NF-κB: A Multifaceted Transcription Factor Regulated at Several Levels. *ChemBioChem* 5: 1348-1358.

Sherr, C.J. 2006. Divorcing ARF and p53: an unsettled case. *Nature Reviews Cancer* 6: 663-673.

Shu, K-X., Li, B., and Wu, L-X. 2007. The p53 network: p53 and its downstream genes. *Colloids and Surfaces B: Biointerfaces* 55: 10-18.

Steegenga, W.T., van der Eb, A.J., Jochemsen, A.G. 1996. How Phosphorylation Regulates the Activity of p53. *Journal of Molecular Biology* 263: 103-113.

Storey, J.M., and Storey, K.B. 2004b. Cold Hardiness and Freeze Tolerance. Pp. 473-503 in Storey, K.B. (ed.), *Functional metabolism: regulation and adaptation.* Wiley-Liss, Hoboken, NJ.

Storey, J.M., and Storey, K.B. 1985. Triggering of cryoprotectant synthesis by the initiation of ice nucleation in the freeze tolerant frog, *Rana sylvatica. Journal of Comparative Physiology B* 156: 191-195.

Storey, K.B. 1987. Organ-specific metabolism during freezing and thawing in a freeze-tolerant frog. *American Journal of Physiology* 253: R292-R297.

Storey, K.B. 2004a. Vertebrate freeze tolerance: role of freeze-responsive gene expression. Pp. 299-306 in Barnes, B.M. & Carey, H.V. (eds), *Life in the cold: evolution, mechanism, adaptation, and application.* Biological Papers of the University of Alaska 27, Fairbanks, Alaska.

Storey, K.B. 2004b. Strategies for exploration of freeze responsive genes expression: advances in vertebrate freeze tolerance. *Cryobiology* 48: 134-145.

Storey, K.B. 2008. Beyond gene chips: transcription factor profiling in freeze tolerance. Pp. 101-108 in Lovegrove, B.G. & McKechnie, A.E. (eds.), *Hypometabolism in animals: hibernation, torpor and cryobiology.* University of KwaZulu-Natal, Pietermaritzburg.

Storey, K.B., and Storey, J.M. 2007. Putting life on 'pause' – molecular regulation of hypometabolism. *Journal of Experimental Biology* 210: 1700-1714.

Storey, K.B., and Storey, J.M. 1984. Biochemical adaptation for freezing tolerance in the wood frog, *Rana sylvatica. Journal of Comparative Physiology B* 155: 29-36.

Storey, K.B., and Storey, J.M. 1986. Freeze tolerance and intolerance as strategies of winter survival in terrestrially-hibernating amphibians. *Comparative Biochemistry and Physiology Part A* 83: 613-617.

Storey, K.B., and Storey, J.M. 2004a. Physiology, biochemistry and molecular biology of vertebrate freeze tolerance: the wood frog. Pp. 243-274 in Benson, E., Fuller, B. & Lane, N. (eds), *Life in the frozen state.* CRC Press, Boca Raton.

Taylor, W. and Stark, G. 2001. Regulation of the G2/M transition by p53. *Oncogene* 20: 1803-1815.

Tergaonkar, V. 2006. NFκB pathway: A good signaling paradigm and therapeutic target. *The International Journal of Biochemistry & Cell Biology* 38: 1647-1653.

Viatour, P., Merville, M-P., Bours, V., and Chariot, A. 2005. Phosphorylation of NF-κB and IκB proteins: implications in cancer and inflammation. *TRENDS in Biochemical Sciences* 30: 43-52.

Vogelstein, B., Lane, D., and Levine, A. 2000. Surfing the p53 network. *Nature* 408: 307-310.

Wegener, E., and Krappmann, D. 2008. Dynamic Protein Complexes Regulate NF-κB Signaling. Pp. 237-259 in Klussmann, E., and Scott, J. (eds.), *Protein-protein interactions as New Drug Targets.* Handbook of Experimental Pharmacology 186.

Wietek, C., and O'Neill, L. 2007. Diversity and regulation in the NF-κB system. *TRENDS in Biochemical Sciences* 32: 311-319.

Willmore, W.G. 2004. Control of transcription in eukaryotic cells. Pp. 153-187 in Storey, K.B. (ed.), *Functional metabolism: regulation and adaptation.* Wiley-Liss, Hoboken, NJ.

Zhan, Q. 2005. Gadd45a, a p53- and BRCA1-regulated stress protein, in cellular response to DNA damage. *Mutation Research* 569: 133-143.

Appendix A: Protein kinases known to phosphorylate p53 and the corresponding molecular/cellular outcome

Table 1 | **Protein kinases known to phosphorylate p53**

Kinase(s)	Activated by	Phosphorylation site on p53	Molecular or cellular outcome	References
ATM	DNA damage	Ser15	Apoptosis	130
ATR	γ-radiation, UV light	Ser15, Ser37	Apoptosis	131
AURKA	Overexpression of AURKA	Ser315	Ubiquitylation and degradation of p53	123
CDK (CDC2/CDK2)	UV light	Ser315	Increased p53 transcription	132
CHK1/CHK2	Ionizing radiation	Ser20	Disruption of the MDM2–p53 complex	133,134
CK1	Topoisomerase-directed drugs and DNA damage	Ser6, Ser9, Thr18 (requires prior phosphorylation of Ser15)	Stabilization of p53 through inhibition of MDM2	21,22, 28,135
CSN-associated kinase complex	Unstressed	Thr150, Thr155, Ser149	Degradation	121
DNAPK	DNA damage	Ser15, Ser37	Disruption of the MDM2–p53 complex	136
ERKs	UV light	Ser15	Apoptosis	137
ERK2	Doxorubicin	Thr55	Activation of p53	138
FACT*–CK2	UV light	Ser392	Increased p53 activity	139
GSK3β	Endoplasmic reticulum stress	Ser315, Ser376	Inhibition of p53-mediated apoptosis	140
HIPK2	UV light	Ser46	Facilitates CBP-mediated acetylation of p53 (at Lys382); arrest; apoptosis	141,142
JNK	UV light	Ser20	Apoptosis	143
JNK	DNA damage	Thr81	Stabilization	23
MAPKAPK2	UV light	Ser20	Apoptosis	143
p38 kinase	UV light	Ser15	Apoptosis	137
p38 kinase	UV light	Ser33, Ser46	Stabilized p53; apoptosis	144
p38 kinase	UV light DNA damage	Ser392	Increased DNA-binding activity of p53	145
PKC	Unstressed; constitutively phosphorylated and dephosphorylated with IR light	Ser376 and Ser378	Ubiquitylation and degradation; increased DNA-binding affinity	20,146
PKR‡	Interferon	Ser392	ND	147
TAF1§	Constitutively phosphorylated	Thr55	Degradation of p53/ stabilization of p53	19,122

Bode and Dong 2004

Appendix B: 14-3-3σ nucleotide alignments, protein alignments, and homology trees

A)

Wood frog 14-3-3σ partial nucleotide sequence aligned with African clawed frog (*Xenopus laevis*), chicken (*Gallus gallus*), human (*Homo sapiens*), and mouse (*Mus musculus*) nucleotide sequences. Genbank accession numbers for the four comparison sequences are respectively NM_001086903, NM_001031477, BC020963, and NM_018754. Dashes (-) represent nucleotides in sequences of other species that are identical to the wood frog sequence.

B)

Homology tree comparing the wood frog partial nucleotide sequence with the comparable segments of the African clawed frog, chicken, human, and mouse 14-3-3σ sequences.

A)

```
Wood_frog            ....................................A      1
African_clawed_frog aaagccgtgacggagcagggcgccgagctgtccaacgagg    172
Chicken             aaggcggtggtggagcacggcgacgagctgtccaacgagg    153
Human               aaaggcgccgtggagaagggcgaggagctctcctgcgaag    189
Mouse               aagagcgccgtggaaaagggcgaggagctctcctgcgagg    517

Wood_frog           GAAGGAACCTTCTTTCTGTTGCTTACAAGAATGTGGTTGG     41
African_clawed_frog agc-c-----g--g--g--g--c-----a--c-----a--    212
Chicken             agc-c-----c--c--c--c--c--------c-----g--    193
Human               agc-a-----g--c--a--a--c--t-----c-----g--    229
Mouse               agc-a-----g-----c--a-----------c-----g--    557

Wood_frog           AGCAAGGAGGTCTTCTTGGAGGGTCATTTCCAGCATTGAG     81
African_clawed_frog g-gcc-c-----cg-c-----------c--g---------    252
Chicken             ctgcca-c-c--gg-c-----------c--------c---    233
Human               c-gcca----g--g-c--------gc-g-----t------    269
Mouse               c-gcca---ag-gg-c---------c-g--------c---    597

Wood_frog           CAGAAGTCAGGTGA......ATCGGAAAAGAAGCTGCAAT    115
African_clawed_frog ------a-c-acac......c--t--c------t----gc    286
Chicken             --c--aa-c.................g--g--ggcg-cg    255
Human               -----aagcaac--ggagggc-----gg-----gg--ccg    309
Mouse               ------agcaac--ggagggg--a---g-----ggc-ccg    637

Wood_frog           T............GACTAAAGAATACCGGGAGAAAATAGA    143
African_clawed_frog -............--tc--g--c--t---------g-g--    314
Chicken             acaaagcgcagct-gtg--c--g-----------gg-g--    295
Human               a............-gtgcgt--g-----------gg-g--    337
Mouse               a............-gtg-----g-----------gg----    665

Wood_frog           GTGCGAGCTCAAGAGTGTTTGTGACACGGTTTTGGATCTG    183
African_clawed_frog --cg-----g-g-tcca-c--cac------cc----at--    354
Chicken             agag-----g---g-c--c--ca--gt---gc---gct--    335
Human               -act------c--g-c--g--c-----c--gc---gc---    377
Mouse               -ac--------gag----g--c-----c--ac-c-gc---    705

Wood_frog           CTTAAGGATTTCTTAATTCCTAAAGCCACGCAACCAGAGT    223
African_clawed_frog t-gg-ta-g-at-----ag-c--t--a--ta-t------a    394
Chicken             --gg--a-gca-c-c--caag--g---ggcg-cg-c---a    375
Human               --gg-cagcca-c-c--caagg-g---gg-g-cg-c---a    417
Mouse               --gg-ctcgca-c-c--caaaggg--tggag-tg-----a    745

Wood_frog           GCAAAGTATTTTACCTGAAGATGAAAGGGGACTATTACCG    263
African_clawed_frog -t--g--c--c--t-----a-----g--a--t----t---    434
Chicken             -------g--c--------------g--a-----c-t---    415
Human               --cgg--c--c--------------g--t-----c-----    457
Mouse               --cgc--c--c--------------g--t-----c-----    785

Wood_frog           ATACCTTTCAGAGGTGGCGAAGGATACTGAGAGAACTGAG    303
African_clawed_frog g--t---g-t--a--a--ttgt-gcga---tc---aac-a    474
Chicken             ------gg-c---.......t..................    429
Human               c-----gg-c---.......gt-gccaccg-t--cgac-a    490
```

```
Mouse                 c-----ag-c---.......gt-gccactg-c--tgac-a    818

Wood_frog             ACAATAGACCTCT.......CACAACAAGCTTATCAAGAA    336
African_clawed_frog   --------aaat-.......-c---gg---c--c-----g    507
Chicken               ....................................        429
Human                 ga-gcgc-t-at-gactcag-c-ggtc---c--c--g--g    530
Mouse                 ga-gcgc-t-atcgattctg-c-ggtc---c--c--g--g    858

Wood_frog             GCATTTGACATCAGCAAGGAGAAAATGCAGCCAACCCACC    376
African_clawed_frog   --g-----t--a------a--g-g--------t--g--t-    547
Chicken               ....................................        429
Human                 --ca-g------------a--g-g----c---c---a---    570
Mouse                 --ca-g------------a--g-g----c---t---a---    898

Wood_frog             CCATCCGCTTGGGCTTAGCCCTAAATTTTTCCGTATTCTA    416
African_clawed_frog   -a------c----gc-g--t--t--c-----t-----t--    587
Chicken               ....................................        429
Human                 --------c-----c-g-----g--c--------c---c-    610
Mouse                 --------c-----c-g-----g--c-----a--c---c-    938

Wood_frog             TTATGAAATTCTTAATAGCCCAGAAAAGGCTTGTTCACTG    456
African_clawed_frog   c-----g--c-------at-----gctt--c--ca-----    627
Chicken               ....................................        429
Human                 c--c--g--cgcc--c-----c--gg----catc--t---    650
Mouse                 c--c--g--agcc--c-----c--gg----catc--g---    978

Wood_frog             GCAAAGACTGCATTTGACGAGGCCATCGCCGA........    488
African_clawed_frog   --t--a--g--t-----t-----------a--gcttgata    667
Chicken               ....................................        429
Human                 --c-----ca-t--c-----------g--t--tctgcaca    690
Mouse                 --c-----ca-c--c-----------g-----cctgcaca   1018
```

B)

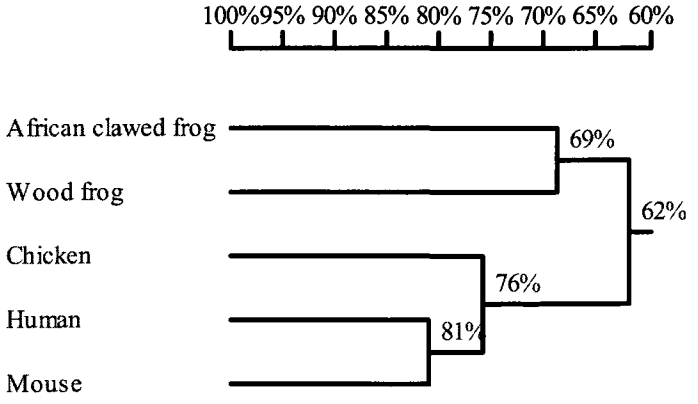

C)

Wood frog 14-3-3σ partial amino acid sequence aligned with the African clawed frog (*Xenopus laevis*), chicken (*Gallus gallus*), human (*Homo sapiens*), and mouse (*Mus musculus*) nucleotide sequences. Genbank accession numbers for the chicken, human, and mouse comparison sequences are respectively AAS92204.1, AAC52030.1, and AAF36093.1. The African clawed frog amino acid sequence was not in the Genbank database but was obtained by translating the nucleotide sequence seen in Fig. 3.10 (from NM_001086903) to the corresponding amino acids using Expasy. Three residues in the wood frog sequence were unique substitutions as compared with the sequences for all the other animals; these are shown in bold underline and are residues 19, 75 and 91 of the partial wood frog sequence.

D)

Homology tree for 14-3-3σ amino acid sequences

C)

```
Wood frog           ....................................      0
African clawed frog .................mekteliqkaklaeqaeryddm    22
Chicken             .................marnhqvqkaklaeqaeryedm    22
Human               .................merasliqkaklaeqaeryedm    22
Mouse               .................merasliqkaklaeqaeryedm    22

Wood frog           .................RRNLLSVAYKNVV.GARRSSWRV    22
African clawed frog atcmkavteqgaelsnee------------.-g---a---    61
Chicken             adfmkavvehgdelsnee------------.-cq--a---    61
Human               aafmkgavekgeelscee------------g-.q-aa---    61
Mouse               aafmksavekgeelscee------------v-.q-aa---    61

Wood frog           ISSIEQKS.GES.EKKL.QLTKEYREKIECELKSVCDTVL    59
African clawed frog -------t.dt-.d---.--i-d----v-s--r-i-t---    98
Chicken             -----h-t.e-g.dd-a.--vn-----v-e---g--nv--    98
Human               l-------ne-gs-e-gpe.vr-----v-t--qg------   100
Mouse               l-------ne-gs-e-gpe.v------v-t--rg------   100

Wood frog           DLLKD.FLIPKATQPECKVFYLKMKGDYYRYLSEVA.KDT    97
African clawed frog e--.-ky--an--n--s-----------f---a---cg-.   136
Chicken             g--.ekh--k--gda-s-----------f---a-......   131
Human               g--.-sh--ke-gda-sr--------------a---tg-.   138
Mouse               g--.-sh--kg-gda-sr--------------a---tg-.   138

Wood frog           ERTETIDLSQQAYQEAFDISKEKMQPTHPIRLGLALNFSV   137
African clawed frog d-kq--en--g----------ke-----------------   176
Chicken             ....................................      131
Human               dkkri--sars-----m----ke-p--n------------   178
Mouse               dkkri--sars-----m----ke-p--n---p--------   178

Wood frog           FYYEILNSPEKACSLAKTAFDEAIA.............     162
African clawed frog -------n--l--t----------eldtlnedsykdstl   216
Chicken             ....................................      131
Human               -h---a----e-i-----t----m-dlhtlsedsykdstl   218
Mouse               -h---a----e-i-----t----m-dlhtlsedsykdstl   218

Wood frog           ....................................      161
African clawed frog imqllrdnltlwtsdsageecdaaegaenrhpghqppspq   256
Chicken             ....................................      131
Human               imqllrdnltlwtadnagee.....g......geapqepqs  248
Mouse               imqllrdnltlwtadsagee.....g......gdwpeepq   247
```

D)

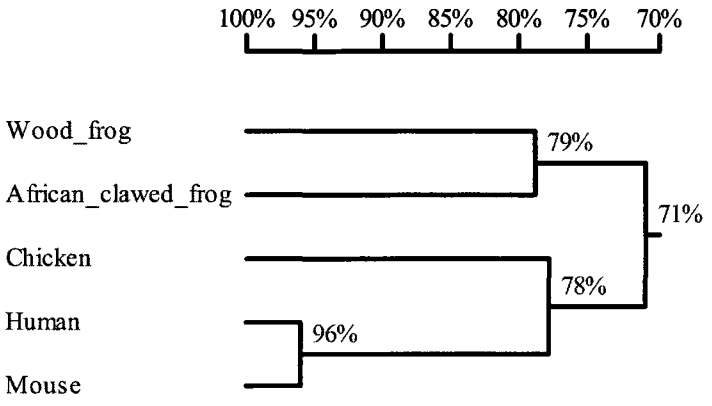
100% 95% 90% 85% 80% 75% 70%
Wood_frog
African_clawed_frog
Chicken
Human
Mouse
79%
71%
78%
96%

Appendix C: GADD45α nucleotide alignments, protein alignments, and homology trees

A)

Wood frog GADD45α partial nucleotide sequence aligned with the African clawed frog (*Xenopus laevis*), western clawed frog (*Xenopus tropicalis*), chicken (*Gallus gallus*), human (*Homo sapiens*), and zebrafish (*Danio rerio*) nucleotide sequences. Genbank accession numbers for the comparison species are respectively: NM_001086068, NM_001016151, DQ358721, NM_001924, and BC075932. Dashes (-) represent nucleotides in the sequences of other species that are identical to the wood frog sequence.

B)

Homology tree comparing the wood frog partial nucleotide sequence with the comparable segments of the African clawed frog, Western clawed frog, chicken, human, and mouse GADD45α sequences.

A)

```
Wood_frog             ..........................GCTCTACAGATT     12
African_clawed_frog   tactgatgataaagacaatcaggatgtc---t--------   377
Western_clawed_frog   tactgacgatacctacgatcaggatatc---t-------c   328
Chicken               cgccgacgaggaagaagaaggagacgcg-----g--a--c   222
Human                 ggcggacgaggacgacgacagagatgtg-----g-----c   514
Zebrafish             cactgacgacgacgatgtgaaggatgtg--g--t------   308

Wood_frog             CACTTCACTCTGATCCAGGCTTTCTGCTGCGAGAATGACA     52
African_clawed_frog   --t-----c-----------a--t-----t----------   417
Western_clawed_frog   --------c-----------a--t-----t----------   368
Chicken               --t------t-a-----a----------------c----   262
Human                 --------c-----------g--t-----------c----   554
Zebrafish             -----------c----------------------c----   348

Wood_frog             TCAACATCCTGAGAGTGAGCAACATGAGCCGGCTGGCTGA     92
African_clawed_frog   ----------------------------t--------c--   457
Western_clawed_frog   ---------------------------------a-----   408
Chicken               -----------c-g--c------cc-gct--ct----cc-   302
Human                 -----------c-c--c------cc-g----------g--   594
Zebrafish             -----------c-c----a-----c-c-g--c--c--ga-   388

Wood_frog             GATCCTGGGCGGCTCTGACAAGCCGGGAGAACCTGCCGAC    132
African_clawed_frog   ------------------------a--g--------t--t   497
Western_clawed_frog   ------------------------t--g--------t--t   448
Chicken               -t-gt--cttcc-gac-g-gg---t-a-cc-.........   333
Human                 -c-----ct-ttggagac-g-cg-t--ccccg-g--gag-   634
Zebrafish             c-----c--g---g-a-g--t--ac--gagcgagcagatg   428

Wood_frog             ........................CTGCATTGTATTCTAA    148
African_clawed_frog   ........................----------------   513
Western_clawed_frog   ........................----------------   464
Chicken               ..............cccactgat--c-----cg-ct-gg   358
Human                 gagggcgccgagcagcccccggac-----c--cg-g--gg   674
Zebrafish             gact.....................----c--c-----gg   447

Wood_frog             TCAACAACCCGCACGCTTCTCAGCTAAAGGATCCCGCCAT    188
African_clawed_frog   ----------a--t-aa-ta---a-c--------t--tc-   553
Western_clawed_frog   ------g---a--t-aa-ta---g-g--------t--tc-   504
Chicken               ---cg--t--c-----c--c--atgg--------a--gc-   398
Human                 -g-cg--t--a--tt-a-----atgg--------t---t-   714
Zebrafish             ---cggtt--a--t--g--cacatgg---a-c--g--tc-   487

Wood_frog             CAACAAAGTGAGCAACTTCTGCAAAGAGAGCCGCTACCTG    228
African_clawed_frog   ---ag------tttgt-a---------a--t--t--t---   593
Western_clawed_frog   ---ag------tttgt-a------------t--t------   544
Chicken               g-gtc-gc---tgtg-------cgg-----t-----ta--   438
Human                 a-gtc--c-t-tttgt--t---cgg--a--t------a--   754
Zebrafish             ggga-------a-cg--------g-----------gta--   527

Wood_frog             GATCAGTGGGTTCCCGTGATCAACCTGCCCGAGCGA....    264
African_clawed_frog   --c--a-----g--t-----t--------a------tgat   633
Western_clawed_frog   --c--------g--t-----t--------a------tgat   584
Chicken               -----------g--g-----------c-----a--gtgac   478
Human                 -----a--------a-----t--t--c--t--a--gtgat   794
Zebrafish             -----------g---a-t--------t--a------tgag   567
```

B)

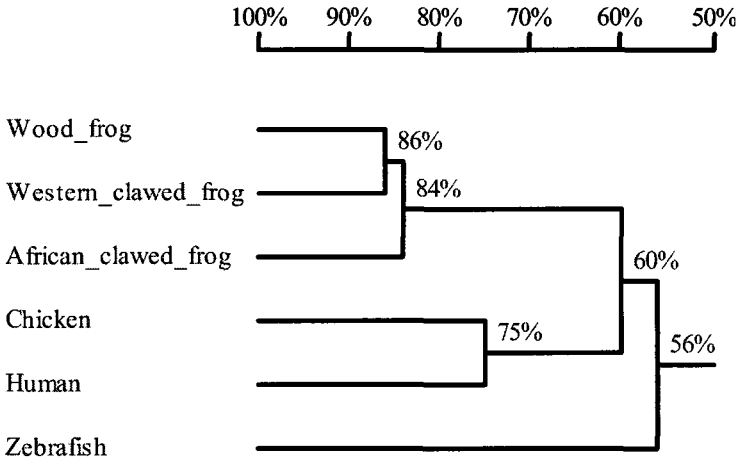
100%
90%
80%
70%
60%
50%
Wood_frog
Western_clawed_frog
African_clawed_frog
Chicken
Human
Zebrafish
86%
84%
60%
75%
56%

C)

Wood frog GADD45α partial amino acid sequence aligned with the African clawed frog (*Xenopus laevis*), western clawed frog (*Xenopus tropicalis*), chicken (*Gallus gallus*), human (*Homo sapiens*), and zebrafish (*Danio rerio*) nucleotide sequences. Genbank accession numbers for the comparison species are respectively: NP_001079537.1, NP_001016151.1, ABC88379.1, NP_001915.1, and NP_001002216.1. Dashes (-) represent nucleotides in the sequences of other species that are identical to the wood frog sequence.

D)

Homology tree for GADD45α amino acid sequences

C)

```
Wood_frog             ....................................      0
African_clawed_frog   mtleeqlsgdqsigkmesvgnaleevlheaklqrtitigv   40
Western_clawed_frog   mtleeqlsgdqsigkmesvgnaleevlckaklqrtitigv   40
Chicken               mtleelpgdqrtagrmeqagdaleevlskalsqrsltlgv   40
Human                 mtleefsageqktermdkvgdaleevlskalsqrtitvgv   40
Zebrafish             mtfee.pcgdnatermdsvekaleevltaalpqgcitvgv   39

Wood_frog             ..........................ALQIHFTLIQA      11
African_clawed_frog   yeaakllnvdpdnvvlcllatddkdnqdv-----------   80
Western_clawed_frog   yeaakllnvdpdnvvlcllatddtydqdi-----------   80
Chicken               yeaakllnvdpdnvvlcllaadeeeegda-----------   80
Human                 yeaakllnvdpdnvvlcllaadedddrdv-----------   80
Zebrafish             yeaakslnvdpdnvvlcllatdeedvkdv-----------   79

Wood_frog             FCCENDINILRVSNMSRLAEILGGS.D.KP....G.EP.A   43
African_clawed_frog   -------------------------.-.--....-.--.-   112
Western_clawed_frog   -------------------------.-.--....-.--.-   112
Chicken               --------------pa---ql-lpd........g-p--pt   112
Human                 --------------pg----l-llet-ag-aase-a-qpp   120
Zebrafish             ------------n--r------..e.gm--...g-.-s.m   111

Wood_frog             DLHCILINNPHASQLKDPAINKVSNFCKESRYLDQWVPVI   83
African_clawed_frog   -----------el-i----lke-icy--------------   152
Western_clawed_frog   --------s--el-v----lke-icy--------------   152
Chicken               ----v-vt------w----lsqlmc--r----m-------   152
Human                 ----v-vt---s--w----lsqlic--r----m-------   160
Zebrafish             ----v-vt--qs-tw----ls-lnr--rd--g--------   151

Wood_frog             NLPER..                                    88
African_clawed_frog   ----.r.                                    157
Western_clawed_frog   -----..                                    157
Chicken               ----..r                                    157
Human                 ----.r.                                    165
Zebrafish             -----..                                    156
```

D)

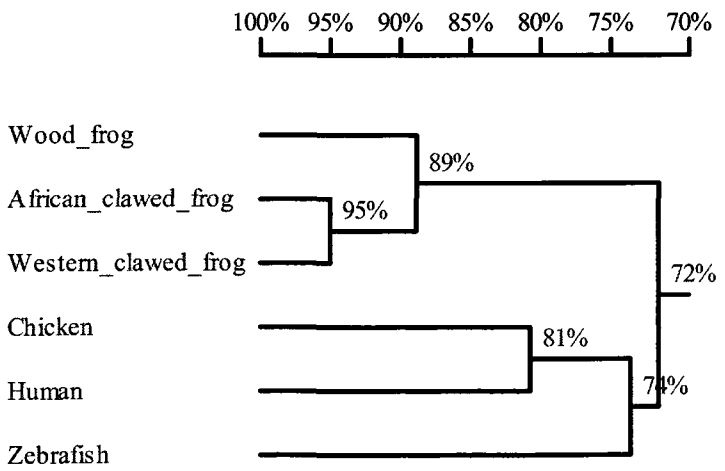

Appendix D: Ferritin Heavy Chain nucleotide alignments, protein alignments, and homology trees

A)

Wood frog ferritin heavy chain partial nucleotide sequence aligned with the sequences (Genbank accession numbers in parentheses) from bullfrog, *Rana catesbeiana* (M15655), African clawed frog, *Xenopus laevis* (BC170382), Western clawed frog, *Xenopus tropicalis* (NM_203677), Asiatic toad, *Bufo gargarizans* (DQ437112), chicken, *Gallus gallus*, (NM_205086.1), human, *Homo sapiens* (BC000857) and mouse, *Mus musculus* (NM_010239). Dashes (-) represent nucleotides in the other sequences that are identical to the wood frog sequence. Dots (.) represent areas in the sequence where nucleotides are absent.

B)

Homology tree for ferritin heavy chain nucleotide sequences comparing the partial sequence from wood frog with the same region of the bullfrog, Asiatic toad, African clawed frog, western clawed frog, chicken, human, and mouse sequences.

A)

```
Wood_frog           .....................................GAA      3
Bullfrog            aaagtcacgaagagagggagcatgctgagaaattgat---    344
African_clawed_frog agagtcacgaggaaagggagcacgccgaaaagttcctc--    375
Western_clawed_frog agagtcatgaggaaagggagcatgccgaaaagttcctc--    326
Asiatic_toad        agagccatgaagagcgagagcatgctgagaagttact---    356
Chicken             agtcccacgaggagcgtgaacatgctgagaagctgat---    363
Human               aatctcatgaggagagggaacatgctgagaaactgat---    450
Mouse               aatctcatgaggagagggagcatgccgagaaactgat---    360

Wood_frog           ATATCAAAACAAGCGTGGGGGACGCGTTGTCCTGCAGGAC     43
Bullfrog            gg----g-----a--------t---a-------------t    384
African_clawed_frog ---c--------a--------c--t--c-----t-----t    415
Western_clawed_frog ---c--------a--------c----cc-----t-----t    366
Asiatic_toad        g-----g--------------c---a--------------    396
Chicken             gctg------c--a-g--t------a-ct--t--------    403
Human               gctg--g---c-a--a--t--c--aa-ct----t-----t    490
Mouse               gctg--g---c----a--t--c--aa-ct----------t    400

Wood_frog           GTCAAGAAACCAGAGCGTGATGAATGGGGTAACACCCTGG     83
Bullfrog            ----------------------------------------    424
African_clawed_frog a-------------------c------a------------    455
Western_clawed_frog a-------------------c-------------------    406
Asiatic_toad        a-t--------t--a-t------g---acc-----t----    436
Chicken             a----------g--t--------c----ag--tgga---a    443
Human               a-------------ct-------c----ag-g-ggg---a    530
Mouse               a-a-----------c--------c----ag-g-ggg---a    440

Wood_frog           ATGCCATGCAGGCTGCTCTGCAGCTGGAAAAGACCGTGAA    123
Bullfrog            -g---------------------------------t-----    464
African_clawed_frog -a-----------c--------at----g----------    495
Western_clawed_frog -a-----------c--------------g-----t-----    446
Asiatic_toad        -g--------------------------g-----t-----    476
Chicken             c---a---g--tg---c-----c-----g----at-----    483
Human               ----a---g--tg---at-a--tt-------a-at-----    570
Mouse               ----a---g--tg---a-----ct---------gt-----    480

Wood_frog           TCAGGCTCTTCTGGACCTGCACAAGCTGGCATCTGACAAA    163
Bullfrog            ------c-----------------ag---g---------g    504
African_clawed_frog c-----ct-g-----t-----------------c-----g    535
Western_clawed_frog c------t-a-----t----------------------g    486
Asiatic_toad        c-----c---t----t--t------g----c---------    516
Chicken             c---t-g--gt-a--g--------at-----a----a--g    523
Human               ----t-a--a-----a--------a-----ca--------    610
Mouse               ----t-a--a-----a--------a-----ta-------g    520

Wood_frog           GTTGACCCCCATCTGTGTGATTTCCTGGAAACGGAATACC    203
Bullfrog            --------------------c---t----g--t-------    544
African_clawed_frog -----t--t--g--c-----c-----t---t-t--g---t    575
Western_clawed_frog ac---t--t-----c--c--c---------t-t--g---t    526
Asiatic_toad        --------t--a--t-----c---------t-t--g---t    556
Chicken             aa------a--ct-------c---a-t--g--tc-c----    563
Human               aa----------t-------c---a-t--g--ac-t----    650
```

```
Mouse                 aa---t-----ct-a-----c---a-t--g---t-t--t-    560

Wood_frog             TGGAGGAACAGGTGAAGGATATTAAACACTTTGGAGATTA    243
Bullfrog              ----------------tc------g--gc----------    584
African_clawed_frog   ------------------cc--g--gg-gc-------c--    615
Western_clawed_frog   ------------------cc--g--gg-gc-------c--    566
Asiatic_toad          ----a--------a----c------g--gc-------c--    596
Chicken               ----t--g--------a-cc--c--g--gc-g--t--cc-    603
Human                 --a-t--g--------a-cc--c---g-a--g--t--cc-    690
Mouse                 --agt-----------atcc------g-ac-g--t--cc-    600

Wood_frog             CATCACCAACCTGAAACGCCTTGGGCTGCCCGAGAACGGC    283
Bullfrog              ---------------g--------------ac--------    624
African_clawed_frog   ---------------g---------g----gc----t---    655
Western_clawed_frog   ------a--------g---------g----gc----t---    606
Asiatic_toad          ---------------g---------g-a--ac--------    636
Chicken               tg-g---------cggaaga-g---gca---a--t-t---    643
Human                 -g-g------t--cgcaaga-g--agc------atct---    730
Mouse                 -g-g------t-acgcaaga-g--tgcc--t--agct---    640

Wood_frog             ATGGGCGAGTACCTGTTCGACAAA.................    307
Bullfrog              -----------------t-----gcacaccatgggagaga    664
African_clawed_frog   ----------------------gcacaccctgggggaga    695
Western_clawed_frog   ----------------------gcacaccctgggggaga    646
Asiatic_toad          ----------------------gcacaccatgggagaga    676
Chicken               ----ca-----------t-----gcacaccctcggggaaa    683
Human                 t---cg--a--t--c--t-----gcacaccctgggagaca    770
Mouse                 ----ca--a--t--c--t-----gcacaccctgggacacg    680
```

B)

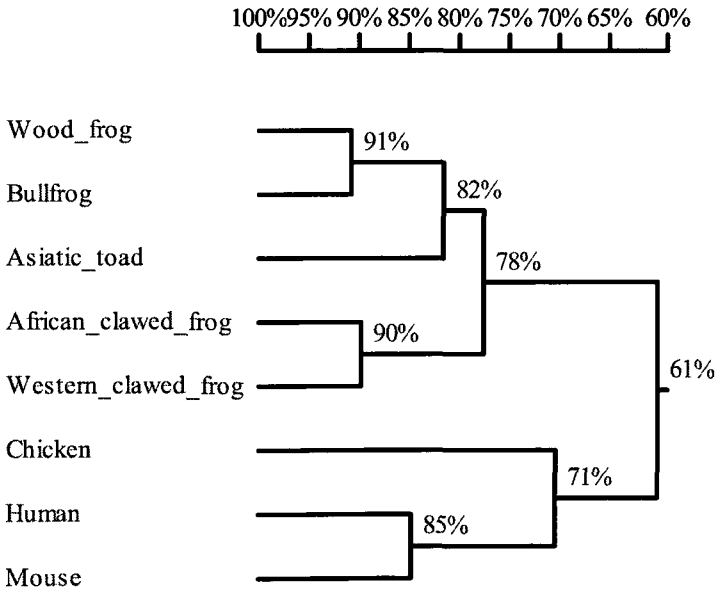

C)

Wood frog ferritin heavy chain partial amino acid sequence aligned with the sequences (Genbank accession numbers in parentheses) from bullfrog, *Rana catesbeiana* (ACO52052.1), African clawed frog, *Xenopus laevis* (NP_001079580.1), Western clawed frog, *Xenopus tropicalis* (NP_989008.1), Asiatic toad *Bufo gargarizans* (ABD75379.1), chicken, *Gallus gallus*, (NP_990417.1), human, *Homo sapiens* (AAA52437.1) and mouse, *Mus musculus* (NP_034369.1). Dashes (-) represent nucleotides in the other sequences that are identical to the wood frog sequence. Dots (.) represent areas in the sequence where nucleotides are absent.

D)

Homology tree for ferritin heavy chain amino acid sequences

C)

```
Wood_frog            ....................................      0
Bullfrog             ....mnsqvrqnfhqdceaalnrqvnlelyasyvylsmsy     36
African_Clawed_frog  ....mqsqvrqnfnsdceaainrmvnlemyasyvylsmsy     36
Western_clawed_frog  ....mqsqvrqnfnsdceaainrmvnmelyasyvylsmsy     36
Asiatic_toad         ....mesqvrqnfhrdceaainrmvnmelyasytylsmsf     36
Chicken              matp.psqvrqnyhqdceaainrqinlelyasyvylsmsy     39
Human                mttastsqvrqnyhqdseaainrqinlelyasyvylsmsy     40
Mouse                mttaspsqvrqnyhqdaeaainrqinlelyasyvylsmsc     40

Wood_frog            ............................KYQNKRGGR      9
Bullfrog             yfdrddvalrnfakyflhqsheerehaeklm-m--q----     76
African_Clawed_frog  yfdrddvalhhvakffkeqsheerehaekfl---------     76
Western_clawed_frog  yfdrddvalhhvakffkeqsheerehaekfl---------     76
Asiatic_toad         yfdrddvalhnvakffkeqsheerehaekll---------     76
Chicken              yfdrddvalknfakyflhqsheerehaeklm-l--q----     79
Human                yfdrddvalknfakyflhqsheerehaeklm-l--q----     80
Mouse                yfdrddvalknfakyflhqsheerehaeklm-l--q----     80

Wood_frog            VVLQDVKKPERDEWGNTLDAMQAALQLEKTVNQALLDLHK     49
Bullfrog             if-------d-----sg-e-lec------n---s---v--    116
African_Clawed_frog  -----i--------s---e--------------------    116
Western_clawed_frog  a----i------------e--------------------    116
Asiatic_toad         i----i----l---t---e--------------------    116
Chicken              if---i---d--d-e-g-t--ec--h---n---s--e---    119
Human                if---i---dc-d-esg-n--ec--h---n---s--e---    120
Mouse                if---i---d--d-esg-n--ec--h---s---s--e---    120

Wood_frog            LASDKVDPHLCDFLETEYLEEQVKDIKHFGDYITNLKRLG     89
Bullfrog             --tern----------h--d----s--el--hv---rkm-    156
African_Clawed_frog  --------q------s--------am-el-----------    156
Western_clawed_frog  -----t---------s--------am-el-----------    156
Asiatic_toad         v-------q------s--------a--ql-----------    156
Chicken              --te-n-------i--h--d----a--ql--hv---rkm-    159
Human                --t--n-------i--h--n----a--el--hv---rkm-    160
Mouse                --t--n-------i--y--s----s--el--hv---rkm-    160

Wood_frog            LPENGMGEYLFDK............                102
Bullfrog             a-q---a------htlgeshd....                177
African_Clawed_frog  v-q----------htlges.....s                176
Western_clawed_frog  v-q----------htlgess.....                176
Asiatic_toad         v-q----------htmgesss....                177
Chicken              a-ky--a------htlgesds....                180
Human                a--s-la------htlgdsdne.s.                183
Mouse                a--a--a------htlghgd.es..                182
```

D)

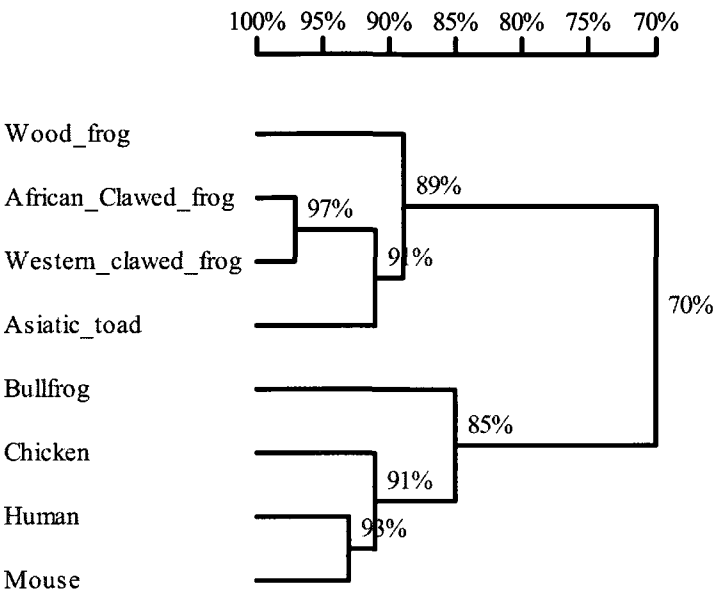
100% 95% 90% 85% 80% 75% 70%
Wood_frog
African_Clawed_frog
Western_clawed_frog
Asiatic_toad
Bullfrog
Chicken
Human
Mouse
97%
91%
89%
70%
85%
91%
93%